THE PHYSICAL REVIEW

A JOURNAL OF EXPERIMENTAL AND THEORETICAL PHYSICS

CONDUCTED BY

THE AMERICAN PHYSICAL SOCIETY

BOARD OF EDITORS

Managing Editor JOHN T. TATE, University of Minnesota, Minneapolis

G. BEMENT, P. W. BRIDGMAN, L. W. MCKEEHAN, L. B. LOEB, H. G. MOSELEY,
M. D. SAYRE, R. U. SOSMAN, C. J. DAVISSON, F. K. RICHTMYER

AUGUST 15, 1929

Effect of Retardation on the Interaction of Two Electrons – – – – – – G. Breit

Satellites of the K-Ray Lines $L\alpha_1$, $L\beta_1$ and $L\beta_2$ – – F. K. Richtmyer and R. D. Richtmyer

Raman Spectra of Polyatomic Gases – – S. C. Dickinson, R. T. Dillon and F. Rasetti

Influence of Foreign Gases on the Intensities of the Magnesium Resonance Lines 4571 and 4703 – – – – – –

THE AMERICAN PHYSICAL SOCIETY

OFFICERS OF THE SOCIETY

[illegible]	HENRY G. GALE	University of Chicago, Chicago, Ill.
[illegible]	W. F. G. SWANN	Bartol Research Foundation, Philadelphia, Pa.
[illegible]	W. L. SEVERINGHAUS	Columbia University, New York City
[illegible]	G. B. PEGRAM	Columbia University, New York City
[illegible]	JOHN T. TATE	University of Minnesota, Minneapolis, Minn.
[illegible] Secretary for [illegible] Coast	I. B. LAM	University of California, Berkeley, Calif.

THE PHYSICAL REVIEW

[illegible] by the American Physical Society at 450 Ahnaip St., Menasha, Wis. [illegible] office: University of Minnesota, Minneapolis, Minn. Two volumes annually, [illegible] issues per volume.

[illegible] series. From July 1, 1893, to January 1, 1913, the REVIEW was conducted by Ed[illegible] L. Nichols, Ernest Merritt and Frederick Bedell, with the financial support of Cor[illegible] University. The first four volumes were issued annually; subsequent volumes, semi[illegible]ly; thirty-five volumes in all.

[illegible] series. On January 1, 1913, the REVIEW was transferred to the American [illegible]al Society as announced on the first page of the new series which was then begun. [illegible] there it has been conducted by a Board of Editors elected by the Society. Semi[illegible]al volumes begin in January and July. Since July 1, 1919, the REVIEW has been issued [illegible] a month.

[illegible]dvertisers are referred to page 2 of the advertisements for further information.

[illegible]ual subscription, throughout the Postal Union, $10.00 in advance.

[illegible]gle copies of current volume, $1.60.

[illegible]eneral Index, 1893-1912, $4.00, in advance.

[illegible] Volumes, $6.00 per volume; Back Numbers, $1.00 per copy for issues prior to [illegible], 1919 (Vols. 1-13), $.60 per copy for issues subsequent thereto. Postage is free [illegible]mittance accompanies order; otherwise postage is extra. No bound volumes can be [illegible]. The REVIEW offers to purchase a limited number of First Series, Vol. 1, No. 1 [illegible].00 each); Second Series, Vol. 7, No. 1, January 1916; Vol. 7, No. 2, February [illegible] Vol. 7, No. 4, April 1916; and Vol. 7, No. 5, May 1916 (at $2.00 each).

[illegible]dvertisements. Rates will be supplied by the Editor on request. Copy for each num[illegible]ust be received at Minneapolis two weeks prior to the dates of issue; old copy is [illegible] until new copy is received. Send electrotypes direct to the printers, George Banta [illegible]shing Co., Menasha, Wis.

[illegible]scount of ten percent is allowed subscription agencies and members of the American [illegible]al Society.

[illegible]anges of address and Complaints of failure to receive the REVIEW, in the case of [illegible]rs of the Physical Society, should be addressed to the Treasurer; in the case of [illegible] subscribers to 450 Ahnaip St., Menasha, Wis.; or to the Editor. New copies can [illegible] free in response to complaint of non-delivery only if notice of non-delivery is [illegible] within three months of date of issue.

[illegible]ditorial Correspondence should be addressed to the PHYSICAL REVIEW, University of [illegible]ota, Minneapolis, Minn.

Entered at the postoffice at Menasha, Wis., as second class matter.
[illegible] for mailing at special rate of postage provided for in section 1103, Act of October 3, 1917, authorized September 6, 1918.

Second Series *August 15, 1929* *Vol. 34, No. 4*

THE

PHYSICAL REVIEW

THE EFFECT OF RETARDATION ON THE INTERACTION OF TWO ELECTRONS

By G. Breit
Department of Research in Terrestrial Magnetism, Washington, D. C.

(Received May 31, 1929)

Abstract

An approximate wave-equation (6) is set up which takes into account terms of the order $(v/c)^2$ in the interaction of two electrons. This equation (6) is reduced to a form (48) which can be interpreted in terms of electronic spins. Disregarding the effect of retardation the two electrons are described by formula (10). This is reduced to a form (36) which can also be described in terms of spins. It is shown that the retarded equation (48) differs from the non-retarded (36) by terms which affect the fine structur of orthohelium and which have not been known so far.

The derivation of the wave-equation (6) is made first in configuration space and later by the Heisenberg-Pauli theory of wave-fields. The latter method is used only to terms of the first order in the Coulomb interaction. It is shown from the consideration of (36) that it cannot be the correct equation and that the modifications due to retardation introduced in (6) and (48) are necessary. These modifications are appreciable only for spectra of elements with low atomic number.

1. Introduction

DIRAC'S equation for the electron enables one to derive the electronic spin and to assign values both to its angular momentum and magnetic moment. In applying his equation to spectroscopic problems it is usually sufficient to express the two small components ψ_1, ψ_2 in terms of the large components ψ_3, ψ_4 and to carry through the calculation to within terms in $(v/c)^2$. This has been done by Darwin. The present paper is an attempt to set up an equation similar to Dirac's for two electrons. The equation set up is only an approximation to within terms in $(v/c)^2$ for the energy. One's first guess in setting up such an equation is (10) below. The interaction-energy is constructed analogously to the classical

$$\frac{e^2}{r}\left[1-\frac{v^{\mathrm{I}}v^{\mathrm{II}}}{c^2}\right]$$

the first term referring to the electrostatic energy and the second to the magnetic.[1]

[1] This equation has been suggested independently by Pauli and Heisenberg. Heisenberg arrived at the result by interpreting Dirac's α's as expressions for the velocity—(v/c) while

Since in the classical theory the difference between retarded and non-retarded potentials makes itself felt in this approximation it becomes necessary to consider this difference in quantum theory as well. As a starting point Darwin's classical Hamiltonian is used. Dirac's matrices α_μ are introduced in such a way as to leave the canonical equations unaltered with the same interpretation of the α_μ as in Dirac's equation. This forms the subject of section 2. In sections 3 and 4 the retarded and non-retarded equations (6) and (10) are reduced to equations in the larger ψ components and expressed in terms of Pauli's two-row spin matrices. It is then possible to discuss the magnetic interaction of the electrons in terms of their spins and to compare them with the form which Heisenberg used in discussing the two-electron problem.

Using the new Heisenberg-Pauli theory of wave-fields it is possible to derive the retarded equation (6) to within terms of the first order in the Coulomb interaction. This derivation is made in section 5. Although all that can be maintained at present is that (6) is correct to within terms of the first order in the Coulomb interaction it is likely, since (6) has been also derived from considerations in the configuration space, that it is the correct result in the approximation $(v/c)^2$.

It can be said with certainty that (10) is not the correct equation to within this order and that therefore Gaunt's work on orthohelium will have to be extended to take into account the last term in the result of reducing (6) [See (48)].[2]

2. Derivation of Retarded and Nonretarded Equations in the Configuration Space

Dirac's equation for a single electron enables one to derive not only the proper values of the energy but also the equations of motion of the electron. This equation is

$$\left(p_0+\sum_{k=1,2,3}\alpha_k p_k+\alpha_4 mc\right)\psi=0,\quad p_0=-\frac{h}{2\pi i}\frac{\partial}{c\partial t}+(e/c)A_0,$$
$$p_k=\frac{h}{2\pi i}\frac{\partial}{\partial x_k}+(e/c)A_k \tag{1}$$

Pauli got it by considerations forming an extension to those of Jordan and Klein with quantizing wave-amplitudes. Essentially the same equation has been used by Eddington and particularly Gaunt who applied it to the fine structure of orthohelium. Professor Pauli kindly suggested to the writer to reduce (10) in a manner similar to that used by Darwin in reducing Dirac's equation. The writer is very grateful to him for his advice and criticism. It is also a pleasure to express his thanks to Professor Heisenberg for discussions about the new Heisenberg-Pauli theory of wave-fields and his encouraging interest in this work.

[2] Estimates indicate that Gaunt's results are improved by this modification. On account of not having sufficiently certain expressions for the proper functions of the 2^3P state of He it is not possible to speak definitely of agreement with experiment.

The results (6) and (48) are simply extended to the case of several electrons by summation over electron-pairs. Also obvious extensions can be made for particles of unequal mass.

the Cartesian coordinates of the electron being x_1, x_2, x_3 the time t; $A_0(A_1, A_2, A_3)$ the scalar and the vector potential respectively, the charge of the electron $-e$, and c the velocity of light. Solving for the Hamiltonian E we have $E/c=-(e/c)A_0-\sum_{k=1,2,3}\alpha_k(p_k+(e/c)A_k)-\alpha_4 mc$. We obtain with this E.

$$\frac{dx_k}{cdt}=\frac{2\pi i}{h}[(E/c), x_k]=\frac{2\pi i}{ch}(Ex_k-x_kE)=-\alpha_k \tag{2}$$

and also

$$\frac{dp_1}{dt}=\frac{\partial\left(\frac{e}{c}A_1\right)}{\partial t}+\frac{2\pi i}{h}[E,p_1]=e\left(\frac{\partial A_0}{\partial x_1}+\frac{1}{c}\frac{\partial A_1}{\partial t}\right)+e(\alpha_2 H_3-\alpha_3 H_2) \tag{3}$$

where $\boldsymbol{H}=\text{curl } \boldsymbol{A}$. It is seen that in (2) Dirac's matrices α_k are representations of $-\dot{x}_k/c$ and that (3) gives the momentum force equation, the left side being the momentum and the right the electric plus the magnetic Lorentz force.[3]

For two electrons it should be similarly required that the matrix expression for the energy should give consistent equations of motion just as Dirac's gives (2) and (3). The approximate Lagrangian and Hamiltonian functions taking into account the retardation of potentials have been derived on the classical theory by Darwin.[4] These are respectively

$$L=-m_1c^2(1-\beta_1^2)^{1/2}-m_{II}c^2(1-\beta_{II}^2)^{1/2}-e_1e_{II}/r + (e_1e_{II}/2c^2)[(\dot{\boldsymbol{r}}_1\dot{\boldsymbol{r}}_{II})r^{-1}+(\dot{\boldsymbol{r}}_1\boldsymbol{r})(\dot{\boldsymbol{r}}_{II}\boldsymbol{r})r^{-3}] \tag{4}$$

$$H=p_1^2/2m_1+p_{II}^2/2m_{II}-p_1^4/8c^2m_1^3-p_{II}^4/8c^2m_{II}^3 - e_1A_0^{I}-e_{II}A_0^{II}+(e_1/cm_1)(\boldsymbol{p}_1\boldsymbol{A}^{I})+(e_{II}/cm_{II})(\boldsymbol{p}_{II}\boldsymbol{A}^{II}) + e_1e_{II}/r-(e_1e_{II}/2c^2m_1m_{II})[(\boldsymbol{p}_1\boldsymbol{p}_{II})/r+(\boldsymbol{p}_1\boldsymbol{r})(\boldsymbol{p}_{II}\boldsymbol{r})/r^3] \tag{5}$$

Here the two electrons are distinguished by roman numerals I, II. Darwin's notation is somewhat changed, the electronic charge being denoted by $-e$ and the vector $\boldsymbol{r}$ and distance r without subscripts refer to the vector from electron I to II. The form of (5) suggests to try for two electrons

$$\left(p_0+\sum_{k=1,2,3}(\alpha_k^{I}p_k^{I}+\alpha_k^{II}p_k^{II})+(\alpha_4^{I}+\alpha_4^{II})mc + (e^2/2c)\left(\sum_k\alpha_k^{I}\alpha_k^{II}r^{-1}+(\boldsymbol{\alpha}^{I}\boldsymbol{r})(\boldsymbol{\alpha}^{II}\boldsymbol{r})r^{-3}\right)\right)\psi=0. \tag{6}$$

where now

$$p_0=-\frac{h}{2\pi i}\frac{\partial}{c\partial t}+(e/c)(A_0^{I}+A_0^{II})-e^2/cr$$

[3] Expression (2) has been communicated to the writer by letter by Dr. P. A. M. Dirac in the summer of 1928. Essentially the same point of view involving also (3) has been subsequently published by Eddington (Proc. Roy. Soc. **A122**, 358 (1929)).

[4] Darwin, Phil. Mag. **39**, 537 (1920).

$$p_k^{\mathrm{I}}=\frac{h}{2\pi i}\frac{\partial}{\partial x_k^{\mathrm{I}}}+(e/c)A_k^{\mathrm{I}};\mathfrak{a}^{\mathrm{I}}=(\alpha_1^{\mathrm{I}},\alpha_2^{\mathrm{I}},\alpha_3^{\mathrm{I}})$$

$$p_k^{\mathrm{II}}=\frac{h}{2\pi i}\frac{\partial}{\partial x_k^{\mathrm{II}}}+(e/c)A_k^{\mathrm{II}};\mathfrak{a}^{\mathrm{II}}=(\alpha_1^{\mathrm{II}},\alpha_2^{\mathrm{II}},\alpha_3^{\mathrm{II}}).$$

A^{I}, A^{II} are respectively the potentials of electrons I, II disregarding their interaction and the wave function ψ has sixteen components which will be written in what follows in the form ψ_{mn} $(m, n=1, 2, 3, 4)$ the first index m referring to electron I and the second n to II. The matrices α_k^{I}, α_k^{II} operate respectively on the upper and lower index. Thus by definition if a^{I} and b^{II} be any of these matrices

$$(a^{\mathrm{I}}b^{\mathrm{II}}\psi)_{m,n}=\sum_{k,l}a_{mk}^{\mathrm{I}}b_{nl}^{\mathrm{II}}\psi_{kl} \tag{7}$$

Equation (6) is thus equivalent to 16 equations involving 16 variables ψ_{mn}. It is clear by performing a calculation similar to that used in deriving (2) from (1) that using (6)

$$\frac{dx_k^{\mathrm{II}}}{dt}=-c\alpha_k^{\mathrm{I}} \qquad \frac{dx_k^{\mathrm{II}}}{dt}=-c\alpha_k^{\mathrm{II}} \tag{8}$$

so that the matrices representing velocities are the same as for one electron. Similarly we find imitating (3) that

$$\frac{dp_k^{\mathrm{I}}}{dt}=e\left(\frac{\partial A_0^{\mathrm{I}}}{\partial x_k^{\mathrm{I}}}+\frac{\partial A_k^{\mathrm{I}}}{c\partial t}\right)+\sum e\alpha_j^{\mathrm{I}}\left(\frac{\partial A_j^{\mathrm{I}}}{\partial x_k^{\mathrm{I}}}-\frac{\partial A_k^{\mathrm{I}}}{\partial x_j^{\mathrm{I}}}\right)$$

$$+\frac{\partial}{\partial x_k^{\mathrm{I}}}[-e^2/r+(e^2/2cr)((\mathfrak{a}^{\mathrm{I}}\mathfrak{a}^{\mathrm{II}})+(\mathfrak{a}^{\mathrm{I}}\mathfrak{r})(\alpha^{\mathrm{II}}\mathfrak{r})/r^2)] \tag{9}$$

and that the same equation follows from (5) on the classical theory provided it is remembered that the p_μ in (5) do not include the potentials as they do in (6). The values for the energy from (5) and (6) are also found to agree to within terms in $(v/c)^2$ provided it is remembered that α_4 should be replaced by $(1-\beta^2)^{1/2}$.[5]

If instead of using (5) the effect of retardation is neglected and the attempt is made to take into account only the magnetic interaction between the electrons corresponding to an interaction energy $(e^2/r)(1-v^{\mathrm{I}}v^{\mathrm{II}}/c^2)$ we obtain instead of (6)

$$\left(p_0+\sum_k(\alpha_k^{\mathrm{I}}p_k^{\mathrm{I}}+\alpha_k^{\mathrm{II}}p_k^{\mathrm{II}})+(\alpha_4^{\mathrm{I}}+\alpha_4^{\mathrm{II}})mc+(e^2/cr)(\mathfrak{a}^{\mathrm{I}}\mathfrak{a}^{\mathrm{II}})\right)\psi=0. \tag{10}$$

[5] If instead of writing (6) we try to use in the interaction term expressions of the form $(1/2m)\Sigma_k p_k+\alpha_k p_k$) then it is found that the simple form of (8) is no longer true and that it also becomes difficult to get simultaneously the correct value of H and the equations of motion. If the matrices represent the velocity components of a single electron, it would be surprising if for two electrons the velocity components were represented in part by the differential operators p.

This is the equation used by Gaunt and Eddington[6], and claimed by them to be correct. As we shall see the consequences of (10) are in some respects unreasonable. Further (6) will be derived to within first order terms in the interaction from the general theory of Heisenberg and Pauli. The work involved in reducing (10) to a form convenient for spectroscopic applications can be conveniently applied to (6). We, therefore reduce (10) first.

3. Reduction of Nonretarded Equation to Larger Components

We follow here a method used by Darwin in discussing Dirac's equation. It makes it possible to reduce equation (10) which involves 16 components (see (7)) to an approximate equation with 4 components expressed in terms of Pauli's spin matrices. The approximation desired is that needed in most spectroscopic applications and includes terms in $(v/c)^2$. The matrices α are taken to be

$$\alpha_1=\begin{pmatrix}0&0&0&1\\0&0&1&0\\0&1&0&0\\1&0&0&0\end{pmatrix}\quad \alpha_2=\begin{pmatrix}0&0&0&-i\\0&0&i&0\\0&-i&0&0\\i&0&0&0\end{pmatrix}\quad \alpha_3=\begin{pmatrix}0&0&1&0\\0&0&0&-1\\1&0&0&0\\0&-1&0&0\end{pmatrix}$$

$$\alpha_4=\begin{pmatrix}1&0&0&0\\0&1&0&0\\0&0&-1&0\\0&0&0&-1\end{pmatrix}. \tag{11}$$

Writing

$$a^{\mathrm{I}}=p_1{}^{\mathrm{I}}+ip_2{}^{\mathrm{I}},\ b^{\mathrm{I}}=p_1{}^{\mathrm{I}}-ip_1{}^{\mathrm{I}},\ c^{\mathrm{I}}=p_3{}^{\mathrm{I}} \tag{12}$$

the (16) equations (10) involve the following types

$$(p_0+2mc)\psi_{1,1}+b^{\mathrm{I}}\psi_{4,1}+c^{\mathrm{I}}\psi_{3,1}+b^{\mathrm{II}}\psi_{1,4}+c^{\mathrm{II}}\psi_{1,3}+\frac{e^2}{cr}\psi_{3,3}=0 \tag{13.1}$$

$$(p_0+2mc)\psi_{2,2}+a^{\mathrm{I}}\psi_{3,2}-c^{\mathrm{I}}\psi_{4,2}+a^{\mathrm{II}}\psi_{2,3}-c^{\mathrm{II}}\psi_{2,4}+\frac{e^2}{cr}\psi_{4,4}=0 \tag{13.2}$$

$$(p_0+2mc)\psi_{1,2}+b^{\mathrm{I}}\psi_{4,2}+c^{\mathrm{I}}\psi_{3,2}+a^{\mathrm{II}}\psi_{1,3}-c^{\mathrm{II}}\psi_{1,4}+\frac{e^2}{cr}(2\psi_{4,3}-\psi_{3,4})=0 \tag{13.3}$$

$$p_0\psi_{1,3}+b^{\mathrm{I}}\psi_{4,3}+c^{\mathrm{I}}\psi_{3,3}+b^{\mathrm{II}}\psi_{1,2}+c^{\mathrm{II}}\psi_{1,1}+\frac{e^2}{er}\psi_{3,1}=0 \tag{14.1}$$

$$p_0\psi_{1,4}+b^{\mathrm{I}}\psi_{4,4}+c^{\mathrm{I}}\psi_{3,4}+a^{\mathrm{II}}\psi_{1,1}-c^{\mathrm{II}}\psi_{1,2}+\frac{e^2}{cr}(2\psi_{4,1}-\psi_{3,2})=0 \tag{14.2}$$

$$p_0\psi_{2,3}+a^{\mathrm{I}}\psi_{3,3}-c^{\mathrm{I}}\psi_{4,3}+b^{\mathrm{II}}\psi_{2,2}+c^{\mathrm{II}}\psi_{2,1}+\frac{e^2}{cr}(2\psi_{3,2}-\psi_{4,1})=0 \tag{14.3}$$

[6] Eddington, reference 3; Gaunt Phil. Trans. Roy. Soc. **228**, 151–196 Pamphlet **A662** (1929); Proc. Roy. Soc. **A122**, 153 (1929).

$$p_0\psi_{2,4}+a^{\mathrm{I}}\psi_{3,4}-c^{\mathrm{I}}\psi_{4,4}+a^{\mathrm{II}}\psi_{2,1}-c^{\mathrm{II}}\psi_{2,2}+\frac{e^2}{cr}\psi_{4,2}=0 \qquad (14.4)$$

S

$$(p_0-2mc)\psi_{3,3}+b^{\mathrm{I}}\psi_{2,3}+c^{\mathrm{I}}\psi_{1,3}+b^{\mathrm{II}}\psi_{3,2}+c^{\mathrm{II}}\psi_{3,1}+\frac{e^2}{cr}\psi_{1,1}=0 \qquad (15.1)$$

$$(p_0-2mc)\psi_{4,4}+a^{\mathrm{I}}\psi_{1,4}-c^{\mathrm{I}}\psi_{2,4}+a^{\mathrm{II}}\psi_{4,1}-c^{\mathrm{II}}\psi_{4,2}+\frac{e^2}{cr}\psi_{2,2}=0 \qquad (15.2)$$

$$(p_0-2mc)\psi_{4,3}+b^{\mathrm{I}}\psi_{2,4}+c^{\mathrm{I}}\psi_{1,4}+a^{\mathrm{II}}\psi_{3,1}-c^{\mathrm{II}}\psi_{3,2}+\frac{e^2}{cr}(2\psi_{2,1}-\psi_{1,2})=0 \qquad (15.3)$$

It is not necessary to write out the remaining 6 equations since they can be obtained by interchanging I and II. Since $p_0\cong 2mc$ we see that $\psi_{4,4}$, $\psi_{3,3}$, $\psi_{3,4}$, $\psi_{4,3}$ are large while the remaining $\psi_{n,m}$ are small. Using equations (13), (14) we let to start with $p_0=2mc$ and solve for $\psi_{1,1}$, $\psi_{1,2}$, $\psi_{1,3}$ in terms of the four large ψ's neglecting for the present all terms of order higher than v/c. Equations (14) determine the order of magnitude of $\psi_{1,3}$, $\psi_{1,4}$, $\psi_{2,3}$, $\psi_{2,4}$ as v/c. Using these values in (13) the order of $\psi_{1,1}$, $\psi_{1,2}$, $\psi_{2,2}$ is $(v/c)^2$ and to the first approximation these may be neglected. The results for the first approximation may be expressed most conveniently by means of Pauli's matrices with two rows and columns which represent the spin. We let

$$\sigma_1=\begin{pmatrix} 0 & -1 \\ -1 & 0 \end{pmatrix},\quad \sigma_2=\begin{pmatrix} 0 & i \\ -i & 0 \end{pmatrix},\quad \sigma_3=\begin{pmatrix} -1 & 0 \\ 0 & 1 \end{pmatrix}. \qquad (16)$$

[These are the negative of Pauli's matrices. It is for the present purpose somewhat more convenient to have the sign changed as done here.] The two row matrices are used as operators on the suffixes 3, 4 only.

Using the relations:

$$\begin{aligned}((\boldsymbol{p}\boldsymbol{\sigma}^{\mathrm{I}})\psi)_{3,3}&=-(b\psi_{4,3}+c\psi_{3,3})\ ;\ ((\boldsymbol{p}\boldsymbol{\sigma}^{\mathrm{I}})\psi)_{3,4}=-(b\psi_{4,4}+c\psi_{3,4})\ ;\ ((\boldsymbol{p}\boldsymbol{\sigma}^{\mathrm{I}})\psi)_{4,3}\\ &=-(a\psi_{3,3}-c\psi_{4,3})\ ;\ ((\boldsymbol{p}\boldsymbol{\sigma}^{\mathrm{I}})\psi)_{4,4}=-(a\psi_{3,4}-c\psi_{4,4})\\ ((\boldsymbol{p}\boldsymbol{\sigma}^{\mathrm{II}})\psi)_{3,3}&=-(b\psi_{3,4}+c\psi_{3,3})\ ;\ ((\boldsymbol{p}\boldsymbol{\sigma}^{\mathrm{II}})\psi)_{3,4}=-(a\psi_{3,3}-c\psi_{3,4})\ ;\ ((\boldsymbol{p}\boldsymbol{\sigma}^{\mathrm{II}})\psi)_{4,3}\\ &=-(b\psi_{4,4}+c\psi_{4,3})\ ;\ ((\boldsymbol{p}\boldsymbol{\sigma}^{\mathrm{II}})\psi)_{4,4}=-(a\psi_{4,3}-c\psi_{4,4})\end{aligned} \qquad (17)$$

$$\begin{aligned}((\boldsymbol{\sigma}^{\mathrm{I}}\boldsymbol{\sigma}^{\mathrm{II}})\psi)_{3,3}&=\psi_{3,3}\ ;\ ((\boldsymbol{\sigma}^{\mathrm{I}}\boldsymbol{\sigma}^{\mathrm{II}})\psi)_{3,4}=2\psi_{4,3}-\psi_{3,4}\ ;\ ((\boldsymbol{\sigma}^{\mathrm{I}}\boldsymbol{\sigma}^{\mathrm{II}})\psi)_{4,3}\\ &=2\psi_{3,4}-\psi_{4,3}\ ;\ ((\boldsymbol{\sigma}^{\mathrm{I}}\boldsymbol{\sigma}^{\mathrm{II}})\psi)_{4,4}=\psi_{4,4}\end{aligned} \qquad (18)$$

and letting

$$\chi^{\mathrm{I}}=(\boldsymbol{p}^{\mathrm{I}}\boldsymbol{\sigma}^{\mathrm{I}})\psi,\quad \chi^{\mathrm{II}}=(\boldsymbol{p}^{\mathrm{II}}\boldsymbol{\sigma}^{\mathrm{II}})\psi \qquad (19)$$

we have to a first approximation

$$p_0=2mc\ ;\ \psi_{1,1}=\psi_{1,2}=\psi_{2,1}=\psi_{2,2}=0$$

$$\begin{aligned}&\psi_{1,3}=(2mc)^{-1}\overset{\mathrm{I}}{\chi}_{3,3}\ ;\ \psi_{1,4}=(2mc)^{-1}\overset{\mathrm{I}}{\chi}_{3,4}\ ;\ \psi_{2,3}=(2mc)^{-1}\overset{\mathrm{I}}{\chi}_{4,3}\ ;\ \psi_{2,4}=(2mc)^{-1}\overset{\mathrm{I}}{\chi}_{4,4}\\ &\psi_{3,1}=(2mc)^{-1}\overset{\mathrm{II}}{\chi}_{3,3}\ ;\psi_{4,1}=(2mc)^{-1}\overset{\mathrm{II}}{\chi}_{4,3}\ ;\psi_{3,2}=(2mc)^{-1}\overset{\mathrm{II}}{\chi}_{3,4}\ ;\psi_{4,2}=(2mc)^{-1}\overset{\mathrm{II}}{\chi}_{4,4}\end{aligned} \qquad (20)$$

Substituting these values in (13.1), (13.2), (13.3) we derive values for $\psi_{1,1}$, $\psi_{1,2}$, $\psi_{2,2}$, $\psi_{2,1}$ to the order $(v/c)^2$ which on using (17) and (18) again reduce to

$$\psi_{1,1}=\eta_{3,3}\ ;\ \psi_{2,2}=\eta_{4,4}\ ;\ \psi_{1,2}=\eta_{3,4}\ ;\ \psi_{2,1}=\eta_{4,3} \tag{21}$$

where

$$\eta=-\frac{e^2}{4mc^2}\,\frac{1}{r}(\sigma^{\mathrm{I}}\sigma^{\mathrm{II}})\psi+\frac{(p^{\mathrm{I}}\sigma^{\mathrm{I}})(p^{\mathrm{II}}\sigma^{\mathrm{II}})}{4m^2c^2}\psi\,. \tag{22}$$

Also substituting (21) in (14.1), (14.2), (14.3), (14.4) and again using (17) and (18) we get to the order $(v/c)^3$

$$\begin{aligned}
&\psi_{1,3}=p_0^{-1}(\chi^{\mathrm{I}}+\xi^{\mathrm{I}})_{3,3}\ ;\quad \psi_{1,4}=p_0^{-1}(\chi^{\mathrm{I}}+\xi^{\mathrm{I}})_{3,4}\ ;\quad \psi_{2,3}=p_0^{-1}(\chi^{\mathrm{I}}+\xi^{\mathrm{I}})_{4,3}\ ;\\
&\qquad\qquad \psi_{2,4}=p_0^{-1}(\chi^{\mathrm{I}}+\xi^{\mathrm{I}})_{4,4}\\
&\psi_{3,1}=p_0^{-1}(\chi^{\mathrm{II}}+\xi^{\mathrm{II}})_{3,3}\ ;\quad \psi_{4,1}=p_0^{-1}(\chi^{\mathrm{II}}+\xi^{\mathrm{II}})_{4,3}\ ;\quad \psi_{3,2}=p_0^{-1}(\chi^{\mathrm{II}}+\xi^{\mathrm{II}})_{3,4}\ ;\\
&\qquad\qquad \psi_{4,2}=p_0^{-1}(\chi^{\mathrm{II}}+\xi^{\mathrm{II}})_{4,4}
\end{aligned} \tag{23}$$

where

$$\begin{aligned}
\xi^{\mathrm{I}}&=-\frac{e^2}{4mc^2}\left\{(p^{\mathrm{II}}\partial^{\mathrm{II}})(\partial^{\mathrm{I}}\partial^{\mathrm{II}})(r^{-1}\psi)+2r^{-1}(\sigma^{\mathrm{I}}\sigma^{\mathrm{II}})(p^{\mathrm{II}}\partial^{\mathrm{II}})\psi\right\}+\frac{(p^{\mathrm{I}}\sigma^{\mathrm{I}})(p^{\mathrm{II}}\sigma^{\mathrm{II}})^2}{4m^2c^2}\psi\\
\xi^{\mathrm{II}}&=-\frac{e^2}{4mc^2}\left\{(p^{\mathrm{I}}\partial^{\mathrm{I}})(\partial^{\mathrm{I}}\partial^{\mathrm{II}})(r^{-1}\psi)+2r^{-1}(\partial^{\mathrm{I}}\partial^{\mathrm{II}})(p^{\mathrm{I}}\partial^{\mathrm{I}})\psi\right\}+\frac{(p^{\mathrm{II}}\sigma^{\mathrm{II}})(p^{\mathrm{I}}\sigma^{\mathrm{I}})^2}{4m^2c^2}\psi
\end{aligned} \tag{24}$$

We have now obtained expressions for all the $\psi_{n,m}$ correct to the order $(v/c)^2$ in terms of $\psi_{3,3}, \psi_{3,4}, \psi_{4,3}, \psi_{4,4}$. We substitute these values into (15.1), (15.2), (15.3). The term p_0-2mc is itself of order mv^2/c or $(E-mc^2)/c$. Our problem is to determine $E-mc^2$ correctly to within the third term in an expansion according to powers of (v/c). Hence we should require that on dividing equations (15) by c all the other terms should be known to an accuracy $(v/c)^4$. Since a^{I}/c, b^{I}/c, c^{I}/c are of the order v/c the accuracy $(v/c)^3$ in determining $\psi_{4,1}$, $\psi_{3,1}$ etc. suffices and similarly since e^2/c^2r is of the order $(v/c)^2$ the accuracy $(v/c)^2$ in determining $\psi_{1,1}$, $\psi_{1,2}$, $\psi_{2,2}$, $\psi_{2,1}$ is also satisfactory. Performing the substitution of (21), (23) into (15.1), (15.2), (15.3) we have using (17), (18) once more

$$\left\{(p_0-2mc)\psi-(p^{\mathrm{I}}\partial^{\mathrm{I}})p_0^{-1}(\chi^{\mathrm{I}}+\xi^{\mathrm{I}})-(p^{\mathrm{II}}\partial^{\mathrm{II}})p_0^{-1}(\chi^{\mathrm{II}}+\xi^{\mathrm{II}})+\frac{e^2}{cr}(\partial^{\mathrm{I}}\partial^{\mathrm{II}})\eta)\right\}_{\alpha,\beta}=0 \tag{25}$$

where

$$\alpha,\beta=3\quad\text{or}\quad 4.$$

This is the result of eliminating in (10) the smaller components and expressing them in terms of the larger ones. It now remains to substitute into (25) equations (19), (22), (24) and to make the result linear in σ^{I}, σ^{II}. We do this by means of the formulas

$$\begin{aligned}
&\sigma_1\sigma_2=-i\sigma_3,\ \ \sigma_2\sigma_3=-i\sigma_1,\ \ \sigma_3\sigma_1=-i\sigma_2\\
&\sigma_1^2=\sigma_2^2=\sigma_3^2=1,\ \ \sigma_i\sigma_k+\sigma_k\sigma_i=0\quad(i\neq k).
\end{aligned} \tag{26}$$

Performing the substitution and collecting terms we have:

$$\Big\{(p_0-2mc)-(\boldsymbol{p}^{\mathrm{I}}\boldsymbol{\vartheta}^{\mathrm{I}})p_0^{-1}(\boldsymbol{p}^{\mathrm{I}}\boldsymbol{\vartheta}^{\mathrm{I}})-(\boldsymbol{p}^{\mathrm{II}}\boldsymbol{\vartheta}^{\mathrm{II}})p_0^{-1}(\boldsymbol{p}^{\mathrm{II}}\boldsymbol{\vartheta}^{\mathrm{II}})$$
$$+\frac{e^2}{4m^2c^3}[(\boldsymbol{p}^{\mathrm{I}}\boldsymbol{\vartheta}^{\mathrm{I}})(\boldsymbol{p}^{\mathrm{II}}\boldsymbol{\vartheta}^{\mathrm{II}})(\boldsymbol{\vartheta}^{\mathrm{I}}\boldsymbol{\vartheta}^{\mathrm{II}})r^{-1}+(\boldsymbol{p}^{\mathrm{I}}\boldsymbol{\vartheta}^{\mathrm{I}})r^{-1}(\boldsymbol{\vartheta}^{\mathrm{I}}\boldsymbol{\vartheta}^{\mathrm{II}})(\boldsymbol{p}^{\mathrm{II}}\boldsymbol{\vartheta}^{\mathrm{II}})$$
$$+(\boldsymbol{p}^{\mathrm{II}}\boldsymbol{\vartheta}^{\mathrm{II}})r^{-1}(\boldsymbol{\vartheta}^{\mathrm{I}}\boldsymbol{\vartheta}^{\mathrm{II}})(\boldsymbol{p}^{\mathrm{I}}\boldsymbol{\vartheta}^{\mathrm{I}})+r^{-1}(\boldsymbol{\vartheta}^{\mathrm{I}}\boldsymbol{\vartheta}^{\mathrm{II}})(\boldsymbol{p}^{\mathrm{I}}\boldsymbol{\vartheta}^{\mathrm{I}})(\boldsymbol{p}^{\mathrm{II}}\boldsymbol{\vartheta}^{\mathrm{II}})]$$
$$-\frac{(\boldsymbol{p}^{\mathrm{I}}\boldsymbol{\vartheta}^{\mathrm{I}})^2(\boldsymbol{p}^{\mathrm{II}}\boldsymbol{\vartheta}^{\mathrm{II}})^2}{4m^3c^3}-\frac{e^4}{4mc^3}\,\frac{(\boldsymbol{\vartheta}^{\mathrm{I}}\boldsymbol{\vartheta}^{\mathrm{II}})^2}{r^2}\Big\}\psi=0. \tag{27}$$

The term $e^2/4m^2c^3[\ ]$ consisting of four members may be transformed conveniently by using a symbol $\langle\ \rangle$ to indicate that the differential operators $\boldsymbol{p}^{\mathrm{I}}$, $\boldsymbol{p}^{\mathrm{II}}$ apply only within the $\langle\ \rangle$. We have then, remembering that $\boldsymbol{p}^{\mathrm{I}}\boldsymbol{p}^{\mathrm{II}}r^{-1}\psi = \langle\boldsymbol{p}^{\mathrm{I}}r^{-1}\rangle\boldsymbol{p}^{\mathrm{II}}\psi+\langle\boldsymbol{p}^{\mathrm{II}}r^{-1}\rangle\boldsymbol{p}^{\mathrm{I}}\psi+\langle\boldsymbol{p}^{\mathrm{I}}\boldsymbol{p}^{\mathrm{II}}r^{-1}\rangle\psi+r^{-1}\boldsymbol{p}^{\mathrm{I}}\boldsymbol{p}^{\mathrm{II}}\psi$ understanding p and σ as vectors

$$(p^{\mathrm{I}}\sigma^{\mathrm{I}})(p^{\mathrm{II}}\sigma^{\mathrm{II}})(\sigma^{\mathrm{I}}\sigma^{\mathrm{II}})(r^{-1}\psi)+(p^{\mathrm{I}}\sigma^{\mathrm{I}})r^{-1}(\sigma^{\mathrm{I}}\sigma^{\mathrm{II}})(p^{\mathrm{II}}\sigma^{\mathrm{II}})\psi+(p^{\mathrm{II}}\sigma^{\mathrm{II}})r^{-1}(\sigma^{\mathrm{I}}\sigma^{\mathrm{II}})(p^{\mathrm{I}}\sigma^{\mathrm{I}})\psi$$
$$+r^{-1}(\sigma^{\mathrm{I}}\sigma^{\mathrm{II}})(p^{\mathrm{I}}\sigma^{\mathrm{I}})(p^{\mathrm{II}}\sigma^{\mathrm{II}})\psi=\langle(p^{\mathrm{I}}\sigma^{\mathrm{I}})r^{-1}\rangle((p^{\mathrm{II}}\sigma^{\mathrm{II}})(\sigma^{\mathrm{I}}\sigma^{\mathrm{II}})+(\sigma^{\mathrm{I}}\sigma^{\mathrm{II}})(p^{\mathrm{II}}\sigma^{\mathrm{II}}))\psi$$
$$+r^{-1}((p^{\mathrm{I}}\sigma^{\mathrm{I}})(p^{\mathrm{II}}\sigma^{\mathrm{II}})(\sigma^{\mathrm{I}}\sigma^{\mathrm{II}})+(\sigma^{\mathrm{I}}\sigma^{\mathrm{II}})(p^{\mathrm{I}}\sigma^{\mathrm{I}})(p^{\mathrm{II}}\sigma^{\mathrm{II}}))\psi+\langle(p^{\mathrm{II}}\sigma^{\mathrm{II}})r^{-1}\rangle((p^{\mathrm{I}}\sigma^{\mathrm{I}})(\sigma^{\mathrm{I}}\sigma^{\mathrm{II}})$$
$$+(\sigma^{\mathrm{I}}\sigma^{\mathrm{II}})(p^{\mathrm{I}}\sigma^{\mathrm{I}}))\psi+\langle(p^{\mathrm{I}}\sigma^{\mathrm{I}})(p^{\mathrm{II}}\sigma^{\mathrm{II}})(\sigma^{\mathrm{I}}\sigma^{\mathrm{II}})r^{-1}\rangle\psi+r^{-1}((p^{\mathrm{I}}\sigma^{\mathrm{I}})(\sigma^{\mathrm{I}}\sigma^{\mathrm{II}})(p^{\mathrm{II}}\sigma^{\mathrm{II}})$$
$$+(p^{\mathrm{II}}\sigma^{\mathrm{II}})(\sigma^{\mathrm{I}}\sigma^{\mathrm{II}})(p^{\mathrm{I}}\sigma^{\mathrm{I}}))\psi=2\langle(p^{\mathrm{I}}\sigma^{\mathrm{I}})r^{-1}\rangle(p^{\mathrm{I}}\sigma^{\mathrm{I}})\psi+2\langle(p^{\mathrm{II}}\sigma^{\mathrm{II}})r^{-1}\rangle(p^{\mathrm{I}}\sigma^{\mathrm{II}})\psi$$
$$+\langle(p^{\mathrm{I}}\sigma^{\mathrm{I}})(p^{\mathrm{II}}\sigma^{\mathrm{II}})(\sigma^{\mathrm{I}}\sigma^{\mathrm{II}})r^{-1}\rangle\psi+2r^{-1}((p^{\mathrm{I}}\sigma^{\mathrm{I}})(p^{\mathrm{II}}\sigma^{\mathrm{I}})+(p^{\mathrm{II}}\sigma^{\mathrm{I}})(p^{\mathrm{I}}\sigma^{\mathrm{I}}))\psi=4r^{-1}(p^{\mathrm{I}}p^{\mathrm{II}})\psi$$
$$+\langle(p^{\mathrm{I}}\sigma^{\mathrm{I}})(p^{\mathrm{II}}\sigma^{\mathrm{II}})(\sigma^{\mathrm{I}}\sigma^{\mathrm{II}})r^{-1}\rangle\psi+2(\langle p^{\mathrm{I}}r^{-1}\rangle p^{\mathrm{II}})+(\langle p^{\mathrm{II}}r^{-1}\rangle p^{\mathrm{I}})$$
$$-i[\langle p^{\mathrm{I}}r^{-1}\rangle\times p^{\mathrm{II}}]\sigma^{\mathrm{I}}-i[\langle p^{\mathrm{II}}r^{-1}\rangle\times p^{\mathrm{I}}]\sigma^{\mathrm{II}})\psi. \tag{28}$$

Here the p_k^{I} and p_k^{II} were treated as ordinary differential operators because on division by c the whole term is of the order $(v/c)^4$ so that the higher order terms arising from the noncommutability of the p's may be neglected. Use has been made in the above of formulas following from (26) *viz.* for any two commuting vectors $\boldsymbol{A}$, $\boldsymbol{B}$

$$(\boldsymbol{A}\boldsymbol{\vartheta})(\boldsymbol{B}\boldsymbol{\vartheta})=(\boldsymbol{A}\boldsymbol{B})-i[\boldsymbol{A}\times\boldsymbol{B}]\boldsymbol{\vartheta} \tag{29}$$

where $[\boldsymbol{A}\times\boldsymbol{B}]$ is the vector product of $\boldsymbol{A}$ and $\boldsymbol{B}$. Since the last term in (28) is the result of applying (29) to $2\langle(p^{\mathrm{I}}\sigma^{\mathrm{I}})r^{-1}\rangle(p^{\mathrm{II}}\sigma^{\mathrm{I}})+2\langle(p^{\mathrm{II}}\sigma^{\mathrm{II}})r^{-1}\rangle(p^{\mathrm{I}}\sigma^{\mathrm{II}})$ only one of p's operates on ψ while the other operates on r^{-1}. Again using (29) we have

$$\begin{aligned}(p^{\mathrm{I}}\sigma^{\mathrm{I}})(p^{\mathrm{II}}\sigma^{\mathrm{II}})(\sigma^{\mathrm{I}}\sigma^{\mathrm{II}})&=(p^{\mathrm{I}}\sigma^{\mathrm{I}})\{(p^{\mathrm{II}}\sigma^{\mathrm{I}})+i[p^{\mathrm{II}}\times\sigma^{\mathrm{II}}]\sigma^{\mathrm{I}}\}\\&=(p^{\mathrm{I}}p^{\mathrm{II}})-i[p^{\mathrm{I}}\times p^{\mathrm{II}}]\sigma^{\mathrm{I}}+i\{p^{\mathrm{I}}[p^{\mathrm{II}}\times\sigma^{\mathrm{II}}]-i[p^{\mathrm{I}}\times[p^{\mathrm{II}}\times\sigma^{\mathrm{II}}]]\sigma^{\mathrm{I}}\}\\&=(p^{\mathrm{I}}p^{\mathrm{II}})-i[p^{\mathrm{I}}\times p^{\mathrm{II}}](\sigma^{\mathrm{I}}-\sigma^{\mathrm{II}})+(p^{\mathrm{II}}\sigma^{\mathrm{I}})(p^{\mathrm{I}}\sigma^{\mathrm{II}})-(\sigma^{\mathrm{I}}\sigma^{\mathrm{II}})(p^{\mathrm{I}}p^{\mathrm{II}}).\end{aligned} \tag{30}$$

If this operates on $1/r$ it is simply

$$\langle(p^{\mathrm{I}}\sigma^{\mathrm{I}})(p^{\mathrm{II}}\sigma^{\mathrm{II}})(\sigma^{\mathrm{I}}\sigma^{\mathrm{II}})r^{-1}\rangle=\langle(p^{\mathrm{II}}\sigma^{\mathrm{I}})(p^{\mathrm{I}}\sigma^{\mathrm{II}})r^{-1}\rangle. \tag{30'}$$

We have therefore finally

$$\begin{aligned}&\frac{e^2}{4m^2c^3}[(\boldsymbol{p}^{\mathrm{I}}\boldsymbol{\vartheta}^{\mathrm{I}})(\boldsymbol{p}^{\mathrm{II}}\boldsymbol{\vartheta}^{\mathrm{II}})(\boldsymbol{\vartheta}^{\mathrm{I}}\boldsymbol{\vartheta}^{\mathrm{II}})r^{-1}\psi+(\boldsymbol{p}^{\mathrm{I}}\boldsymbol{\vartheta}^{\mathrm{I}})r^{-1}(\boldsymbol{\vartheta}^{\mathrm{I}}\boldsymbol{\vartheta}^{\mathrm{II}})(\boldsymbol{p}^{\mathrm{II}}\boldsymbol{\vartheta}^{\mathrm{II}})\psi\\&\quad+(\boldsymbol{p}^{\mathrm{II}}\boldsymbol{\vartheta}^{\mathrm{II}})r^{-1}(\boldsymbol{\vartheta}^{\mathrm{I}}\boldsymbol{\vartheta}^{\mathrm{II}})(\boldsymbol{p}^{\mathrm{I}}\boldsymbol{\vartheta}^{\mathrm{I}})\psi+r^{-1}(\boldsymbol{\vartheta}^{\mathrm{I}}\boldsymbol{\vartheta}^{\mathrm{II}})(\boldsymbol{p}^{\mathrm{I}}\boldsymbol{\vartheta}^{\mathrm{I}})(\boldsymbol{p}^{\mathrm{II}}\boldsymbol{\vartheta}^{\mathrm{II}})\psi]\\&=\frac{e^2}{m^2c^3r}(\boldsymbol{p}^{\mathrm{I}}\boldsymbol{p}^{\mathrm{II}})\psi+\frac{e^2}{4m^2c^3}\langle(\boldsymbol{p}^{\mathrm{II}}\boldsymbol{\vartheta}^{\mathrm{I}})(\boldsymbol{p}^{\mathrm{I}}\boldsymbol{\vartheta}^{\mathrm{II}})r^{-1}\rangle\\&\quad+\frac{e^2}{2m^2c^3}((\langle\boldsymbol{p}^{\mathrm{I}}r^{-1}\rangle\boldsymbol{p}^{\mathrm{II}})+(\langle\boldsymbol{p}^{\mathrm{II}}r^{-1}\rangle\boldsymbol{p}^{\mathrm{I}})-i[\langle\boldsymbol{p}^{\mathrm{I}}r^{-1}\rangle\times\boldsymbol{p}^{\mathrm{II}}]\boldsymbol{\vartheta}^{\mathrm{I}}-i[\langle\boldsymbol{p}^{\mathrm{II}}r^{-1}\rangle\times\boldsymbol{p}^{\mathrm{I}}]\boldsymbol{\vartheta}^{\mathrm{II}})\psi\end{aligned}\tag{31}$$

In computing $(\boldsymbol{p}^{\mathrm{I}}\boldsymbol{\sigma}^{\mathrm{I}})p_0^{-1}(\boldsymbol{p}^{\mathrm{I}}\boldsymbol{\sigma}^{\mathrm{I}})$ we may not disregard the noncommutability of the $\boldsymbol{p}$'s because this term on division by c is of the order $(v/c)^2$. We have:

$$(\boldsymbol{p}^{\mathrm{I}}\boldsymbol{\vartheta}^{\mathrm{I}})p_0^{-1}(\boldsymbol{p}^{\mathrm{I}}\boldsymbol{\vartheta}^{\mathrm{I}})=(2mc)^{-1}(\boldsymbol{p}^{\mathrm{I}}\boldsymbol{\vartheta}^{\mathrm{I}})[1-(2mc^2)^{-1}(E-2mc^2+eV)](\boldsymbol{p}^{\mathrm{I}}\boldsymbol{\vartheta}^{\mathrm{I}})$$

where

$$V=A_0^{\mathrm{I}}+A_0^{\mathrm{II}}-\frac{e^2}{r}\tag{32}$$

or

$$\begin{aligned}(\boldsymbol{p}^{\mathrm{I}}\boldsymbol{\sigma}^{\mathrm{I}})p_0^{-1}(\boldsymbol{p}^{\mathrm{I}}\boldsymbol{\vartheta}^{\mathrm{I}})&=(2mc)^{-1}\sum\left(\frac{h}{2\pi i}\frac{\partial}{\partial x_k^{\mathrm{I}}}+\frac{e}{c}A_k^{\mathrm{I}}\right)\sigma_k^{\mathrm{I}}[1-(2mc^2)^{-1}(E-2mc^2\\&\qquad+eV)]\sum\left(\frac{h}{2\pi i}\frac{\partial}{\partial x_k^{\mathrm{I}}}+\frac{e}{c}A_k^{\mathrm{I}}\right)\sigma_k^{\mathrm{I}}\\&=(2mc)^{-1}\left(\sum\left(\frac{h}{2\pi i}\frac{\partial}{\partial x_k^{\mathrm{I}}}+\frac{e}{c}A_k^{\mathrm{I}}\right)\sigma_k^{\mathrm{I}}\right)^2\\&\qquad-(2mc)^{-1}(\boldsymbol{p}^{\mathrm{I}}\boldsymbol{\vartheta}^{\mathrm{I}})(2mc^2)^{-1}(E-2mc^2+eV)(\boldsymbol{p}^{\mathrm{I}}\boldsymbol{\vartheta}^{\mathrm{I}})\end{aligned}$$

where in the second part of the expression the difference between p_k^{I} and $(h/2\pi i)\partial/\partial x_k^{\mathrm{I}}$ is not essential since that part on division by c is of the order $(v/c)^4$. We have therefore

$$\begin{aligned}(\boldsymbol{p}^{\mathrm{I}}\boldsymbol{\sigma}^{\mathrm{I}})p_0^{-1}(\boldsymbol{p}^{\mathrm{I}}\boldsymbol{\sigma}^{\mathrm{I}})&=(2mc)^{-1}\sum(p_k^{\mathrm{I}})^2-\frac{eh}{4\pi mc^2}(\boldsymbol{H}^{\mathrm{I}}\boldsymbol{\vartheta}^{\mathrm{I}})-\frac{E-2mc^2+eV}{4m^2c^3}\sum(p_k^{\mathrm{I}})^2\\&\qquad-\frac{ehi}{8\pi m^2c^3}(\mathcal{E}^{\mathrm{I}}\boldsymbol{p}^{\mathrm{I}})-\frac{eh}{8\pi mc^3}\left[\mathcal{E}^{\mathrm{I}}\times\frac{\boldsymbol{p}^{\mathrm{I}}}{m}\right]\boldsymbol{\vartheta}^{\mathrm{I}}\end{aligned}\tag{33}$$

where

$$\begin{aligned}\boldsymbol{H}^{\mathrm{I}}&=\operatorname{curl}\boldsymbol{A}^{\mathrm{I}}\\\mathcal{E}^{\mathrm{I}}&=-\operatorname{grad}^{\mathrm{I}}V=-\left(\frac{\partial}{\partial x_1^{\mathrm{I}}},\frac{\partial}{\partial x_2^{\mathrm{I}}},\frac{\partial}{\partial x_3^{\mathrm{I}}}\right)V.\end{aligned}\tag{33'}$$

The term $(\boldsymbol{p}^{\mathrm{I}}\boldsymbol{\vartheta}^{\mathrm{I}})^2(\boldsymbol{p}^{\mathrm{II}}\boldsymbol{\sigma}^{\mathrm{II}})^2$, entering as $(v/c)^4$, we neglect in it A_k and obtain

$$(\boldsymbol{p}^{\mathrm{I}}\boldsymbol{\vartheta}^{\mathrm{I}})^2(\boldsymbol{p}^{\mathrm{II}}\boldsymbol{\vartheta}^{\mathrm{II}})^2=\sum(p_k^{\mathrm{I}})^2\sum(p_k^{\mathrm{II}})^2=(\boldsymbol{p}^{\mathrm{I}})^2(\boldsymbol{p}^{\mathrm{II}})^2\tag{34}$$

Using (26)

$$(\vartheta^{\mathrm{I}}\vartheta^{\mathrm{II}})^2=3-2\,(\vartheta^{\mathrm{I}}\vartheta^{\mathrm{II}}) \tag{35}$$

Substituting (31), (33), (34), (35) into (27) we have

$$\Big\{E-2mc^2+eV-\frac{1}{2m}\Big(1-\frac{E-2mc^2+eV}{2mc^2}\Big)\sum((p_k^{\mathrm{I}})^2+(p_k^{\mathrm{II}})^2)$$
$$+\frac{he}{4\pi mc}[(H^{\mathrm{I}}\vartheta^{\mathrm{I}})+(H^{\mathrm{II}}\vartheta^{\mathrm{II}})]+\frac{ehi}{8\pi m^2c^2}[(\mathcal{E}^{\mathrm{I}}p^{\mathrm{I}})+(\mathcal{E}^{\mathrm{II}}p^{\mathrm{II}})]$$
$$+\frac{he}{8\pi mc^2}\Big(\Big[\mathcal{E}^{\mathrm{I}}\times\frac{p^{\mathrm{I}}}{m}\Big]\vartheta^{\mathrm{I}}+\Big[\mathcal{E}^{\mathrm{II}}\times\frac{p^{\mathrm{II}}}{m}\Big]\vartheta^{\mathrm{II}}\Big)+\frac{e^2}{c^2r}\Big(\frac{p^{\mathrm{I}}}{m}\cdot\frac{p^{\mathrm{II}}}{m}\Big)$$
$$-\Big(\frac{eh}{4\pi mc}\Big)^2\langle(\nabla^{\mathrm{II}}\vartheta^{\mathrm{I}})(\nabla^{\mathrm{I}}\vartheta^{\mathrm{II}})r^{-1}\rangle+\frac{e^2hi}{4\pi m^2c^2}\Big[\Big(\frac{r^{\mathrm{II}}-r^{\mathrm{I}}}{r^3}\cdot p^{\mathrm{I}}\Big)+\Big(\frac{r^{\mathrm{I}}-r^{\mathrm{II}}}{r^3}\cdot p^{\mathrm{II}}\Big)\Big]$$
$$-\frac{e^2h}{4\pi mc^2}\Big(\Big[\frac{r^{\mathrm{II}}-r^{\mathrm{I}}}{r^3}\times\frac{p^{\mathrm{II}}}{m}\Big]\vartheta^{\mathrm{I}}+\Big[\frac{r^{\mathrm{I}}-r^{\mathrm{II}}}{r^3}\times\frac{p^{\mathrm{I}}}{m}\Big]\vartheta^{\mathrm{II}}\Big)-\frac{(p^{\mathrm{I}})^2(p^{\mathrm{II}})^2}{4m^3c^2}$$
$$-\frac{e^4}{4mc^2}\,\frac{3-2(\vartheta^{\mathrm{I}}\vartheta^{\mathrm{II}})}{r^2}\Big\}\psi=0.$$

Solving for $E-2mc^2+eV$

$$\Big\{E-2mc^2+eV-\frac{1}{2m}((p^{\mathrm{I}})^2+(p^{\mathrm{II}})^2)+\frac{(p^{\mathrm{I}})^4+(p^{\mathrm{II}})^4}{8m^3c^2}+\frac{e^2}{r}\Big(\frac{p^{\mathrm{I}}}{mc}\cdot\frac{p^{\mathrm{II}}}{mc}\Big)$$
$$+\frac{he}{4\pi mc}[(H^{\mathrm{I}}\vartheta^{\mathrm{I}})+(H^{\mathrm{II}}\vartheta^{\mathrm{II}})]+\frac{ehi}{8\pi m^2c^2}[(\mathcal{E}^{\mathrm{I}}p^{\mathrm{I}})+(\xi^{\mathrm{II}}p^{\mathrm{II}})+2e\Big(\frac{r^{\mathrm{II}}-r^{\mathrm{I}}}{r^3}\cdot p^{\mathrm{I}}\Big)$$
$$+2e\Big(\frac{r^{\mathrm{I}}-r^{\mathrm{II}}}{r^3}\cdot p^{\mathrm{II}}\Big)\Big]+\frac{he}{8\pi mc^2}\Big(\Big[\mathcal{E}^{\mathrm{I}}\times\frac{p^{\mathrm{I}}}{m}\Big]\vartheta^{\mathrm{I}}+\Big[\mathcal{E}^{\mathrm{II}}\times\frac{p^{\mathrm{II}}}{m}\Big]\vartheta^{\mathrm{II}}$$
$$+2e\Big[\frac{r^{\mathrm{I}}-r^{\mathrm{II}}}{r^3}\times\frac{p^{\mathrm{II}}}{m}\Big]\vartheta^{\mathrm{I}}+2e\Big[\frac{r^{\mathrm{II}}-r^{\mathrm{I}}}{r^3}\times\frac{p^{\mathrm{I}}}{m}\Big]\vartheta^{\mathrm{II}}\Big)$$
$$-\Big(\frac{eh}{4\pi mc}\Big)^2\langle(\nabla^{\mathrm{II}}\vartheta^{\mathrm{I}})(\nabla^{\mathrm{I}}\vartheta^{\mathrm{II}})r^{-1}\rangle-\frac{e^4}{4mc^2}(3-2(\vartheta^{\mathrm{I}}\vartheta^{\mathrm{II}}))r^{-2}\Big\}\psi=0. \tag{36}$$

This is the result of reducing equation (10) with 16 components to equations in the 4 larger components. Comparing this with equation (24) of Heisenberg[7] we see that all of these terms are included in his (24) with the exception of

$$\frac{(p^{\mathrm{I}})^4+(p^{\mathrm{II}})^4}{8m^3c^2}+\frac{e^2}{r}\Big(\frac{p^{\mathrm{I}}}{mc}\cdot\frac{p^{\mathrm{II}}}{mc}\Big)+\frac{ehi}{8\pi m^2c^2}\,[(\mathcal{E}^{\mathrm{I}}p^{\mathrm{I}})+(\mathcal{E}^{\mathrm{II}}p^{\mathrm{II}})+2e\Big(\frac{r^{\mathrm{II}}-r^{\mathrm{I}}}{r^3}\cdot p^{\mathrm{I}}\Big)$$
$$+2e\Big(\frac{r^{\mathrm{I}}-r^{\mathrm{II}}}{r^3}\cdot p^{\mathrm{II}}\Big)-\frac{e^1}{4mc^2}(3-2(\vartheta^{\mathrm{I}}\vartheta^{\mathrm{II}})r^{-2}.$$

[7] Heisenberg, Zeits. f. Physik 39, 499 (1926).

The first of these may be called the relativity correction to the kinetic energy, the second is the magnetic interaction of the orbits, the third is characteristic of using Dirac's equation, has been discussed by Darwin,[8] for a single electron and will be discussed in more detail below; the fourth term may be called a higher order interaction of the spins but as we shall see later enters here with a wrong factor on account of having neglected retardation. In particular we observe that the fine structure of helium should be exactly the same according to (36) and (10) as according to Heisenberg's (24). In making the comparison with Heisenberg it is necessary to remember that our σ_k^{I}, σ_k^{II} are just the negative of Pauli's and that Heisenberg's last term representing the dipole interaction is given in (36) as $-(eh/4\pi mc)^2\langle(\nabla^{\mathrm{II}}\sigma^{\mathrm{I}})(\nabla^{\mathrm{I}}\sigma^{\mathrm{II}})r^{-1}\rangle$.

Reduction of Retarded Equation to Larger Components

We can now perform a similar calculation for the retarded equation (6). The first approximation and therefore (20) remains the same as before. Using (20), (17), (18) in equations which now correspond to (13.1), (13.2), (13.3)

$$\psi_{1,1}=\eta'_{3,3},\ \psi_{2,2}=\eta'_{4,4},\ \psi_{1,2}=\eta'_{3,4},\ \psi_{2,1}=\eta'_{4,3} \tag{37}$$

where

$$\eta'=-(e^2/8mc^2)((\mathfrak{d}^{\mathrm{I}}\mathfrak{d}^{\mathrm{II}})r^{-1}+(\mathfrak{d}^{\mathrm{I}}\mathbf{r})(\mathfrak{d}^{\mathrm{II}}\mathbf{r})r^{-3})\psi+(\mathfrak{p}^{\mathrm{I}}\mathfrak{d}^{\mathrm{I}})(\mathfrak{p}^{\mathrm{II}}\mathfrak{d}^{\mathrm{II}})\psi/4m^2c^2 \tag{38}$$

use being made of equations such as

$$((\mathfrak{a}^{\mathrm{I}}\mathbf{r})(\mathfrak{a}^{\mathrm{II}}\mathbf{r})\psi)_{1,3}=\frac{1}{2mc}((\mathfrak{d}^{\mathrm{I}}\mathbf{r})(\mathfrak{d}^{\mathrm{II}}\mathbf{r})\chi^{\mathrm{II}})_{3,3} \tag{39}$$

which follow on substituting (20) as well as

$$((\mathfrak{a}^{\mathrm{I}}\mathbf{r})(\mathfrak{a}^{\mathrm{II}}\mathbf{r})\psi)_{n,m}=((\mathfrak{d}^{\mathrm{I}}\mathbf{r})(\mathfrak{d}^{\mathrm{II}}\mathbf{r})\psi)_{n,m}\ ;\ (n,m=3 \text{ or } 4). \tag{40}$$

Using these values for (37) the quantities $\psi_{1,3}$, $\psi_{2,3}$ etc. are evaluated to a higher approximation than (20) and analogous to (23). This again is obtained from the equations which now take place of (14) as

$$\psi_{1,3}=p_0^{-1}(\chi^{\mathrm{I}}+\xi'^{\mathrm{I}})_{3,3}\ ;\ \psi_{1,4}=p_0^{-1}(\chi_0{}^{\mathrm{I}}+\xi'^{\mathrm{I}})_{3,4}\ \text{etc.} \tag{41}$$

where

$$\xi'^{\mathrm{I}}=-\frac{e^2}{8mc^2}\left\{(\mathfrak{p}^{\mathrm{II}}\mathfrak{d}^{\mathrm{II}})\left(\frac{(\mathfrak{d}^{\mathrm{I}}\mathfrak{d}^{\mathrm{II}})}{r}+\frac{(\mathfrak{d}^{\mathrm{I}}\mathbf{r})(\mathfrak{d}^{\mathrm{II}}\mathbf{r})}{r^3}\right)+2\left(\frac{(\mathfrak{d}^{\mathrm{I}}\mathfrak{d}^{\mathrm{II}})}{r}+\frac{(\mathfrak{d}^{\mathrm{I}}\mathbf{r})(\mathfrak{d}^{\mathrm{II}}\mathbf{r})}{r^3}\right)(\mathfrak{p}^{\mathrm{II}}\mathfrak{d}^{\mathrm{II}})\right\}\psi$$
$$+\frac{(\mathfrak{p}^{\mathrm{I}}\mathfrak{d}^{\mathrm{I}})(\mathfrak{p}^{\mathrm{II}}\mathfrak{d}^{\mathrm{II}})^2}{4m^2c^2}\psi \tag{42}$$

Putting these values into the modified (15) we have

$$\left\{(p_0-2mc)\psi-(\mathfrak{p}^{\mathrm{I}}\mathfrak{d}^{\mathrm{I}})p_0^{-1}(\chi^{\mathrm{I}}+\xi'^{\mathrm{I}})-(\mathfrak{p}^{\mathrm{II}}\mathfrak{d}^{\mathrm{II}})p_0^{-1}(\chi^{\mathrm{II}}+\xi'^{\mathrm{II}})\right.$$
$$\left.+\frac{e^2}{2c}\left(\frac{(\mathfrak{d}^{\mathrm{I}}\mathfrak{d}^{\mathrm{II}})}{r}+\frac{(\mathfrak{d}^{\mathrm{I}}\mathbf{r})(\mathfrak{d}^{\mathrm{II}}\mathbf{r})}{r^3}\right)\eta\right\}_{\alpha,\beta}=0 \tag{43}$$

[8] C. C. Darwin, Proc. Roy. Soc. **118**, 654 (1928).

where $\alpha, \beta = 3$ or 4. Substituting into this (19), (38), (42) we obtain

$$\Big\{ p_0 - 2mc - (\boldsymbol{p}^{\mathrm{I}}\boldsymbol{\vartheta}^{\mathrm{I}})p_0^{-1}(\boldsymbol{p}^{\mathrm{I}}\boldsymbol{\vartheta}^{\mathrm{I}}) - (\boldsymbol{p}^{\mathrm{II}}\boldsymbol{\vartheta}^{\mathrm{II}})p_0^{-1}(\boldsymbol{p}^{\mathrm{II}}\boldsymbol{\vartheta}^{\mathrm{II}}) + \frac{e^2}{8m^2c^3}\big[(\boldsymbol{p}^{\mathrm{I}}\boldsymbol{\vartheta}^{\mathrm{I}})(\boldsymbol{p}^{\mathrm{II}}\boldsymbol{\vartheta}^{\mathrm{II}})X$$
$$+ (\boldsymbol{p}^{\mathrm{I}}\boldsymbol{\vartheta}^{\mathrm{I}})X(\boldsymbol{p}^{\mathrm{II}}\boldsymbol{\vartheta}^{\mathrm{II}}) + (\boldsymbol{p}^{\mathrm{II}}\boldsymbol{\vartheta}^{\mathrm{II}})X(\boldsymbol{p}^{\mathrm{I}}\boldsymbol{\vartheta}^{\mathrm{I}}) + X(\boldsymbol{p}^{\mathrm{I}}\boldsymbol{\vartheta}^{\mathrm{I}})(\boldsymbol{p}^{\mathrm{II}}\boldsymbol{\vartheta}^{\mathrm{II}})\big]$$
$$- \frac{(\boldsymbol{p}^{\mathrm{I}}\boldsymbol{\vartheta}^{\mathrm{I}})^2(\boldsymbol{p}^{\mathrm{II}}\boldsymbol{\vartheta}^{\mathrm{II}})^2}{4m^3c^3} - \frac{e^4}{16mc^3}X^2\Big\}\psi = 0 \tag{44}$$

where

$$X = \frac{(\boldsymbol{\vartheta}^{\mathrm{I}}\boldsymbol{\vartheta}^{\mathrm{II}})}{r} + \frac{(\boldsymbol{\vartheta}^{\mathrm{I}}\boldsymbol{r})(\boldsymbol{\vartheta}^{\mathrm{II}}\boldsymbol{r})}{r^3}\,. \tag{44'}$$

In addition to (31), (33), (34) we need also the following expressions:

$$(\boldsymbol{p}^{\mathrm{I}}\boldsymbol{\vartheta}^{\mathrm{I}})(\boldsymbol{p}^{\mathrm{II}}\boldsymbol{\vartheta}^{\mathrm{II}})\frac{(\boldsymbol{\vartheta}^{\mathrm{I}}\boldsymbol{r})(\boldsymbol{\vartheta}^{\mathrm{II}}\boldsymbol{r})}{r^3} + (\boldsymbol{p}^{\mathrm{I}}\boldsymbol{\vartheta}^{\mathrm{I}})\frac{(\boldsymbol{\vartheta}^{\mathrm{I}}\boldsymbol{r})(\boldsymbol{\vartheta}^{\mathrm{II}}\boldsymbol{r})}{r^3}(\boldsymbol{p}^{\mathrm{II}}\boldsymbol{\vartheta}^{\mathrm{II}}) + (\boldsymbol{p}^{\mathrm{II}}\boldsymbol{\vartheta}^{\mathrm{II}})\frac{(\boldsymbol{\vartheta}^{\mathrm{I}}\boldsymbol{r})(\boldsymbol{\vartheta}^{\mathrm{II}}\boldsymbol{r})}{r^3}(\boldsymbol{p}^{\mathrm{I}}\boldsymbol{\vartheta}^{\mathrm{I}})$$
$$+ \frac{(\boldsymbol{\vartheta}^{\mathrm{I}}\boldsymbol{r})(\boldsymbol{\vartheta}^{\mathrm{II}}\boldsymbol{r})}{r^3}(\boldsymbol{p}^{\mathrm{I}}\boldsymbol{\vartheta}^{\mathrm{I}})(\boldsymbol{p}^{\mathrm{II}}\boldsymbol{\vartheta}^{\mathrm{II}}) = 4\sum \frac{(x_i^{\mathrm{II}} - x_i^{\mathrm{I}})(x_j^{\mathrm{II}} - x_j^{\mathrm{I}})}{r^3} p_i^{\mathrm{I}} p_j^{\mathrm{II}}$$
$$+ 2(\langle \boldsymbol{p}^{\mathrm{II}} r^{-1}\rangle, \boldsymbol{p}^{\mathrm{II}} - \boldsymbol{p}^{\mathrm{I}}) - 2i\big[\langle \boldsymbol{p}^{\mathrm{II}} r^{-1}\rangle \times \boldsymbol{p}^{\mathrm{I}}\big]\boldsymbol{\vartheta}^{\mathrm{II}} - 2i\big[\langle \boldsymbol{p}^{\mathrm{I}} r^{-1}\rangle \times \boldsymbol{p}^{\mathrm{II}}\big]\boldsymbol{\vartheta}^{\mathrm{I}}$$
$$+ \langle (\boldsymbol{p}^{\mathrm{I}}\boldsymbol{\vartheta}^{\mathrm{II}})(\boldsymbol{p}^{\mathrm{II}}\boldsymbol{\vartheta}^{\mathrm{I}})r^{-1}\rangle \tag{45}*$$

which when combined with (31) gives

$$\frac{e^2}{8m^2c^3}\big[(\boldsymbol{p}^{\mathrm{I}}\boldsymbol{\vartheta}^{\mathrm{I}})(\boldsymbol{p}^{\mathrm{II}}\boldsymbol{\vartheta}^{\mathrm{II}})X + (\boldsymbol{p}^{\mathrm{I}}\boldsymbol{\vartheta}^{\mathrm{I}})X(\boldsymbol{p}^{\mathrm{II}}\boldsymbol{\vartheta}^{\mathrm{II}}) + (\boldsymbol{p}^{\mathrm{II}}\boldsymbol{\vartheta}^{\mathrm{II}})X(\boldsymbol{p}^{\mathrm{I}}\boldsymbol{\vartheta}^{\mathrm{I}}) + X(\boldsymbol{p}^{\mathrm{I}}\boldsymbol{\vartheta}^{\mathrm{I}})(\boldsymbol{p}^{\mathrm{II}}\boldsymbol{\vartheta}^{\mathrm{II}})\big]$$
$$= \frac{e^2}{2m^2c^3}\Big(r^{-1}(\boldsymbol{p}^{\mathrm{I}}\boldsymbol{p}^{\mathrm{II}}) + \sum \frac{(x_i^{\mathrm{II}} - x_i^{\mathrm{I}})(x_j^{\mathrm{II}} - x_j^{\mathrm{I}})}{r^3} p_i^{\mathrm{I}} p_j^{\mathrm{II}}\Big)$$
$$+ \frac{e^2}{4m^2c^3}\langle (\boldsymbol{p}^{\mathrm{II}}\boldsymbol{\vartheta}^{\mathrm{I}})(\boldsymbol{p}^{\mathrm{I}}\boldsymbol{\vartheta}^{\mathrm{II}})r^{-1}\rangle - \frac{e^2 i}{2m^2c^3}\big(\big[\langle \boldsymbol{p}^{\mathrm{I}} r^{-1}\rangle \times \boldsymbol{p}^{\mathrm{II}}\big]\boldsymbol{\vartheta}^{\mathrm{I}}$$
$$+ \big[\langle \boldsymbol{p}^{\mathrm{II}} r^{-1}\rangle \times \boldsymbol{p}^{\mathrm{I}}\big]\boldsymbol{\vartheta}^{\mathrm{II}}\big). \tag{46}$$

It should be noted here for future reference that $(\langle \boldsymbol{p}^{\mathrm{II}} r^{-1}\rangle, \boldsymbol{p}^{\mathrm{II}} - \boldsymbol{p}^{\mathrm{I}})$ *in* (45) *has been cancelled by a similar term in* (31). Using (29) we also have

$$X^2 = \frac{6 - 4(\boldsymbol{\vartheta}^{\mathrm{I}}\boldsymbol{\vartheta}^{\mathrm{II}})}{r^2} + \frac{2(\boldsymbol{\vartheta}^{\mathrm{I}}\boldsymbol{r})(\boldsymbol{\vartheta}^{\mathrm{II}}\boldsymbol{r})}{r^4}\,. \tag{47}$$

Substituting (33), (34), (46) into (44) and solving for $E - 2mc^2 + eV$ as has been done in deriving (36) we have

$$\Big\{ E - 2mc^2 + eV - \frac{1}{2m}((\boldsymbol{p}^{\mathrm{I}})^2 + (\boldsymbol{p}^{\mathrm{II}})^2) + \frac{(\boldsymbol{p}^{\mathrm{I}})^4 + (\boldsymbol{p}^{\mathrm{II}})^4}{8m^3c^2} + \frac{e^2}{2m^2c^2}(r^{-1}(\boldsymbol{p}^{\mathrm{I}}\boldsymbol{p}^{\mathrm{II}})$$
$$+ \sum r^{-3}(x_i^{\mathrm{II}} - x_i^{\mathrm{I}})(x_j^{\mathrm{II}} - x_j^{\mathrm{I}})p_i^{\mathrm{I}} p_j^{\mathrm{II}}) + \frac{he}{4\pi mc}\big[(\boldsymbol{H}^{\mathrm{I}}\boldsymbol{\vartheta}^{\mathrm{I}}) + (\boldsymbol{H}^{\mathrm{II}}\boldsymbol{\vartheta}^{\mathrm{II}})\big]$$

* For derivation see appendix.

$$+\frac{ehi}{8\pi m^2c^2}[(\mathcal{E}^{\mathrm{I}}\boldsymbol{p}^{\mathrm{I}})+(\mathcal{E}^{\mathrm{II}}\boldsymbol{p}^{\mathrm{II}})]+\frac{he}{8\pi mc^2}\left(\left[\mathcal{E}^{\mathrm{I}}\times\frac{\boldsymbol{p}^{\mathrm{I}}}{m}\right]\sigma^{\mathrm{I}}+\left[\mathcal{E}^{\mathrm{II}}\times\frac{\boldsymbol{p}^{\mathrm{II}}}{m}\right]\sigma^{\mathrm{II}}\right.$$
$$\left.+2e\left[\frac{\boldsymbol{r}^{\mathrm{I}}-\boldsymbol{r}^{\mathrm{II}}}{r^3}\times\frac{\boldsymbol{p}^{\mathrm{II}}}{m}\right]\vartheta^{\mathrm{I}}+2e\left[\frac{\boldsymbol{r}^{\mathrm{II}}-\boldsymbol{r}^{\mathrm{I}}}{r^3}\times\frac{\boldsymbol{p}^{\mathrm{I}}}{m}\right]\vartheta^{\mathrm{II}}\right)-\left(\frac{eh}{4\pi mc}\right)^2\langle(\nabla^{\mathrm{II}}\vartheta^{\mathrm{I}})(\nabla^{\mathrm{I}}\vartheta^{\mathrm{II}})r^{-1}\rangle$$
$$\left.-\frac{e^4}{8mc^2}\left(\frac{3-2(\vartheta^{\mathrm{I}}\vartheta^{\mathrm{II}})}{r^2}+\frac{(\vartheta^{\mathrm{I}}\mathrm{r})(\vartheta^{\mathrm{II}}\mathrm{r})}{r^4}\right)\right\}\psi=0. \tag{48}$$

This is the result of reducing equation (6) with 16 components to equations in the four larger components just as (36) is the result of reducing equation (10). This equation (48) is presumably the correct one to use since it has been derived using a correction for retardation in (6). It is further seen that it contains terms

$$(e^2/2m^2c^2)\left[r^{-1}(\boldsymbol{p}^{\mathrm{I}}\boldsymbol{p}^{\mathrm{II}})+\sum_{i,j}r^{-3}(x_i^{\mathrm{II}}-x_i^{\mathrm{I}})(x_j^{\mathrm{II}}-x_j^{\mathrm{I}})p_i^{\mathrm{I}}p_j^{\mathrm{II}}\right]$$

which are the quantum theory analogon of the classical $(e^2/2c^2)[(v^{\mathrm{I}}v^{\mathrm{II}})r^{-1}+(v^{\mathrm{I}}\boldsymbol{r})(v^{\mathrm{II}}\boldsymbol{r})r^{-3}]$. The $e^2hi/4\pi m^2c^2(\boldsymbol{r}(\boldsymbol{p}^{\mathrm{I}}-\boldsymbol{p}^{\mathrm{II}}))$ occurring with $(\mathcal{E}\boldsymbol{p})$ in (36) are absent here. So far as the $(\mathcal{E}\boldsymbol{p})$ combinations go these terms would mean that in an atom with nuclear charge Ze the whole bracket multiplied by $ehi/8\pi m^2c^2$ is

$$((Ze\boldsymbol{r}_{\mathrm{I}}r_{\mathrm{I}}^{-3}-3e^2(\boldsymbol{r}_{\mathrm{I}}-\boldsymbol{r}_{\mathrm{II}}))\boldsymbol{p}^{\mathrm{I}})+((Ze\boldsymbol{r}_{\mathrm{II}}r_{\mathrm{II}}^{-3}-3e^2(\boldsymbol{r}_{\mathrm{II}}-\boldsymbol{r}_{\mathrm{I}})r^{-3})\boldsymbol{p}^{\mathrm{II}})$$

so that if the electron I is far out the effective screened nuclear charge for p^{I} is $Z-3$ instead of $Z-1$. In equation (48) however the effective screened nuclear charge is $Z-1$. This argument is not conclusive because the terms $(\boldsymbol{r}r^{-3}(\boldsymbol{p}^{\mathrm{I}}-\boldsymbol{p}^{\mathrm{II}}))$ can be absorbed in $e^2/rm^2c^2)(\boldsymbol{p}^{\mathrm{I}}\boldsymbol{p}^{\mathrm{II}})$ provided this is changed into $(e^2/2m^2c^2)(p^{\mathrm{I}}r^{-1}p^{\mathrm{II}}+p^{\mathrm{II}}r^{-1}p^{\mathrm{I}})$. The question cannot be decided unless it is possible to know[9] in what order the factors p^{I}, p^{II}, r^{-1} correspond to the classical $v^{\mathrm{I}}v^{\mathrm{II}}/r$. In (48) the order of factors in corresponding expressions is readily verified to be immaterial.

Quite unambiguously we can see, however from the fact that (36) does not contain the combination

$$r^{-1}(\boldsymbol{p}^{\mathrm{I}}\boldsymbol{p}^{\mathrm{II}})+\sum_{i\neq j}r^{-3}(x_i^{\mathrm{II}}-x_i^{\mathrm{I}})(x_j^{\mathrm{II}}-x_j^{\mathrm{I}})p_i^{\mathrm{I}}p_j^{\mathrm{II}}$$

that it cannot be a correct result. We must require that for cases where the effects of spins are negligible the result should agree with Darwin's (5). This is the case for (48) and not for (36) and therefore (48) rather than (36) is the correct equation. A generalization to the cases of particles of unequal mass can easily be made. The result is

$$\left\{E-(m_{\mathrm{I}}+m_{\mathrm{II}})c^2+eV-(\boldsymbol{p}_{\mathrm{I}}^2/2m_{\mathrm{I}})-(\boldsymbol{p}_{\mathrm{II}}^2/2m_{\mathrm{II}})+(\boldsymbol{p}_{\mathrm{I}}^4/8m_{\mathrm{I}}^3c^2)+(\boldsymbol{p}_{\mathrm{II}}^4/8m_{\mathrm{II}}^3c^2)\right.$$

[9] According to Jordan and Klein [Zeits. f. Physik **45**, 751 (1927)] the order $\frac{1}{2}(p^{\mathrm{I}}r^{-1}p^{\mathrm{II}}+p^{\mathrm{II}}r^{-1}p^{\mathrm{I}})$ is the correct one to use. This is in agreement with the results below.

$$+(e^2/2m_{\rm I}m_{\rm II}c^2)\left[(\boldsymbol{p}^{\rm I}\boldsymbol{p}^{\rm II})r^{-1}+\sum_{i,j}r^{-3}(x_i^{\rm II}-x_i^{\rm I})(x_j^{\rm II}-x_j^{\rm I})p_i^{\rm I}p_j^{\rm II}\right]$$

$$+(he/4\pi c)\left[(\boldsymbol{H}^{\rm I}\sigma^{\rm I})m_{\rm I}^{-1}+(\boldsymbol{H}^{\rm II}\sigma^{\rm II})m_{\rm II}^{-1}\right]+(ehi/8\pi c^2)\left[(\mathcal{E}^{\rm I}\boldsymbol{p}^{\rm I})m_{\rm I}^{-2}+(\mathcal{E}^{\rm II}\boldsymbol{p}^{\rm II})m_{\rm II}^{-2}\right.$$

$$+(he/8\pi c^2)(m_{\rm I}^{-2}[\mathcal{E}^{\rm I}\times\boldsymbol{p}^{\rm I}]\sigma^{\rm I}+m_{\rm II}^{-2}[\mathcal{E}^{\rm II}\times\boldsymbol{p}^{\rm II}]\sigma^{\rm II}+2(m_{\rm I}m_{\rm II}r^3)^{-1}\{[(\boldsymbol{r}^{\rm I}-\boldsymbol{r}^{\rm II})$$

$$\left.\times\boldsymbol{p}^{\rm II}]\sigma^{\rm I}+[(\boldsymbol{r}^{\rm II}-\boldsymbol{r}^{\rm I})\times\boldsymbol{p}^{\rm I}]\sigma^{\rm II}\}\right)-(eh/4\pi c)^2(m_{\rm I}m_{\rm II})^{-1}\langle(\nabla^{\rm II}\sigma^{\rm I})(\nabla^{\rm I}\sigma^{\rm II})r^{-1}\rangle$$

$$-(e^4/4(m_{\rm I}+m_{\rm II})c^2)\left[(3-2(\sigma^{\rm I}\sigma^{\rm II}))r^{-2}+(\sigma^{\rm I}\boldsymbol{r})(\sigma^{\rm II}\boldsymbol{r})r^{-4}\right]\Big\}\psi=0. \qquad (48')$$

For $m_{\rm II}=\infty$ this degenerates into the equation for a single electron.

Derivation by Heisenberg-Pauli Theory of Wave Fields

We use the results of Heisenberg and Pauli in the form of their equations (109), (110)

$$-E^{(2)}=\sum_{st,r\lambda}{}'e^2h/4\pi)(E_s-E_t+h\nu_{r\lambda})^{-1}(N_s{}^0+1)N_t{}^0(d_{st}{}^{r\lambda}-ic_{st}{}^{r\lambda})(d_{ts}{}^{r\lambda}+ic_{ts}{}^{r\lambda})$$
$$+\sum_{st,r\lambda}(e^2/4\pi\nu_{r\lambda})N_s{}^0(d_{ss}{}^{r\lambda}+ic_{ss}{}^{r\lambda})N_t{}^0(d_{tt}{}^{r\lambda}+ic_{tt}{}^{r\lambda}) \qquad (109\ H.P.)$$

applying to the case of Einstein-Bose statistics for matter and for our purpose an equivalent expression for the case of matter obeying the exclusion principle. Here E_s, E_t are possible energy values of a single unperturbed electron neglecting therefore its interaction with other electrons. The system consists initially of $N_s{}^0$ electrons in state s, $N_t{}^0$ electrons in state t and no light quanta. On account of interactions between matter and radiation light quanta appear. Their frequency is $\nu_{r\lambda}$ where r refers to a particular set of vibrations in Jean's cube and $\lambda=1, 2, 3, 4$. For the reasons which make it necessary to introduce the index λ the reader must be referred to the paper of Heisenberg and Pauli. We use the notation

$$c_{st}{}^{r\lambda}=\int u_\rho{}^{*s}\alpha_{\rho\sigma}{}^i u_\sigma{}^t v_i{}^{r\lambda}dV$$

$$d_{st}{}^{r\lambda}=\int u_\rho{}^{*s}u_\rho{}^t v_0{}^{r\lambda}dV \qquad (101\ H.P.)$$

$$\phi_i=Q^{r\lambda}v_i{}^{r\lambda},\quad \phi_0=P^{r\lambda}v_0{}^{r\lambda} \qquad (97\ H.P.)$$

meaning by $u_\rho{}^s$, the proper functions of Dirac's equation corresponding to E_s. Also letting κ_r, λ_r, μ_r be integers ϕ_0 the scalar potential ϕ_i/c $(i=1, 2, 3)$ the vector potential

$$\phi_1=(8/L^3)^{1/2}q_1{}^r\cos\pi L^{-1}\kappa_r x\sin\pi L^{-1}\lambda_r y\sin\pi L^{-1}\mu_r z$$
$$\phi_0=(8/L^3)^{1/2}q_0{}^r\sin\pi L^{-1}\kappa_r x\sin\pi L^{-1}\lambda_r y\sin\pi L^{-1}\mu_r z \qquad (84\ H.P.)$$
$$2L\nu_r=c\nu_r{}';\ \nu_r{}^{12}{}_{,1}=\kappa_r{}^2+\lambda_r{}^2+\mu_r{}^2;\ \nu_{r,0}{}'^2(\epsilon+\delta)=\epsilon(1-\delta)\nu_{r,1}{}'^2.$$

In these formulas the integers κ, λ, μ determine the modes of vibration of Jean's cube, ϵ and δ are small constants which are made zero in the limit. They evaluate in their (116)

$$-\sum(2\pi\nu_{r\lambda})^{-1}d_{st}{}^{r\lambda}{}_{nm}=\int r^{-1}{}_{P,P'}u_p{}^{*s}(P)u_p{}^{t}(P)u_\sigma{}^{*n}(P')u_\sigma{}^{m}(P')dVdV'$$

$r_{p,p'}$ being the distance between the point $P=(x, y, z)$ and $P'=(x', y', z')$. Whenever the same dummy suffix occurs twice a summation is performed with respect to it. They have also shown that to within the approximation in which $E_s-E_t+h\nu_{r\lambda}$ can be replaced by $h\nu_{r\lambda}$ the cross product terms $d_{st}c_{ts}$ contribute nothing and that the terms $c_{st}c_{ts}$ give a term in

$$\int r^{-1}{}_{pp'}u_p{}^{*s}(P)\alpha^i{}_{p\sigma}u_\sigma{}^{t}(P)\cdot u_\mu{}^{*t}(P')\alpha^i{}_{\mu\nu}u_\nu{}^{s}(P')dVdV'.$$

These two terms due to $d_{st}d_{ts}$ and $c_{st}c_{ts}$ give as a result equation (10) which we have used to deduce (36).

The way to get corrections for retardation is indicated also in their paper. They state that the difference between $(E_s-E_t+h\nu_{r\lambda})^{-1}$ and $(h\nu_{r\lambda})^{-1}$ gives these corrections.

Since the $c_{st}c_{ts}$ terms contribute results involving products of two α's their effects are of terms in $(v/c)^2$. For the purpose of this paper we want only an approximation to this order $(v/c)^2$. It is sufficient therefore to consider in $c_{st}c_{ts}$ the first approximation to $(E_s-E_t+h\nu_{r\lambda})^{-1}=(h\nu_{r\lambda})^{-1}$. The $d_{st}d_{ts}$ terms, however, are of order 1. For them we must expand $(E_s-E_t+h\nu_{r\lambda})^{-1}$. Now their (112) is replaced by

$$\sum_{r\lambda}((h\nu_{r\lambda})^{-1}+(E_t-E_s)(h\nu_{r\lambda})^{-2}+(E_t-E_s)^2(h\nu_{r\lambda})^{-3})d_{st}d_{ts}. \tag{49}$$

The evaluation of the first term of this is performed by them by letting

$$\sum_{r\lambda}\nu_{r\lambda}{}^{-1}v_0{}^{r\lambda}(P)v_0{}^{r\lambda}(P')=G(P,P')$$

and then showing that for $\delta\to 0$

$$\Delta_P G(P,P')=64\pi^2L^{-3}\sum_r \sin\pi L^{-1}H_r x\sin\pi L^{-1}\lambda_r y\sin\pi L^{-1}\mu_r z$$

$$\sin\pi L^{-1}H_r x'\sin\pi L^{-1}\lambda_r y'\sin\pi L^{-1}\mu_r z'=8\pi^2\delta(P-P')\ (114)(H.P)$$

whence it is deduced that

$$G(P,P')=-2\pi r^{-1}{}_{PP'}. \tag{115}(H.P.)$$

For reasons which will be seen presently it is more advisable for us to perform here a direct calculation. We let $L\to\infty$. In the limit we can then replace summations by integrals. In order to be dealing with free particles we must simultaneously remove them from the walls of the enclosure. Thus we also increase x, y, z keeping $x-L/2, y-L/2, z-L/2$ constant. Under these conditions the walls of the enclosure recede from the particles to infinity and the coordinates of the particles with respect to the center of the enclosure are kept constant. We have then

$$G(P,P')=-(64/\pi)\int_0^\infty\int_0^\infty\int_0^\infty(\omega_1^2+\omega_2^2+\omega_3^2)^{-1}\sin\omega_1x\sin\omega_2y\sin\omega_3z$$
$$\sin\omega_1x'\sin\omega_2y'\sin\omega_3z'd\omega_1d\omega_2d\omega_3. \quad (50)$$

The product of sines in the integral can be combined into a sum of eight products of which (1/8) $\cos\omega_1(x-x')\cos\omega_2(y-y')\cos\omega_3(z-z')$ is the only one of importance. The others contain one or more factors of the type $\cos\omega_1(x+x')$. These considered as functions of ω alternate very rapidly because $x+x'\cong L$. The contribution of these other terms is therefore negligible. We have further

$$4\cos\omega_1X\cos\omega_2Y\cos\omega_3Z=\cos(\omega_1X+\omega_2Y+\omega_3Z)+\cos(-\omega_1X+\omega_2Y+\omega_3Z)$$
$$+\cos(\omega_1X-\omega_2Y+\omega_3Z)+\cos(\omega_1X+\omega_2Y-\omega_3Z). \quad (50')$$

In using integrals such as (50) we are concerned therefore with

$$\int_0^\infty\int_0^\infty\int_0^\infty f(\omega_1^2+\omega_2^2+\omega_3^2)\cos\omega_1X\cos\omega_2Y\cos\omega_3Zd\omega_1d\omega_2d\omega_3$$
$$=\frac{1}{8}\int_{-\infty}^{+\infty}\int_{-\infty}^{+\infty}\int_{-\infty}^{+\infty}f(\omega_1^2+\omega_2^2+\omega_3^2)\cos(\omega_1X+\omega_2Y+\omega_3Z)d\omega_1d\omega_2d\omega_3 \quad (51)$$

by (50′). Since the last integral extends over all the space ω it can be written

$$\frac{1}{8}\int_{-\infty}^{+\infty}\int\int {}^{2}{}_{1}\omega)f+\omega_2^2+\omega_3^2)\cos(\omega_1R)d\omega_1d\omega_2d\omega_3\ ;\ R^2=X^2+Y^2+Z^2 \quad (51')$$

Substituting these values into (50) we have

$$G(P,P')=-(1/\pi)\int_\omega f(\omega_1^2+\omega_2^2+\omega_3^2)\cos(\omega_1R)d\omega_1d\omega_2d\omega_3. \quad (52)$$

For the three terms in (49) in the case of $\epsilon=-1$ (this procedure is justified at the end of the paper) we need to evaluate this expression with $f=\Omega^{-2}$, Ω^{-3}, Ω^{-4} where $\Omega^2=\omega_1^2+\omega_2^2+\omega_3^2$. We have

$$\int_\omega\Omega^{-2}\cos(\omega_1R)d\omega_1d\omega_2d\omega_3=2\pi^2/R \quad (53)$$

$$\int_\omega\Omega^{-4}[\cos(\omega_1R)-1]d\omega_1d\omega_2d\omega_3=-\pi^2R \quad (54)$$

$$\int_\omega\Omega^{-3}[\cos(\omega_1R)-1]d\omega_1d\omega_2d\omega_3=\text{const.} \quad (55)$$

By means of (53), (50)

$$G(P,P')=-2\pi/R \quad (57)$$

which is (115) of *H. P.*

Next in (52) we replace the summation by the first term corresponding to (57). With this understanding we have:

$$\sum_{s,t,r,\lambda} (e^2h/4\pi)(E_s-E_t)^2 d_{st}{}^{r\lambda} d_{ts}{}^{r\lambda} (h\nu_{r\lambda})^{-3} =$$

$$(e^2/4\pi h^2) \int\int u_\rho{}^{*s}(P) u_\rho{}^t(P) u_\sigma{}^{*t}(P') u_\sigma{}^s(P') \sum_{r,\lambda} (\nu_{r\lambda})^{-3} v_0{}^{r\lambda}(P) v_0{}^{r\lambda}(P') (E_s-E_t)^2 dV dV'$$

Writing

$$F(P,P') = \sum_{r,\lambda} \nu_{r\lambda}^{-3} v_0{}^{r\lambda}(P) v_0{}^{r\lambda}(P') \tag{58}$$

we find

$$F(P,P') = -4\pi c^{-2} \int_\omega \Omega^{-4} (\cos(\omega_1 R) - 1) d\omega_1 d\omega_2 d\omega_3 = 4\pi^3 c^{-2} R \tag{59}$$

where (55) has been applied and 1 has been subtracted from $\cos \omega_1 R$. This amounts to adding and subtracting in the integrand Ω^{-4} four times. The result is unchanged because as we shall see an additive constant in (59) has no effect. Thus:

$$\sum_{s,t,r,\lambda} (e^2h/4\pi)(h\nu_{r\lambda})^{-3} (E_s-E_t)^2 d_{st}{}^{r\lambda} d_{ts}{}^{r\lambda}$$

$$= \pi^2 e^2 h^{-2} \sum_{s,t} \int\int (E_s-E_t)^2 c^{-2} R u_\rho{}^{*s} u_\rho{}^t (u_\sigma{}^{*t} u_\sigma{}^s)' dV dV'. \tag{60}$$

Using (1) we have:

$$\frac{1}{c}(E_t + eA_0) u_\rho{}^t + \sum_{k=1,2,3} \left(\frac{h}{2\pi i} \frac{\partial}{\partial x_k} + \frac{e}{c} A_k \right) \alpha_{\rho\tau}{}^k u_\tau{}^t + mc\alpha_{\rho\tau}{}^4 u_\tau{}^t = 0$$

$$\frac{1}{c}(E_s + eA_0) u_\rho{}^{*s} + \sum_{k=1,2,3} \left(-\frac{h}{2\pi i} \frac{\partial}{\partial x_k} + \frac{e}{c} A_k \right) u_\tau{}^{*s} \alpha_{\tau\rho}{}^k + mc u_\tau{}^{*s} \alpha_{\tau\rho}{}^4 = 0.$$

Multiplying the first of these by $u_\rho{}^{*s}$, the second by $u_\rho{}^t$ and subtracting we have:

$$\frac{1}{c}(E_t - E_s) u_\rho{}^{*s} u_\rho{}^t + \sum_k \frac{h}{2\pi i} \left(u_\rho{}^{*s} \alpha_{\rho\tau}{}^k \frac{\partial u_\tau{}^t}{\partial x_k} + \frac{\partial (u_\tau{}^{*s} \alpha_{\tau\rho}{}^k)}{\partial x_k} u_\rho{}^t \right) = 0$$

which may be written on summation as

$$\frac{1}{c}(E_t - E_s) u_\rho{}^{*s} u_\rho{}^t + \sum_k \frac{h}{2\pi i} \frac{\partial}{\partial x_k} (u_\rho{}^{*s} \alpha_{\rho\tau}{}^k u_\tau{}^t) = 0 \tag{61}$$

analogously to the conservation theorem being in fact that theorem for the part of the current four vector due to cross product terms of states t, s. Formula (61) shows that an additive constant in (59) can contribute nothing since it disappears on partial integration. Similarly it shows using (55) that

the second term in (49) contributes nothing. Substituting (61) into (60) we have

$$\sum_{s,t,r,\lambda} \frac{e^2h}{4\pi} \frac{(E_s-E_t)^2}{(h\nu_{r\lambda})^2} d_{st}{}^{r\lambda} d_{ts}{}^{r\lambda} = \frac{e^2}{4} \int r_{pp'} \frac{\partial(u_\rho{}^{*s}\alpha_{\rho\tau}{}^k u_\tau{}^t)}{\partial x_k} \frac{\partial(u_\sigma{}'^{*t}\alpha^l{}_{\sigma\kappa} u_\kappa{}'^s)}{\partial x_l'} dVdV'.$$

Combining this with

$$(e^2h/4\pi) \sum_{r,\lambda} (h\nu_{r\lambda})^{-1} d_{st}{}^{r\lambda} d_{ts}{}^{r\lambda} = -(e^2/2) \int r^{-1}{}_{pp'} u_\rho{}^{*s} u_\rho{}^t u_\sigma{}'^{*t} u_\sigma{}'^s dVdV'$$

and

$$(e^2h/4\pi) \sum_{r,0} (h\nu_{r\lambda})^{-1} c_{st}{}^{r\lambda} c_{ts}{}^{r\lambda} = \frac{e^2}{2} \int r^{-1}{}_{pp'} u_\rho{}^{*s} \alpha_{p\sigma}{}^i u_\sigma{}^t (u_\mu{}^{*t} \alpha_{\mu\nu}{}^i u_\nu{}^s)' dVdV'$$

so that (118) and (119) of *H. P.* is still true but corresponds now to

$$\begin{aligned} A_{st,ts} = \int r^{-1}{}_{pp'} \Big\{ & u_\rho{}^{*s} u_\rho{}^t (u_\sigma{}^{*t} u_\sigma{}^s)' - u_\rho{}^{*s} \alpha_{p\sigma}{}^i u_\sigma{}^t (u_\mu{}^{*t} \alpha_{\mu\nu}{}^i u_\nu{}^s)' \\ & - (1/2) \sum_{k,l=1,2,3} \frac{\partial(u_\rho{}^{*s}\alpha_{\rho\tau}{}^k u_\tau{}^t)}{\partial x_k} \frac{\partial(u_\mu{}^{*t}\alpha_{\mu\nu}{}^l u_\nu{}^s)'}{\partial x_l'} \Big\} dVdV' \\ = \int \Big\{ & r_{PP'}{}^{-1} u_\rho{}^{*s} u_\rho{}^t (u_\sigma{}^{*t} u_\sigma{}^s)' - \frac{1}{2} \Big(\frac{\delta_{lk}}{r_{PP'}} \\ & + \sum_{k,l} \frac{(x_k - x_k')(x_l - x_l')}{r_{PP'}} \Big) u_\rho{}^{*s} \alpha_{\rho\tau}{}^k u_\tau{}^t (u_\mu{}^{*t} \alpha_{\mu\nu}{}^l u_\nu{}^s)' \Big\} dVdV' \qquad (62) \end{aligned}$$

We have performed here two partial integrations and also used the fact that terms due to retardation contribute nothing to $A_{ss,tt}$. By an accent put over a parenthesis we mean that the parenthesis is to be evaluated at (x', y', z').

This result (62) means that the interaction energy in the configuration space is of the form used in (6) since that form according to ordinary quantum mechanics gives as a first approximation to the interaction energy the expression (62). The method of approximations used gives so far only the first approximation in the Coulomb interaction between the electrons. It does not necessarily follow therefore that (6) is correct to within all terms in $(v/c)^2$. But if we combine this derivation with the arguments given in the first section it seems at least very likely that (6) is the correct equation.

It is satisfying to note that just as Darwin's form (5) takes into account retardation by considering second order corrections to the electrostatic potential so our retarded equation owes its retarded terms to the third member of (49). The first order correction vanished both in Darwin's classical calculation and here.

The equation (6) and its reduced form (48) differs, as stated before, from (10) and (36) by the presence of $-e^4(8mc^2)^{-1}(\mathfrak{d}^{\mathrm{I}}\mathbf{r})(\mathfrak{d}^{\mathrm{II}}\mathbf{r})r^{-4}$ which should affect the fine structure of orthohelium. In order to see its effect it is convenient to combine it with the term just preceding it which represents dipole interaction. These two terms together contribute to the energy the amount:

$$\mu^2\left[\frac{(\vartheta^{\mathrm{I}}\vartheta^{\mathrm{II}})}{r^3}+\left(-\frac{3}{r^5}+\frac{2\pi^2e^2m}{h^2r^4}\right)(\vartheta^{\mathrm{I}}r)(\vartheta^{\mathrm{II}}r)\right] \text{ where } \mu=\frac{eh}{4\pi mc}\cdot$$

Only the second part of this expression contributes to the fine structure on account of the presence of $(\vartheta^{\mathrm{I}}r)(\vartheta^{\mathrm{II}}r)$. Retardation makes itself felt here through the term in r^{-4}. Its effect is seen to decrease the influence of the ordinary dipole interaction. For helium in the 2^3P state the retardation term is roughly 1/3 of the dipole term.

A preliminary calculation of the orthohelium fine structure using an equation equivalent to (36) has been made by Heisenberg[7]. Recently an attempt to refine Heisenberg's calculations has been made by Gaunt[6]. Gaunt also uses an equation similar to (36). It is clear from Gaunt's calculation that the result is uncertain on account of not knowing a sufficiently good approximation for the proper functions of the 2^3P state of helium. Preliminary calculations of the new term in (48) show it is not in contradiction with experimental values for it improves Gaunt's present result. It is premature, however, to claim agreement with experiment before the proper functions of the 2^3P state are worked out and the perturbation calculation for the fine structure is made with them in such a way as to be sure about the accuracy of the result.

All the terms in (48) with the exception of the last one due to retardation in the action of the electrostatic potential can be interpreted physically in terms of the spin model and in fact have been written down and used by Heisenberg before the discovery of the Dirac equation. The effect of retardation is to introduce interactions which have no simple explanation in terms of the spin. Since Dirac's equation is based on much more solid ground than the spin model the new terms have in all probability a physical existence. In the case of electrons they would be expected to be capable of experimental detection only in the spectra of elements of low atomic number. There is also a possibility of testing the formula on the fine structure of band spectra[10]. If Dirac's equation applies to protons it may also be possible to test the existence of the new terms in such cases as radiation probabilities of ortho and parahydrogen. If we are interested in higher approximations than $(v/c)^2$ it is more convenient not to use the expansion (49) but to consider pairs of terms

$$N_t^0N_s^0(E_s-E_t+h\nu_{r\lambda})^{-1}(d_{st}^{r\lambda}-ic_{st}^{r\lambda})(d_{ts}^{r\lambda}+ic_{ts}^{r\lambda})$$
$$+N_s^0N_t^0(E_t-E_s+h\nu_{r\lambda})^{-1}(d_{ts}^{r\lambda}-ic_{ts}^{r\lambda})(d_{st}^{r\lambda}+ic_{st}^{r\lambda}).$$

The evaluation of this expression is laborious and need not be given in detail here. For the limit $\delta=0$ we find for instance

$$-(e^2h/4\pi)\sum_{r\lambda}N_s^0N_t^0[d_{st}^{r\lambda}d_{ts}^{s\lambda}(E_s-E_t+h\nu_{r\lambda})^{-1}+d_{ts}^{r\lambda}d_{st}^{r\lambda}(E_t-E_s+h\nu_{r\lambda})^{-1}]$$
$$=e^2\int u^{*s}u^t\{\cos(2\pi r_{pp'}/\lambda_{st})$$
$$-(1/2)(1+\epsilon^{-1})(2\pi r_{pp'}/\lambda_{st})\sin(2\pi r_{pp'}/\lambda_{st})(1/r_{pp'})(u^{*t}u^s)'dVdV'$$

[10] H. A. Kramers, Zeits. f. Physik 53, 422 (1929).

where

$$\lambda_{st}=ch/\left|E_s-E_t\right|.$$

Applying the conservation of charge (61) we get for the second part of the integral and similar expressions for the $d^{r\lambda}_{st}c^{r\lambda}_{ls}-d^{r\lambda}_{ls}c^{r\lambda}_{st}$ as well as $c^{r\lambda}_{st}c^{r\lambda}_{ls}$ contribu-

$$-(e^2/2)(1+\epsilon^{-1})\int\frac{\partial(u^{*s}\alpha^i u^t)}{\partial x^i}\left(\sin\frac{2\pi r_{PP'}}{\lambda_{st}}\right)\left(\frac{2\pi r_{PP'}}{\lambda_{st}}\right)^{-1}\frac{\partial(u^{*t}\alpha^k u^s)'}{\partial x_k'}dVdV'$$

tions to the interaction energy. The first of these contributes only terms in $1+\epsilon^{-1}$ while the last gives $(u^{*s}\alpha^i u^t)(1/r_{pp'})\cos(2\pi r_{pp'}/\lambda_{st})(u^{*t}\alpha^i u^s)'$ combinations as well. On adding all the terms it is found that $1+\epsilon^{-1}$ disappears on using (61) and partial integration. The terms independent of ϵ combine into

$$\begin{aligned}A_{st,ts}=\int&(u_p^{*s}u_s^t\{1/r_{PP'}\}(u_\sigma^{*t}u_\sigma^s)'\\&-u_p^{*s}\alpha_{p\sigma}{}^i u_\sigma^t\{1/r_{PP'}\}(u_\mu^{*t}\alpha_{\mu\nu}{}^i u_\nu^s)')dVdV'\end{aligned}\tag{63}$$

where

$$\{1/r_{PP'})\}=(1/r_{PP'})\cos(2\pi r_{PP'}/\lambda_{st})$$

may be said to be the retarded value of $1/r_{pp'}$ for the transition (st).

The calculations can be shortened by observing to start with that all terms in $1+\epsilon^{-1}$ must disappear since otherwise the interaction energy would become infinite for $\epsilon=0$. This means that at this stage of the calculation we may work with $\epsilon=-1$. The calculation then becomes quite short.

This short cut is a close equivalent of the procedure followed in classical electrodynamics in deriving the retarded potentials. The non quantized field equations of Heisenberg and Pauli can be solved as a sum of two parts provided conservation of charge holds. The first part is given by the usual retarded potentials in the form of the well known integrals. On account of the conservation of charge these integrals cause the coefficient of $1+\epsilon^{-1}$ to disappear and can therefore be calculated as though ϵ were -1. It is these retarded potentials that determine the interaction between particles. The other part of the general solution depends on ϵ and is obtained by solving the field equations as though the current s_α were 0. In the classical theory this part of the solution has nothing to do with the interaction. The disappearance of ϵ is thus entirely due to the conservation of charge both in the quantized and classical field equations.

In (63) the phase under the cosine is that which would exist for light waves of wave-length λ_{st}

$$\lambda_{st}=ch/\left|E_s-E_t\right|\tag{64}$$

corresponding to emissions and absorptions between states s and t.

The correction which we have used in (6) is from this point of view due to the second term in the expansion $\cos x=1-x^2/2$ of the phase factor. We expect the correction to apply therefore only for small values of $r_{pp'}/\lambda_{st}$.

Appendix. Derivation of (45)

We let $y_i=(x_i^{II}-x^I{}_i)/r^{3/2}$ and expand as follows:

$$\frac{(\mathfrak{d}^I\boldsymbol{r})(\mathfrak{d}^{II}\boldsymbol{r})}{r^3}(\boldsymbol{p}^I\mathfrak{d}^I)(\boldsymbol{p}^{II}\mathfrak{d}^{II})+(\boldsymbol{p}^I\mathfrak{d}^I)(\boldsymbol{p}^{II}\mathfrak{d}^{II})\frac{(\mathfrak{d}^I\boldsymbol{r})(\mathfrak{d}^{II}\boldsymbol{r})}{r^3}$$

$$+(\boldsymbol{p}^I\mathfrak{d}^I)\frac{(\mathfrak{d}^I\boldsymbol{r})(\mathfrak{d}^{II}\boldsymbol{r})}{r^3}(\boldsymbol{p}^{II}\mathfrak{d}^{II})+(\boldsymbol{p}^{II}\mathfrak{d}^{II})\frac{(\mathfrak{d}^I\boldsymbol{r})(\mathfrak{d}^{II}\boldsymbol{r})}{r^3}(\boldsymbol{p}^I\mathfrak{d}^I)$$

$$=\sum(\sigma_i^I\sigma_j^{II}\sigma_k^I\sigma_l^{II}y_iy_jp_k^Ip_l^{II}+\sigma_k^I\sigma_l^{II}\sigma_i^I\sigma_j^{II}p_k^Ip_l^{II}y_iy_j+\sigma_k^I\sigma_i^I\sigma_j^{II}\sigma_l^{II}p_k^Iy_iy_jp_l^{II}$$

$$+\sigma_i^{II}\sigma_i^I\sigma_j^{II}\sigma_k^Ip_l^{II}y_iy_jp_k^I)=A+B+C+D \text{ where using (26)}$$

$$A=\sum_{i=k,j=l}\ \sum_{i,j}(y_iy_jp_i^Ip_j^{II}+p_i^Ip_j^{II}y_iy_j+p_i^Iy_iy_jp_j^{II}+p_j^{II}y_iy_jp_i^I)$$

$$B=\sum_{i=k,j\neq l}\ \sum_{i,j\neq l}\sigma_j^{II}\sigma_l^{II}(y_iy_jp_i^Ip_l^{II}-p_i^Ip_l^{II}y_iy_j+p_i^Iy_iy_jp_l^{II}-p_l^{II}y_iy_jp_i^I)$$

$$C=\sum_{i\neq k,j=l}=\sum_{j,i\neq k}\sigma_i^I\sigma_k^I(y_iy_jp_k^Ip_j^{II}-p_k^Ip_j^{II}y_iy_j-p_k^Iy_iy_jp_j^{II}+p_j^{II}y_iy_jp_k^I)$$

$$D=\sum_{i\neq k,j\neq l}=\sum_{i\neq k,j\neq l}\sigma_i^I\sigma_k^I\sigma_j^{II}\sigma_l^{II}(y_iy_jp_k^Ip_l^{II}+p_k^Ip_l^{II}y_iy_j-p_k^Iy_iy_jp_l^{II}-p_l^{II}y_iy_jp_k^I)$$

On carrying out the differentiations $p_i^Ip_j^{II}$

$$A=\sum_{i,j}(4y_iy_jp_i^Ip_j^{II}+2\{p_i^Iy_iy_j\}p_j^{II}+2\{p_j^{II}y_iy_j\}p_i^I+\{p_i^Ip_j^{II}y_iy_j\})$$

$$B=-\sum_{i,j\neq l}\sigma_j^{II}\sigma_l^{II}(2\{p_l^{II}y_iy_j\}p_i^I+\{p_i^Ip_l^{II}y_iy_j\})$$

$$C=-\sum_{j,i\neq k}\sigma_i^I\sigma_k^I(2\{p_k^Iy_iy_j\}p_j^{II}+\{p_k^Ip_j^{II}y_iy_j\})$$

$$D=\sum_{i\neq k,j\neq l}\sigma_i^I\sigma_k^I\sigma_j^{II}\sigma_l^{II}\{p_k^Ip_l^{II}y_iy_j\}$$

Using the value $y_i=(x_i^{II}-x_i^I)/r^{3/2}$ we have

$$\sum_{i,j}\{p_i^Ip_j^{II}y_iy_j\}=\sum_{i,j\neq l}\{p_i^Ip_l^{II}y_iy_j\}\sigma_j^{II}\sigma_l^{II}=\sum_{j,i\neq k}\{p_k^Ip_j^{II}y_iy_j\}\sigma_i^I\sigma_k^I=0$$

$$D=\sum_{i,i+l}\{(\boldsymbol{p}^I\mathfrak{d}^{II})(\boldsymbol{p}^{II}\mathfrak{d}^I)r^{-1}\}-2\sum_{i,j\neq l}\sigma_j^{II}\sigma_l^{II}\{p_l^{II}y_iy_j\}p_i^I=-2i[\{\boldsymbol{p}^{II}r^{-1}\}\times\boldsymbol{p}^I]\mathfrak{d}^{II}-2\sum_{j,i\neq k}\sigma_i^I\sigma_k^I\{p_k^Iy_iy_j\}p_j^{II}$$

$$=-2i[\{\boldsymbol{p}^Ir^{-1}\}\times\boldsymbol{p}^{II}]\mathfrak{d}^I$$

$$2\sum_{i,j}(\{p_i^Iy_iy_j\}p_j^{II}+\{p_j^{II}y_iy_j\}p_i^I)=2(\{\boldsymbol{p}^{II}r^-\}\cdot(\boldsymbol{p}^{II}-\boldsymbol{p}^I)).$$

Substituting these values into A, B, C, D and forming $A+B+C+D$ we get (45).

THE SATELLITES OF THE X-RAY LINES $L\alpha$, $L\beta_1$ and $L\beta_2$

By F. K. Richtmyer* and R. D. Richtmyer
Department of Physics, Cornell University

(Received July 10, 1929)

Abstract

The satellite structure accompanying the x-ray diagram lines $L\alpha$, $L\beta_1$ and $L\beta_2$ has been investigated for the elements Rb(37) to Sn(50). This structure is more complex than has heretofore been assumed. Not only is the number of satellites greater than previously reported, but a continuous spectrum seems to extend for some distance toward shorter wave-lengths beyond the satellites. Tables are given showing wave-lengths, values of ν/R and of $\Delta\nu/R$ ($\Delta\nu$ = difference in frequency between satellite and parent line) for five (seven for some elements) satellites of $L\alpha$; four of $L\beta_1$; and five of $L\beta_2$. The empirical relation previously reported for the $K\alpha$ satellites is found to hold for these L satellites: namely, the square root of the difference in frequency between a satellite and its parent line is a linear function of atomic number —similar to Moseley's law for diagram lines. The difficulties of obtaining values of the wave-lengths of satellites as accurate as are the measured wave-lengths of the corresponding diagram lines, are discussed. It is shown that some of these difficulties may be eliminated by obtaining a densitometer curve for the energy distribution through the parent line at a voltage just below the excitation voltage of the satellites. From measurements on a plate taken at high dispersion it appears that satellites may be resolved into fine-structure components.

X-RAY satellites are those comparatively faint lines in x-ray spectra, which do not fit the usual energy-level diagram, for which reason these lines are frequently called "non-diagram lines." They were first discovered by Siegbahn and Stenstrom[1] in their studies of the wave-lengths of the K-series lines of the elements Na (11) to Zn (30). On the short wave-length side of the $K\alpha$ doublet of Zn (30) a faint line was observed, which became more prominent for elements of lower atomic number, split up into a doublet at Ca (20) and was followed as far as Na (11).

Although the literature on x-ray satellites is not extensive, investigations since the above observation of Siegbahn and Larsen have shown that many x-ray lines have such faint companions, usually on the high-frequency side. Thus, satellites are known to accompany $K\alpha$, $K\beta$, $L\alpha$, $L\beta_1$, $L\beta_2$, $L\gamma_1$, $L\gamma_{2,3}$ and $M\alpha$. However, there seems to have been no systematic search to prove that satellites of other lines do *not* exist; there is some evidence to indicate that there are more satellites accompanying the above-mentioned lines than have been heretofore reported; little is known regarding the excitation potentials of satellites; the range of atomic numbers of the elements emitting a given satellite has not been absolutely fixed; and the current theories of

* The senior author wishes to express his thanks to the Heckscher Research Council of Cornell University for a grant in aid of this research.

[1] Siegbahn and Stenstrom, Phys. Zeits. **17**, 48 and 318 (1916).

the origin of satellites agree only partially with experimental facts. There is need for more complete data on this subject. The present paper[2] is a preliminary report, largely empirical, of measurements of wave-lengths of the satellites of certain of the L lines: $L\alpha$, $L\beta_1$ and $L\beta_2$.

The spectrum plates were made with a Siegbahn vacuum spectrometer. A calcite crystal was used throughout, except for wave-lengths longer than about 5.8A, for which a quartz crystal was used. The voltage applied to the x-ray tube varied somewhat from element to element, but was in the neighborhood of 13 to 15 kv, unidirectional and with a ripple of several percent. Exposures necessary to bring out the satellite structure varied from thirty minutes to three hours, depending on the nature of the cathode material, the lines under investigation, and the permissible tube current.

The wave-lengths of the satellites of a given diagram (or "parent") line were determined by comparison with the known wave-length of the parent line (Siegbahn's values). This measurement presents some difficulties, if precise values of the wave-lengths of the satellites are desired. Either of two prodecures may be followed:

(1) The distance between parent line and satellite on the plate may be determined directly by a micrometer microscope. This method is open to two sources of error. First, the exposures necessary to bring out the satellite structure are so long that the parent line is much over exposed. Not only is it difficult to determine its exact center, but, the parent line thus being very broad, the satellites lie "in its shadow." Because of the rapidly varying density of the photographic plate in this neighborhood, the eye is subject to the well-known errors of psychological contrast in estimating the position of maximum density corresponding to the satellite line on which to set the cross hair of the microscope. Second, even though this position of maximum density on the plate be correctly estimated, such position is *not* the position of maximum *intensity* of the satellite line, since, as before mentioned, the satellite is superimposed on the rapidly varying density at the side of the parent line.

(2) The first of these two sources of error can be eliminated by making a densitometer record through the parent line and its satellite structure, and from this record the correct positions of maximum density determined. Such a record is shown by the full curve A of Fig. 1, which is a tracing of the original densitometer record for $L\alpha$ of Ag (47). (The spectrum plate was exposed thirty minutes at 12.0 kv and 16 m. a.). The four satellites, $L\alpha'$ to $L\alpha^{iv}$ inclusive, are clearly observable at the left of $L\alpha_1$ and the distance between the maximum of $L\alpha_1$ and that of each of the satellites may be readily determined, although with no very high precision. However, such determination is open to the second of the two sources of error mentioned above. Since curve A is a composite of parent line plus satellites, the *correct* positions of maximum *intensity* of the several satellites can be obtained *only* by subtracting from the ordinates of curve A the ordinates of a densito-

[2] A part of this work was done at Uppsala, Sweden, in the laboratory of Professor Siegbahn, to whom the authors wish to express their best thanks for the many courtesies extended.

meter curve of the parent line $L\alpha$ without its satellites. This latter curve cannot, of course, be obtained directly. A procedure frequently followed is to make an estimate of its shape, and therefrom to determine the desired wave-lengths of the satellites. This procedure at best is open to obvious objections.

An alternative, though far from satisfactory, procedure is the following: Existing data seem to show that the excitation potentials of satellites are some twenty to thirty percent higher than those of the corresponding parent lines. Thus the excitation potential of the $L\alpha$ lines of Ag (47) is 3.34 kv. The satellites of this line should not be produced at 3.8 kv. Accordingly, a plate was made of $L\alpha$ of Ag (47) at 3.8 kv and a densitometer record of this plate is shown as curve B of Fig. 1. No satellite structure is observable, although it is to be noted that the curve is unsymmetrical, there being a "foot" on the high frequency side of the line where the satellites appear at higher voltages. This curve enables one to make a somewhat better *guess* as to the correct shape of the curve for $L\alpha$ alone if it could be obtained at 12.0 kv. Such a curve is shown as the dotted curve C of Fig. 1. Finally one obtains curve D by subtracting the ordinates of curve C from those of A. Curve D gives the satellite structure accompanying the diagram line $L\alpha$.

It is observed that this satellite structure seems to consist of two parts: (1) a kind of continuous spectrum c_1 c_2 c_3 upon which are superposed[3] the satellites α' to α^v. Even curve D would have to be analyzed into its component parts in order to give unambiguously the position of the respective maxima. The procedure here outlined seems to be necessary if one wishes to obtain values of the wave-lengths of satellite lines comparable in precision with corresponding values for the parent lines.

However, the number and approximate location of satellites is sufficient for many purposes. Accordingly, the data herein recorded were obtained from the spectrum plates by direct measurement with a micrometer microscope.[4] The order of magnitude of the differences between such direct measurements with the micrometer microscope and those obtained from a densitometer record such as curve A Fig. 1, are indicated in Table I, the second

TABLE I. *Comparison of micrometer microscope with densitometer method of measuring position of satellites with reference to the parent line.*

Satellite	Distance from $L\alpha_1$		
	By micrometer microscope	By densitometer record	Difference, percent
$L\alpha_1'$	2.01 mm	2.01 mm	0.
$L\alpha_1''$	2.77	2.64	4.8
$L\alpha_1'''$	3.34	3.16	5.5
$L\alpha_1^{iv}$	4.64	4.59	1.1

[3] The curves in Fig. 1 should be regarded as diagrammatic, rather than as representing accurately to scale the relative intensities of the component spectral parts.

[4] A very low power microscope—magnification not more than 1.5× or 2.0×—is necessary to render the fainter satellites visible.

column of which gives (in mm) the distances between $L\alpha$ and its first four satellites (for Zr (40)). The third column gives similar data determined from a densitometer record. From the last column it is seen that these differences amount to a few perçent. They vary from satellite to satellite, and with the density of the spectrum plate. A careful study of this point would yield valuable information.

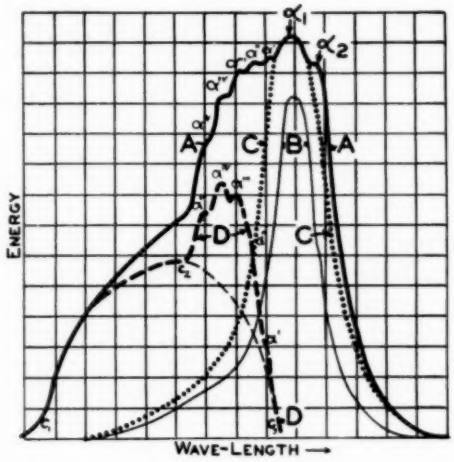

Fig. 1. A: Ag $L\alpha$ with satellites, at 12,000 volts; B: Ag $L\alpha$ at 3,800 volts; C: Estimated shape of Ag $L\alpha$ without satellites at 12,000 volts; D: Estimated structure of Ag $L\alpha$, at 12,000 volts.

RESULTS

Satellites of $L\alpha$. In Siegbahn's tables of x-ray spectral lines[5] only one satellite of $L\alpha$ is listed. This line is called by Siegbahn $L\alpha^3$, and is recorded over the range of elements, As (33) to In (49). However, Siegbahn and Larson[6] later found five satellites of $L\alpha$ of Mo (42), with a possible sixth somewhat doubtful. Druyvesteyn[7] reports five satellites over the range of elements Nb (41) to Ag (47). The present authors have found five satellites for each of the elements from Rb (37) to In (49). On the plates for some of the elements two others, and in the case of one element (Mo (42)) three, are clearly ob-

TABLE II. *Wave-lengths of the satellites of* $L\alpha$, *in X-units.*

	Rb 37	Sr 38	Zr 40	Nb 41	Mo 42	Ru 44	Rh 45	Pd 46	Ag 47	Cd 48	In 49
$L\alpha_1$	7302.7	6847.8	6055.9	5711.3	5394.3	4835.7	4587.8	4356.5	4145.6	3947.8	3763.7
α'	7280.8	6827.3	6038.5	5695.4	5380.0	4823.2	4576.2	4345.3	4134.9	3938.0	3754.5
α''	7274.1	6821.4	6032.5	5689.6	5374.0	4818.1	4571.3	4341.2	4130.6	3934.0	3750.9
α'''	7263.0	6814.3	6026.5	5684.6	5368.9	4812.9	4566.5	4335.9	4125.6	3929.0	3746.2
α^{iv}	7752.0	6800.7	6015.9	5672.1	5359.8	4804.5	4559.3	4329.1	4119.3	3922.2	3740.0
α^{v}	7241.4	6793.1	6008.4	5667.0	5351.4	4797.2	4551.9	4322.2	4112.5	3915.8	3733.2
α^{vi}				5661.0	5343.6	4788.7		4314.2			3730.1
α^{vii}					5336.6						
α^{viii}					5324.0						

[5] The Spectroscopy of X-Rays, p. 118.

[6] Siegbahn and Larson, Arkiv för Matematik, Astronomi och Fysik **18**, 1 (1924).

[7] Druyvesteyn, Het Röntgenspectrum van de tweede Soort. Dissertation, Groningen, 1928.

served. It seems probable that carefully chosen exposure-times would show at least seven satellites for all these elements.

Tables II, III and IV give, respectively, the wave-lengths, values of ν/R and of $\Delta\nu/R$ for these satellites. (ν = frequency; R = Rydberg's constant;

TABLE III. *Values of ν/R for the satellites of $L\alpha$.*

	Rb 37	Sr 38	Zr 40	Nb 41	Mo 42	Ru 44	Rh 45	Pd 46	Ag 47	Cd 48	In 49
$L\alpha_1$	124.79	133.07	150.48	159.56	168.93	188.45	198.63	209.08	219.81	230.83	242.12
α'	125.17	133.47	150.91	160.01	169.39	188.94	199.14	209.62	220.38	231.41	242.72
α''	125.28	133.59	151.06	160.17	169.57	189.14	199.35	209.82	220.61	231.64	242.95
α'''	125.47	133.72	151.21	160.31	169.73	189.35	199.56	210.09	220.89	231.93	243.25
α^{iv}	125.66	133.99	151.48	160.66	170.02	189.67	199.88	210.41	221.22	232.33	243.66
α^{v}	125.84	134.14	151.66	160.80	170.29	189.98	200.20	210.75	221.59	232.70	244.00
α^{vi}				160.97	170.53	190.29		211.14			244.30
α^{vii}					170.75						
α^{viii}					171.15						

$\Delta\nu$ = difference in frequence between satellite and parent line). Only those lines are recorded for which satisfactory micrometer-microscope settings could be made.

A word about terminology: Following Druyvesteyn and others, there seems to be a tendency to indicate satellites by primes ($'$), double primes ($''$), etc. The present authors have adopted this system whenever possible.

TABLE IV. ($\Delta\nu/R$) *for the satellites of $L\alpha$.* $\Delta\nu/R = (\nu/R)_s - (\nu/R)_{L\alpha_1}$

	Rb 37	Sr 38	Zr 40	Nb 41	Mo 42	Ru 44	Rh 45	Pd 46	Ag 47	Cd 48	In 49
$L\alpha'$	0.375	0.400	0.432	0.447	0.464	0.490	0.507	0.542	0.573	0.577	0.598
α''	0.490	0.517	0.583	0.609	0.640	0.691	0.721	0.745	0.805	0.810	0.831
α'''	0.680	0.654	0.733	0.749	0.803	0.895	0.932	1.010	1.076	1.104	1.134
α^{iv}	0.868	0.920	0.996	1.100	1.090	1.220	1.248	1.334	1.415	1.500	1.540
α^{v}	1.048	1.066	1.182	1.243	1.355	1.508	1.572	1.668	1.780	1.875	1.975
α^{vi}				1.412	1.600	1.84		2.06			
α^{vii}					1.82						
α^{viii}					2.22						

(Certain exceptions will be noted below). Accordingly the satellites of $L\alpha$ are called $L\alpha'$, $L\alpha''$, $L\alpha'''$, $L\alpha^{iv}$ . . . . This terminology can be at best only tentative as is indicated by the data in Table V below.

$L\alpha'$ is faint. $L\alpha''$ and $L\alpha'''$ are quite strong and have the appearance of a doublet. $L\alpha^{iv}$ is about as strong as $L\alpha'$. Beginning with $L\alpha^{v}$ the lines become increasingly fainter.

The satellites of In (49) are not well separated and at Sn (50) the satellites seem to be replaced by a band showing little or no structure. Whether higher resolving power and properly chosen exposures will show that this band can be resolved for elements above In (49) remains to be seen.

That greater detail of structure may be revealed by using higher resolving power is clearly indicated by a plate of $L\alpha$ of Ag (47) taken with a quartz crystal in second order, for which the dispersion, at $\lambda = 4.15$A, is nearly four and one half times as great as for a calcite crystal in first order. On this plate the more intense satellites, $L\alpha''$ and $L\alpha'''$ *are each clearly split up into two components.* $L\alpha'$ seems to appear complex, with possibly three components. And several faint lines appear between $L\alpha'$ and $L\alpha_1$. One of these, desig-

nated in Table V as $L\alpha_1$(a) is not separated from $L\alpha_1$ but appears as a "shoulder" on the latter. Table V shows the wave-lengths of these fine structure components as observed with the quartz crystal.

TABLE V. *Fine structure of the satellites of Lα of Ag (47), as observed with a quartz crystal in second order. (Wave-lengths, in X-units).*

Line	Quartz crystal Second order	Calcite crystal First order*
$L\alpha_1$	(4145.64)	(4145.64)
$L\alpha_1$ (a)	4142.25	
$L\alpha_1$ (b$_1$)	4140.03	
$L\alpha_1$ (b$_2$)	4139.29	
$L\alpha_1$ (b$_3$)	4138.56	
$L\alpha_1$ (c) (?)	4136.58	
$L\alpha'$ (a)	4135.41	
$L\alpha'$ (b)	4134.63	4134.9
$L\alpha'$ (c)	4133.90	
$L\alpha''$ (a)	4131.64	
$L\alpha''$ (b)	4130.11	4130.6
$L\alpha'''$ (a)	4125.84	
$L\alpha'''$ (b)	4124.63	4125.6
$L\alpha^{iv}$	4119.21	4119.3

* From Table II, for comparison.

The difference in frequency between a satellite and its parent line increases in a regular way with atomic number, as is shown in Fig. 2 (a) in which $\Delta\nu/R$ for the several satellites of $L\alpha$ are plotted as ordinates against atomic number as abscissa. The resulting straight lines justify the conclusion[8] that for the satellites of $L\alpha$, the *square root of the frequency difference between a given satellite and the parent line is a linear function af atomic number.*

Satellites of $L\beta_1$. Two satellites of $L\beta_1$ have been previously reported. They were called $L\beta_1$ and $L\beta_{13}$ by Coster,[9] who measured them for the elements Rb (37) to Sb (51). Thoreaus[10] reports two satellites for the elements Cu (29) to Br (35) inclusive, which he calls $L\beta'$ and $L\beta''$ and which are identical with Coster's $L\beta_1'$ and $L\beta_{13}$. Druyvesteyn[7] calls these lines $L\beta_1'$ and $L\beta_1''$ respectively. On the plates of $L\beta_1$ taken by the present authors for the elements Nb (41) to Sn (50) these two lines were clearly visible, and

TABLE VI. *Wave-lengths of the satellites of Lβ$_1$, in X-units.*

	Nb 41	Mo 42	Ru 44	Rh45	Pd 46	Ag 47	Cd 48	In 49	Sn 50
$L\beta_1'$	5479.6	5165.8	4611.0	4364.0	4137.3	3926.6	3730.1	3547.8	3377.9
β_1''	5465.7	5153.5	4600.4	4353.0	4126.8	3915.0	3720.4	3539.5	3369.7
β_1'''	5451.5	5139.9	4588.5	4343.1	4116.9	3907.1	3712.5	3531.6	3361.5
β_1^{iv}		5132.5	4581.6	4335.5	4109.5	3899.6	3703.9	3523.5	3352.6
		5125.2	4572.2	4327.4	4103.0	3893.5	3696.4		

[8] F. K. Richtmyer, Phil. Mag. **6**, 64 (1928).
[9] Coster, Phil. Mag. **43**, 1088 and 1105 (1922).
[10] Thoreaus, Phil. Mag. **2**, 107 (1926).

in addition there were two others at still shorter wave-lengths, which we may designate as $L\beta_1'''$ and $L\beta_1^{iv}$. The wave-lengths, values of ν/R and of $\Delta\nu/R$ for these four lines are shown in Tables VI, VII and VIII. The plot

TABLE VII. *ν/R for the satellites of $L\beta_1$.*

	Nb 41	Mo 42	Ru 44	Rh 45	Pd 46	Ag 47	Cd 48	In 49	Sn 50
$L\beta_1$	166.30	176.40	197.63	208.82	220.26	232.07	244.30	256.85	269.77
β_1'	166.72	176.82	198.08	209.35	220.82	232.76	244.94	257.45	270.43
β_1''	167.15	177.28	198.59	209.82	221.35	233.23	245.45	258.02	271.09
β_1'''		177.53	198.89	210.18	221.74	233.67	246.02	258.62	271.59
β_1^{iv}		177.78	199.29	210.57	222.09	234.03	246.51		

TABLE VIII. *$\Delta\nu/R$ for the satellites of $L\beta_1$.*

	Nb 41	Mo 42	Ru 44	Rh 45	Pd 46	Ag 47	Cd 48	In 49	Sn 50
$L\beta_1'$	0.421	0.422	0.455	0.526	0.560	0.688	0.636	0.603	0.655
β_1''	0.853	0.883	0.964	0.999	1.086	1.156	1.152	1.174	1.315
β_1'''		1.130	1.261	1.363	1.481	1.597	1.715	1.765	1.822
β_1^{iv}		1.386	1.663	1.752	1.825	1.959	2.209		

of $\Delta\nu/R$ as a function of atomic number is shown in Fig. 2 (b). These satellites are relatively weaker, compared to $L\beta_1$, than are the satellites of $L\alpha$ and are hence more difficult to measure. This may account for the greater scattering of the points in Fig. 2 (b) than in Fig. 2 (a).

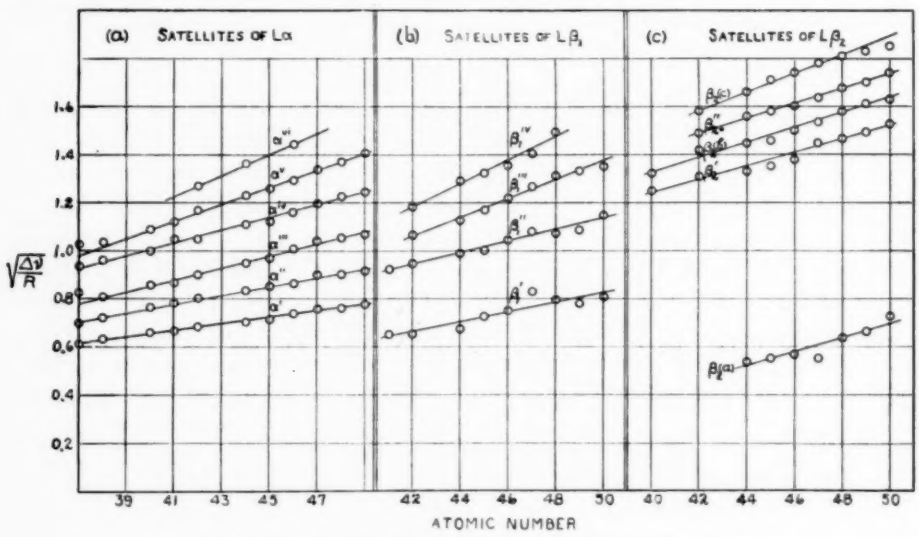

Fig. 2. Linear relation between $(\Delta\nu/R)^{1/2}$ and atomic number.

$L\beta_1''$ is the strongest of this group. Next in order of intensity come $L\beta_1'$ and $L\beta_1'''$. $L\beta_1^{iv}$ is very weak and is difficult to measure, although its existence seems to be definitely established.

A comparison of Figs. 2 (a) and 2 (b) shows that, although the two satellite structures are quite dissimilar in general appearance, yet the frequency differences between satellites and the respective parent lines are all included within the same range of values of $\Delta\nu/R$.

Satellites of $L\beta_2$. The satellite structure accompanying $L\beta_2$ is rather remarkable. Two prominent satellites have long been known, namely: $L\beta_2'$ and $L\beta_2''$ (Siegbahn $L\beta_{11}$ and $L\beta_{12}$). These lines are nearly equal in intensity, are sharper than other L-satellites and are separated farther from the parent line. Our plates show, in addition to these, three other lines. Close to $L\beta_2$ is a very faint, yet fairly well defined line which we have called $L\beta_2$ (a). Between $L\beta_2'$ and $L\beta_2''$ appears a broad, diffuse line. This is much weaker than either $L\beta_2'$ or $L\beta_2''$ and extends nearly from one to the other. We have designated this $L\beta_2$ (b). Beyond $L\beta_2''$ is still another very faint line, $L\beta_2$(c) in our notation. The wave-lengths, values of ν/R and of $\Delta\nu/R$ for these five satellites are given in Tables IX, X and XI. Fig. 2 (c) shows the plot of $\Delta\nu/R$ against atomic number.

TABLE IX. *Wave-lengths of the satellites of* $L\beta_2$ *in X-units.*

	Zr 40	Mo 42	Ru 44	Rh 45	Pd 46	Ag 47	Cd 48	In 49	Sn 50
$L\beta_2$	5573.4	4909.2	4361.9	4122.1	3900.7	3693.8	3506.4	3331.2	3167.9
$L\beta_2$(a)			4355.9	4116.5	3895.3	3689.3	3501.0	3325.9	3162.1
$L\beta_2'$	5520.2	4864.9	4325.0	4088.0	3869.0	3663.7	3477.3	3304.1	3142.3
$L\beta_2$(b)	5514.2	4856.1	4318.1	4082.4	3863.2	3658.7	3472.6	3299.7	3138.8
$L\beta_2''$	5504.8	4850.8	4311.4	4075.6	3857.8	3653.9	3468.2	3296.0	3134.4
$L\beta_2$(c)		4843.0	4304.3	4067.9	3850.2	3646.5	3462.2	3290.5	3130.1

TABLE X. *Values of* ν/R *for the satellites of* $L\beta_2$.

	Zr 40	Mo 42	Ru 44	Rh 45	Pd 46	Ag 47	Cd 48	In 49	Sn 50
$L\beta_2$	163.50	185.62	208.92	221.07	233.62	246.70	259.89	273.56	287.66
$L\beta_2$(a)			209.21	221.37	233.94	247.01	260.29	274.00	288.19
$L\beta_2'$	165.06	187.33	210.69	222.90	235.54	248.71	262.04	275.79	289.98
$L\beta_2$(b)	165.24	187.62	211.02	223.20	235.87	249.05	262.39	276.15	290.31
$L\beta_2''$	165.63	187.83	211.34	223.56	236.19	249.37	262.72	276.45	290.70
$L\beta_2$(c)		188.13	211.68	223.98	236.65	249.86	263.16	276.90	291.09

TABLE XI. $\Delta\nu/R$ *for the satellites of* $L\beta_2$.

	Zr 40	Mo 42	Ru 44	Rh 45	Pd 46	Ag 47	Cd 48	In 49	Sn 50
$L\beta_2$(a)			0.289	0.302	0.325	0.307	0.402	0.437	0.530
$L\beta_2'$	1.562	1.714	1.768	1.830	1.900	2.009	2.154	2.230	2.321
$L\beta_2$(b)	1.739	2.00	2.10	2.13	2.25	2.35	2.50	2.59	2.65
$L\beta_2''$	2.13	2.21	2.42	2.49	2.571	2.668	2.829	2.891	3.044
$L\beta_2$(c)		2.51	2.76	2.91	3.03	3.16	3.27	3.34	3.43

It is not the purpose of the present paper to discuss the bearing of these data on theories concerning the origin of satellite lines.[11] Indeed it seems probable that these theories cannot be advanced much farther until much more information is available. Particularly important are such questions as the excitation potentials of satellites, their relative intensities, and the fine structure which may be revealed by using the highest attainable resolution. Investigations along these lines are in progress in this laboratory.

[11] For a general discussion of this question see F. K. Richtmyer, Franklin Institute, Journal, (paper in press).

RAMAN SPECTRA OF POLYATOMIC GASES

By R. G. Dickinson, R. T. Dillon and F. Rasetti
Norman Bridge Laboratory of Physics and Gates Chemical Laboratory
California Institute of Technology

(Received July 15, 1929)

Abstract

Raman spectra of gaseous CO_2, N_2O, NH_3, CH_4 and C_2H_4 have been photographed using the line $\lambda 2536$ of mercury as the exciting radiation. Vibrational transitions have been observed in all the gases investigated, and rotational transitions in the cases of NH_3 and CH_4. For the frequency shifts due to the vibrational transitions, the following numerical values (in cm^{-1}) have been found:

CO_2: 1264.5; 1285.1; 1387.7; 1408.4.
N_2O: 1281.8
NH_3: 3333.6
CH_4: 2914.8; 3022.1; 3071.5.
C_2H_4: 1342.4; 1623.3; 2880.1; 3019.3; 3240.3; 3272.3.

Raman spectra of liquid NH_3 have been photographed and found to give the two frequency shifts: 3298.4 and 3214.5. In the case of gaseous NH_3, pure rotational transitions lead to a moment of inertia having the value $I_0 = 2.79 \times 10^{-40}$. In the case of methane, the positive and negative branches of the 3022.1 band lead to the value $I_0 = 5.17 \times 10^{-40}$. The relations between these data and infra-red absorption data are discussed.

Introduction

SINCE Raman's experimental discovery of scattered radiation of modified frequency, which was predicted from the hypothesis of light quanta by Smekal and from the correspondence principle of Kramers and Heisenberg, a great deal of experimental material has been reported, chiefly for complicated molecules in the liquid state. In order to obtain data which might be interpretable in terms of models, it seemed desirable to make measurements on some of the simpler polyatomic molecules. It also appeared advantageous to study substances in the gaseous state so as to avoid the perturbations arising from the mutual interaction of molecules in liquids. This interaction produces, for example, a lack of sharpness in the rotational states, so that rotational transitions give rise to continuous spectra instead of sharply defined lines. Moreover, as in the case of ammonia for which data are given below, even the vibrational shifts may differ between the liquid and gaseous states.

Data on Raman spectra of polyatomic gases are very meagre. Ramdas[1] has reported the spectrum given by ethyl ether vapor to be identical with that given by the liquid. Rasetti,[2] has given two vibrational frequencies, 1284 and 1392 cm^{-1}, for gaseous carbon dioxide. R. W. Wood,[3] working with

[1] Ramdas, Ind. J. of Phys. **3**, 131 (1928).
[2] F. Rasetti, Nature **123**, 205 (1929).
[3] R. W. Wood, Phil. Mag. **7**, 744 (1929).

ammonia at atmospheric pressure, has found a Raman shift corresponding to the center of the infra-red band at 3.0μ.

Apparatus and Technique

In the present work, we have employed the apparatus and the improvements in technique already developed by one of us[4] for the investigation of diatomic gases. One of these improvements consists in the use of gas pressures up to fifteen atmospheres thus considerably reducing the exposure time. An equally important improvement resulted from the use of ultra-violet rather than visible light as the primary radiation. The intensity of the scattered radiation increases with the frequency of the exciting light, and may be expected to increase particularly rapidly when this approaches an absorption frequency of the scattering substance.[5] On the other hand, an exciting radiation of too high frequency would be absorbed. The line λ2536 of mercury provided a convenient and strong source in a spectral region suitable for the investigation of a number of gases. Photochemical and fluorescence effects due to shorter wave-lengths of the mercury arc were eliminated by an acetic acid filter.

A Hilger E2 quartz spectrograph was used. A comparison spectrum from an iron arc was recorded on each plate. The frequencies of the Raman lines were evaluated by linear interpolation on a frequency scale between iron lines not more than 20A apart. All the measured Raman lines were excited by λ2536; we have taken[4] the frequency of this line as 39411.1 cm^{-1}

Results

Carbon dioxide. This gas was taken from a commercial cylinder. Purification was not considered necessary since the spectra which would have been given by possible impurities, such as O_2, N_2 and CO were already well known.

The Raman spectrum, which is reproduced in the figure, consisted of a very strong unresolved rotational band close to the exciting line, and four sharp lines whose frequency shifts and approximate relative intensities are given in Table I.

Table I. *Frequency shifts for carbon dioxide.*

$\Delta\nu$ (cm^{-1}):	1264.5	1285.1	1387.7	1408.4
Intensity:	1	10	15	1

It may be pointed out that none of these frequencies coincides with any of those observed in infra-red absorption by Barker,[6] and by Schäfer and Philipps.[7]

Nitrous oxide. The gas used was a product prepared for anaesthetic purposes and given as 99.75% pure.

[4] F. Rasetti, Proc. Nat. Acad. Sci. **15,** 515 (1929); Phys. Rev. **34,** 367 (1929).
[5] F. Rasetti, Proc. Nat. Acad. Sci. **15,** 234 (1929).
[6] E. F. Barker, Astroph. Journ. **55,** 391 (1922).
[7] Schäfer and Philipps, Zeits. f. Physik **36,** 641 (1926).

Only one Raman line was found; this was rather weak but sharp. The frequency shift, $\Delta\nu$, was 1281.8. An infra-red absorption of this frequency would lie at 7.8μ; we are not aware of data showing any band at this wave-

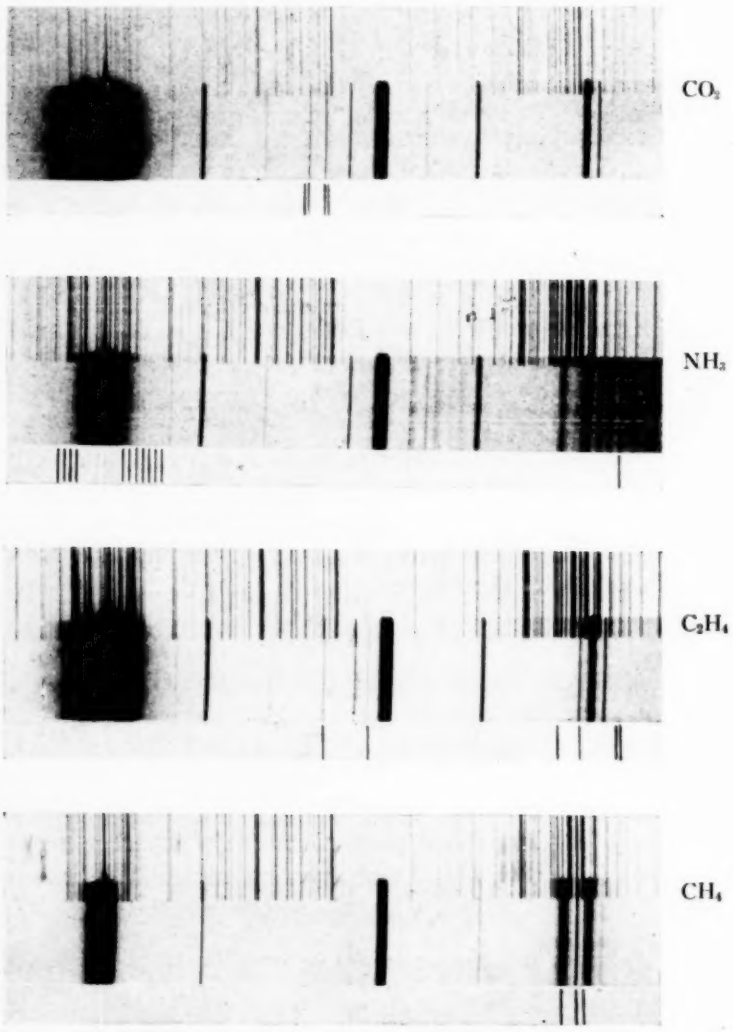

Fig. 1. Raman Spectra of Carbon Dioxide, Ammonia, Methane, and Ethylene excited by the line λ2536 of mercury; the comparison spectrum is that of the iron arc.

length. However, the at least approximate agreement of the frequency measured by us with the difference between the frequencies corresponding to the prominent absorptions given by E. v. Bahr[8] as occurring at 2.86 and 4.49μ, may be significant.

[8] E. v. Bahr, Verh. D. Phys. Ges. **15**, 710 (1913).

Ammonia. The gas was taken from a commercial cylinder, and the exposure tube was filled at a pressure slightly less than that of the saturated vapor at room temperature.

Unresolved fluorescence bands extending from λ2700 through the visible appeared on the plates; but in the region in which the Raman lines occurred, the bands were weak enough not to interfere with the measurements. The spectrum is shown in the figure. In addition to a vibrational line corresponding to $\Delta\nu = 3333.6$, rotational lines could be measured on both sides of the line λ2536. These appear to correspond to a change of ± 2 in rotational quantum number as is shown in Table II. The assumed change in rotational quantum number is given in the first column, and the observed values of the frequency shifts in the second. The calculated values of the frequency shifts given in the third column were obtained from the expression:

TABLE II. *Pure rotational Raman lines from gaseous ammonia.*

Transition	$\Delta\nu$ obs. (cm^{-1})	$\Delta\nu$ calc. (cm^{-1})	diff.
7→9	−334.8	−334.2	−0.6
6→8	−295.3	−295.5	+0.9
5→7	−256.0	−256.5	+0.5
4→6	−217.0	−217.4	+0.4
3→5	−178.7	−178.1	−0.6
2→4	−138.7	−138.7	0.0
1→3	− 99.6	− 99.1	−0.5
4→2	+138.2	+138.7	+0.5
5→3	+178.7	+178.1	−0.6
6→4	+217.4	+217.4	0.0

$$\pm\Delta\nu = (E_{m+2} - E_m)/hc$$

in which E_m, the energy of the mth rotational state was assumed to be given by:

$$E_m/hc = 9.921(m+\tfrac{1}{2})^2 - 0.00063(m+\tfrac{1}{2})^4$$

This rotational band corresponds to a moment of inertia, $I_0 = 2.792 \times 10^{-40}$. This may be compared with the value, 2.77×10^{-40}, obtained by Badger and Cartwright[9] from pure rotational absorption bands, and with the value, 2.83×10^{-40}, deduced by Stinchcomb and Barker[10] from the absorption band at 3.0μ. These authors give for the frequency of the center of this band 3337.0, which agrees fairly well with our value 3333.6.

We have thought it interesting to make an accurate comparison of the Raman shifts given by the liquid and gaseous states of ammonia. Liquid ammonia was distilled into the heavy walled glass tube in which it was to be irradiated, and was sealed up. The exciting radiation was from a mercury arc. The spectrum was photographed with a two-prism glass spectrograph of aperture f8 and a dispersion of about 100 wave-numbers per mm in the blue. The frequencies of the shifted lines were evaluated with an iron arc comparison spectrum as with the quartz instrument. The results are given in Table III.

[9] Badger and Cartwright, Phys. Rev. **33**, 692 (1929).
[10] Stinchcomb and Barker, Phys. Rev. **33**, 305 (1929).

From these results, it appears that liquid ammonia gives two Raman shifts, a strong one having $\Delta\nu = 3298.4$ and a somewhat weaker one having $\Delta\nu = 3214.5$; the disagreement between the frequency shifts in the liquid and gas lies well outside of the experimental error.

Methane. Samples of methane from two different sources were examined. The first sample was prepared by heating a mixture of sodium acetate and soda-lime. The gas was passed through a solution of KOH and then through concentrated H_2SO_4. It was then condensed to the liquid state from which it was evaporated into the apparatus under pressure.

TABLE III. *Raman spectra from liquid ammonia.*

Observed frequency.	Intensity	Exciting wave-length	Exciting frequency	Frequency shift
24176.0	weak	3650.15	27388.4	3212.4
24088.8	med. (broad)	3650.15	27388.4	3299.6
		(3663.27)	(27290.5)	(3201.7)
24053.4	weak	3654.83	27353.3	3299.9
23994.2	medium	3663.27	27290.5	3296.3
21490.9	strong	4046.56	24705.5	3214.6
21407.0	very strong	4046.56	24705.5	3298.5
19722.8	weak	4358.34	22938.1	3216.3
19638.8	weak	4358.34	22938.1	3299.3

The second sample was purified from a natural gas which originally contained 80% methane. A photograph made before purification showed a strong fluorescence which we attributed to heavier hydrocarbons. The treatment of the gas consisted in admitting it at about 800 pounds per sq. in. pressure into a cylindrical bomb filled with absorbent charcoal previously heated and evacuated. While the purified gas was slowly withdrawn from one end of the bomb and expanded into the apparatus, the pressure in the bomb was maintained at 800 pounds by admitting raw gas at the other end. Separate experiments have shown this procedure to give methane of about 99% purity. The methane so purified showed no fluorescence.

TABLE IV. *Rotation-vibrational Raman lines from methane.*

Transition	$\Delta\nu$ obs. (cm^{-1})	$\Delta\nu$ calc. (cm^{-1})	diff.
10→12	3261.2	3261.0	−0.2
9→11	3241.0	3240.7	−0.3
8→10	3220.5	3220.4	−0.1
7→ 9	3199.8	3199.9	+0.1
6→ 8	3178.4	3179.4	+1.0
5→ 7	3159.0	3158.7	−0.3
4→ 6	3137.2	3138.0	+0.8
3→ 5	3117.7	3117.1	−0.6
6→ 4	2901.5	2903.1	+1.6
7→ 5	2881.3	2881.2	−0.1
8→ 6	2859.8	2859.1	−0.7
9→ 7	2837.0	2837.0	0.0
10→ 8	2814.1	2814.7	+0.6

The spectra given by the methane from these two sources were identical; we believe, therefore, that there is little question that any of the observed lines resulted from impurities. The spectrum is shown in the figure.

Three vibrational Raman lines were found in the spectrum. One of them was very strong (relative intensity, 20); it was sharp, and corresponded to a shift $\Delta\nu = 2914.8$. One line was rather weak (intensity, 2) with $\Delta\nu = 3071.5$. The remaining line was of intermediate strength (intensity, 5); it was rather broad and shaded off on the short wave-length side. The frequency shift corresponding to its sharp edge was $\Delta\nu = 3022.1$. On both sides of this last line, a number of weak and approximately equally spaced lines were measured. These appear to constitute the positive and negative branches of the band of which the line at $\Delta\nu = 3022.1$ is the unresolved Q branch. In interpreting this band, a change of ± 2 in rotational quantum number has again been assumed. The results are given in Table IV; in the first column is given the change in rotational quantum number m, in the second, the observed shift, and in the third, the shift calculated from the following expressions for the energy in the normal state and in the excited vibrational state:

$$E_0/hc = 5.363(m+\tfrac{1}{2})^2$$
$$E_1/hc = 3022.1 + 5.313(m+\tfrac{1}{2})^2$$

For the normal state, a moment of inertia $I_0 = 5.17 \times 10^{-40}$ may be calculated from these results. The vibrational shift agrees fairly well with the value 3019, given by Cooley[11] for the band at 3.31μ. The spacing of the lines near the center of this band was found by Cooley to be 9.77 cm^{-1}, which leads to a moment of inertia, $I_0 = 5.66 \times 10^{-40}$. Although this is not very far from our value, the disagreement seems to be well outside the experimental error. The other two vibrational frequencies observed by us do not seem to correspond to any infra-red absorption.

It may be remarked that the frequency 2914.8 observed by us, practically coincides with the difference between two observed infra-red frequencies, 4217 and 1304, which Dennison[12] assumes to be fundamentals. If this is more than a coincidence, Dennison's choice of fundamental frequencies can hardly be correct, because in this case, this very strong Raman line would have its origin in molecules thermally excited with an energy corresponding to the frequency 1304; this appears highly improbable.

Ethylene. The gas used was a commercial product prepared for anaesthetic purposes, and given as 99.2% pure.

The scattering by this gas was particularly strong, so that Raman lines could be photographed in a few hours. The spectrum is shown in the figure. A strong unresolved rotational band appeared close to the exciting line. Six shifts were measured and are given in Table V.

TABLE V. *Frequency shifts for ethylene.*

$\Delta\nu$ (cm^{-1}):	1342.4	1623.3	2880.1	3019.3	3240.3	3272.3
Intensity:	20	15	3	20	2	1

[11] J. P. Cooley, Astroph. Journ. **62,** 73 (1925).
[12] D. M. Dennison, Astroph. Journ. **62,** 84 (1925).

No agreement appears to exist between these frequencies and those of the centers of the infra-red bands as given by Levin and Meyer.[13]

Discusson

One striking fact which appears from these results is that the Raman spectra consist usually of a few sharp lines in contrast with the large number of lines observed in infra-red absorption bands. This is observed also in diatomic molecules and for these, has been discussed theoretically by Hill and Kemble.[14] The Q branch of vibrational-rotational bands (generally unresolved) is much stronger in Raman effect than the positive and negative branches and is practically always the only one observed, while in infra-red absorption spectra the Q branch is absent. The same is apparently true of the Raman spectra of polyatomic molecules. Therefore, we believe that the isolated lines generally observed in these spectra must be interpreted as unresolved Q branches, and that they usually give energy differences between vibrational levels.

Another striking fact, already well-known in the case of liquids, is that the majority of the Raman shifts do not correspond to vibrational frequencies observed in absorption. This is strikingly exemplified by the data on CO_2 where no coincidence is found between the several frequencies observed in Raman effect and the large number in absorption. In many cases, this can no doubt be attributed to the fact first pointed out by Carrelli, Pringsheim and Rosen[15] that shifts corresponding to inactive frequencies (that is, frequencies which are not associated with a variable electric moment of the molecule, and which, therefore, do not give rise to emission or absorption of radiation) can appear in the scattering process. This is due to the fact that the occurrence of a transition between two quantum states in the Raman effect does not depend on the properties of these states only; but, also, on those of all the levels which combine with both of them.[5] It also follows that it is not possible to account for the occurrence or otherwise of all the transitions between vibrational levels without taking into account electronic bands. As very little is at present known about electronic bands in polyatomic molecules, we cannot predict theoretically the intensities of vibrational and rotational lines in Raman effect.

The question arises as to which frequencies are to be considered fundamental in cases, like that of CO_2, where completely different frequencies are found in absorption and in Raman effect. It is an experimental fact and has been deduced theoretically by Manneback,[16] that in diatomic molecules shifts corresponding to the harmonics of the fundamental frequency occur with very low intensity. This appears to be true for polyatomic molecules also. It accordingly seems natural to assume that transitions from the normal state to states in which two different vibrations are simultaneously excited

[13] A. Levin and C. F. Meyer, Journ. Opt. Soc. Am. **16**, 137 (1928).
[14] E. L. Hill and E. C. Kemble, Proc. Nat. Acad. Sci. **15**, 387 (1929).
[15] A. Carrelli, P. Pringsheim and M. Rosen, Zeits. f. Physik **51**, 511 (1928).
[16] C. Manneback, Naturwissenschaften **17**, 364 (1929).

(and have energies corresponding to approximately the sum of the two frequencies), also have small probabilities. If this is true, and if we assume that in the molecules considered, we have no vibration frequencies low enough to give an appreciable proportion of molecules in excited states at room temperature, then the strong lines observed in Raman effect appear to correspond to fundamental frequencies. Combination frequencies may occur among the weaker Raman lines. It is also possible, although it does not seem very likely in the case of the molecules investigated here, that some of the Raman lines may be due to electronic transitions arising from a multiple structure of the normal electronic level as is the case for some diatomic molecules.

THE INFLUENCE OF FOREIGN GASES ON THE INTENSITIES OF THE MAGNESIUM RESONANCE LINES 4571 AND 2852

By John G. Frayne*
California Institute of Technology, Pasadena

(Received June 29, 1929)

Abstract

The Mg line 4571, $3^1S-3^3P_1$, is very weak in the arc while 2852, 3^1S-3^1P, is very intense. The life of the 3^3P_1 state is calculated to be 4×10^{-3} sec., while 3^1P has a life of 3×10^{-9} sec. Collisions of second kind between excited Mg atoms reduce intensity of 4571 in the arc. At a vapor pressure of 10^{-4} mm, the time between collisions of the Mg atoms is 10^{-3} sec. The 4571 line should appear strong at this or lower vapor pressures. Vapor from solid Mg metal at 500°C was excited in an evacuated tube by an electrodeless short-wave discharge. The 4571 line appeared in the discharge as a fairly prominent line.

Effect of foreign gases on 4571. The noble gases enhanced this line, the intensity relative to the triplet 3838 increasing up to about 20 mm in argon and 10 mm in neon and helium and then remaining practically constant. At these pressures, argon increased the line 100 times, Ne about 70 times, and He about 40 times. N_2 and CO increased 4571 up to the limit of pressure, about 2 mm, at which the discharge could be operated. H_2 caused a *slight* increase at a pressure of about 2 mm.

Intensity-pressure curves for noble gases have been reproduced theoretically, proving the assumption that excited Mg atoms suffer collisions of the second kind with the walls, and that action of a noble gas in enhancing the 4571 line is due entirely to the slowing up of diffusion of Mg atoms in 2^3P_1 state to the walls, and to its inefficiency in causing collisions of the second kind with excited Mg atoms.

Effect of foreign gases on 2852. All gases reduce 2852 and all singlets terminating on the 3^1P level. Increasing pressure of H_2 reduces 2852 faster than the singlets. Dissociation of the H_2 molecules by Mg atoms in 3^1P state reduces radiation from that state.

THE Mg line 4571, 3^1S–3^3P_1, is either very weak or entirely absent in the ordinary arc in air. On the other hand, the line 2852, 3^1S–3^1P, is exceptionally strong in the arc. 4571 is found in the flame spectrum and King[1] reports it as a fairly strong line in the low-temperature-furnace spectrum. Foote and Mohler[2] have produced it with considerable intensity in a controlled electron discharge, it being the first line to appear at an accelerating potential of 2.7 volts. Since the transition from the 3^1S to the 3^3P_1 state requires the minimum energy, this line should ordinarily be the strongest line in the spectrum. Its anomalous behavior is therefore of interest. The fact that it appears fairly strong wherever the excited vapor is of low pressure has been explained by Bowen[3] on the same basis as his explanation of nebular lines that arise from metastable states in nitrogen and oxygen.

* National Research Fellow.

[1] A. S. King, Astrophys. J. **48**, 13 (1918).

[2] Foote and Mohler, Phil. Mag. **37**, 33 (1919).

[3] Bowen, Proc. Nat. Acad. Sci. **14**, 30 (1928).

In a recent paper Houston[4] has shown how the transition probabilities of singlet and triplet systems may be calculated. From these calculations the natural life of an excited state may be determined. In Mg the life of the 3^3P_1 state approximates 4×10^{-3} sec. whereas the 3^1P state has a life of 3×10^{-9} sec. These figures show at once, in accordance with Bowen's theory, that the long life of the 3^3P_1 state accounts for the behavior of the 4571 line, collisions of the second kind returning most of the excited atoms to the normal state when the vapor pressure is sufficiently high. Now if the vapor pressure were low enough so that the time between collisions of the excited atoms is of the order of magnitude of the free life of the excited state, transition to the normal state should more likely give rise to radiation. Kinetic theory considerations show that at a vapor pressure of 10^{-4} mm, the time between collisions of Mg atoms is of the order of 10^{-3} sec. At this or lower vapor pressures, the 4571 should be a prominent line. There is one limitation, however, to obtaining the full intensity of the line at these low pressures. The vapor is confined to a vessel, and since the mean free path of the Mg atoms at 10^{-3} mm is several cm, collisions with the walls will be very frequent. Cario and Franck[5] and other observers have suggested that impacts of excited atoms with the walls of a discharge tube are collisions of the second kind. Recently, Pool[6] has found direct experimental evidence for this kind of impact of excited Hg atoms with the walls of the tube. If, then, we wish to obtain the full intensity of the Mg 4571 line at low pressures, we must reduce the frequency of collisions with the walls. This can be done, as we shall see later, by introducing a noble gas to prevent diffusion to the walls.

This experiment was primarily undertaken, at the suggestion of Professor I. S. Bowen, to compare the intensity of the 4571 line excited at low pressure with the intensity of the corresponding line in the arc. This comparison did not prove feasible because of the weakness of the line in the arc. A study of the variation of intensity of the line with vapor pressure was not undertaken on account of the experimental difficulties involved. It is necessary, for example, to heat the discharge tube to 500°C or higher to secure enough vapor for a discharge. It was decided, therefore, to make a study of the line with the vapor at 500°C, and particularly, the effect of foreign gases and vapors on it at this temperature. With the technique developed in this work, it is hoped to carry on a further investigation of the effect of pressure on the line.

Experimental Procedure

A short-wave oscillator supplied the energy for an electrodeless discharge in the Mg vapor at 500°C. According to International Critical Table data, the vapor pressure at this temperature is approximately 10^{-4} mm. A short stick of carefully scraped Mg metal was inserted in a tube 30 cm long, and 4 cm diameter. The presence of vapor from this stick was always indicated

[4] Houston, Phys. Rev. **33,** 297 (1929).
[5] Cario and Franck, Zeits. f. Physik **37,** 619 (1926).
[6] M. L. Pool, Phys. Rev. **33,** 22, (1929).

by the appearance of a brilliant green glow which filled the entire tube. A quartz window was sealed to the Pyrex tube by a graded seal. The spectra were photographed on a E-1 Hilger spectrograph. Intensity measurements were made in the manner described by Frayne and Montgomery.[7]

Experimental Results

Hydrogen. With hydrogen in the tube, it was possible to excite a discharge only between pressures of about 2 mm and 10^{-2}mm. The Mg combined with the H_2 to form MgH_2. This made it necessary to pass in H_2 through a capillary during the excitation of the discharge. The intensity of the 4571 line relative to the triplet 3838 increased slightly with pressure.

Carbon monoxide. CO apparently had an oxidizing effect on the Mg vapor, as it was difficult to keep the discharge going. This gas caused a decided increase in the 4571 line.

Nitrogen. N_2 was studied between 2 and 10^{-2} mm, no discharge being possible above 2 mm. The 4571 line showed a strong increase at 2 mm, while the 2852 line showed a decided decrease. The singlet series also showed a falling off in intensity at the higher N_2 pressures.

Fig. 1. Spectrum of Mg vapor in presence of foreign gases.

Argon. The argon used in this work was not entirely free from nitrogen and oxygen. It was partly purified by operating the discharge in it for a couple of hours. The 4571 line shows an increase at 1 mm, see Fig. 1, and increases rapidly with pressure up to 10 or 20 millimeters. The intensity seems to remain practically constant at higher pressures. The 2852 line as well as all the singlet lines diminish rapidly with pressure.

Neon. Neon behaves similarly to argon. It was very pure and no difficulty was encountered in getting a strong discharge at a pressure of 200 mm. The 4571 line is again enhanced, reaching its saturation value at 10 mm or lower. The increase is not as great as in the case of argon. The diminution of the 2852 line is not very pronounced.

Helium. The helium used in this work was very pure. Its behavior is quite similar to neon.

All the noble gases, argon particularly, diminished the intensity of the singlet series. With an argon pressure of 6 cm, the singlets only appear as very faint lines, and the 2852 line has become so reduced in intensity that

[7] Frayne and Montgomery, Phys. Rev. **33,** 549 (1929).

it is actually weaker on the plate than 4571. This is remarkable when one considers the intensities of these two lines in the arc. The results of observations on the 4571 line are shown in Fig. 2 and those on the 2852 line are shown in Fig. 3.

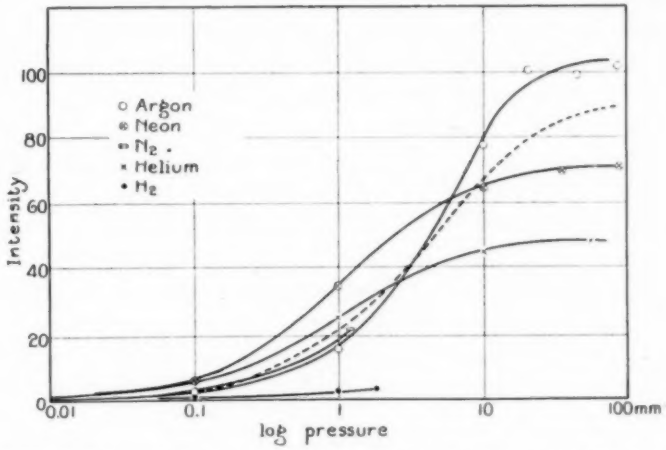

Fig. 2. Relation of intensity of Mg 4571 line to the pressure of foreign gas.

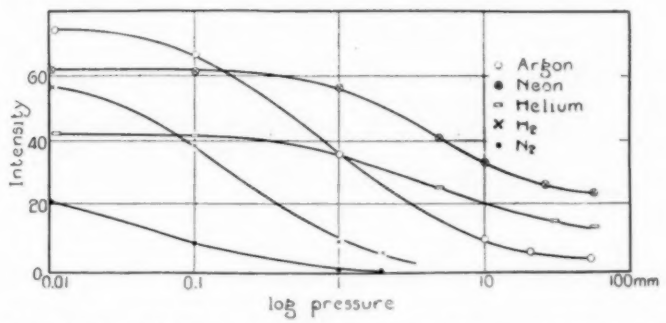

Fig. 3. Relation of intensity of Mg 2852 line to the pressure of foreign gas.

Discussion of Results on 4571.

The curves of Fig. 2 show clearly that of all the permanent gases studied, H_2 alone fails to cause any appreciable increase in the intensity of the 4571 line. Figure 3, however, shows that all the gases bring about a quenching of the 2852 resonance line. The behavior of the 4571 line may be explained as follows. The Mg vapor pressure in the discharge was about 10^{-4} mm and at this low pressure collisions of the second kind of the excited Mg atoms with the walls are very frequent. The introduction of any gas wi l slow up diffusion to the walls, thus diminishing collision with the walls and increasing the possibilities of radiation from the excited 3^3P_1 state. Since the velocity of diffusion varies inversely as the pressure, one would expect the intensity of the line to increase with pressure up to a certain point above which the intensity of the line should remain constant, if there were no collisions of the second kind between the excited Mg atoms and the gas. On the other

hand, the line should show a decrease of intensity if such collisions take place. In this research, it was only possible to attain the "saturation" value of the 4571 line with noble gases in the tube. It was not possible to excite any discharge with N_2, H_2, or CO above a few mm, and consequently, the conditions for obtaining the maximum value of the 4571 line could not be attained. Now Stuart[8] has found that the noble gases are very inefficient in effecting collisions of the second kind with excited atoms. In this research, a slight decrease in intensity of the 4571 line was found in argon above 40 mm, while the intensity appeared to remain constant above 1 cm for neon and helium. This suggests that N_2 impurities are responsible for the slight decrease in argon. Of course, the accuracy of measurement in this type of work is not sufficiently great to detect a small decline in the intensity. The fact that H_2 has little effect on 4571 is probably due to collisions of the second kind between H_2 molecules and the excited Mg atoms. These collisions offset the effect of reduced diffusion to the walls.

Mathematical Theory

The curves in Fig. 2 lend themselves readily to mathematical analysis. Let us consider the tube containing Mg excited atoms distributed across any cross section. We will assume, as above, that these excited atoms undergo collisions of the second kind with the walls of the tube. We will further assume that collisions between Mg excited atoms may be neglected at a pressure of 10^{-4} mm and that there are no collisions of the second kind with the foreign gas present in the tube.

The equation for the steady state in the tube is:

$$\frac{kd^2n}{dr^2}+\frac{k}{r}\frac{dn}{dr}+(c-\tau n)=0$$

where n is the number of excited Mg atoms per cc at a point distant r from the center; k the diffusion coefficient; c the rate at which the excited atoms are being produced; $\tau =$ the transition probability of the excited atoms. The boundary condition is that at the periphery of the tube n shall be zero. On making the substitutions $y=c-\tau n$ and $x=(\tau/k)^{1/2}r=\alpha r$, the equation reduces to

$$\frac{d^2y}{dx^2}+\frac{1}{x}\frac{dy}{dx}-y=0$$

a solution of this equation is:

$$y=a_0\left\{1+\frac{x^2}{2^2}+\frac{x^4}{2^2\cdot 4^2}+\frac{x^6}{2^2\cdot 4^2\cdot 6^2}+\cdots\right\}$$

or

$$n=\frac{c}{\tau}-\frac{a_0}{\tau}\left\{1+\frac{\alpha^2r^2}{2^2}+\frac{\alpha^4r^4}{2^2\cdot 4^2}+\frac{\alpha^6r^6}{2^2\cdot 4^2\cdot 6^2}+\cdots\right\}.$$

[8] Stuart, Zeits. f. Physik **32**, 262 (1925).

If we now let $n=0$ when $r=R$, we may evaluate a_0 and we have

$$n=\frac{c}{\tau}\frac{\frac{\alpha^2(R^2-r^2)}{2^2}+\frac{\alpha^4(R^4-r^4)}{2^2\cdot 4^2}+\frac{\alpha^6(R^6-r^6)}{2^2\cdot 4^2\cdot 6^2}+\cdots}{1+\frac{\alpha^2R^2}{2^2}+\frac{\alpha^4R^4}{2^2\cdot 4^2}+\frac{\alpha^6R^6}{2^2\cdot 4^2\cdot 6^2}\cdots}$$

Now the intensity of the 4571 line will be proportional to the number of atoms in a cross-section of the tube, the number being given by

$$N=2\pi\int_0^R rn\,dr.$$

If we multiply the right hand side of Eq. (1) by $2\pi r\,dr$, and integrate term by term with respect to r, we will have an expression that will be proportional to the intensity of the 4571 line for the given experimental conditions. We obtain

$$N=2\pi c/\tau\left\{\frac{\frac{\alpha^2}{2^2}\frac{R^4}{4}+\frac{\alpha^4}{2^2\cdot 4^2}\frac{R^6}{3}+\frac{\alpha^6}{2^2\cdot 4^2\cdot 6^2}\frac{3R^8}{8}+\cdots}{1+\frac{\alpha^2R^2}{2^2}+\frac{\alpha^4R^4}{2^2\cdot 4^2}+\frac{\alpha^6R^6}{2^2\cdot 4^2\cdot 6^2}}\right\}$$

Since c is unknown we need only evaluate the expression inside the brackets. If we let $R=2$ cm, we obtain the following values

$\alpha^2=0.01$	0.1	1	10	0.100
$N\propto 0.01$	0.094	0.606	1.52	1.75
$p=0.0155$	0.155	1.55	15.5	155

Now $\alpha^2=\tau/k$ and τ is the reciprocal of the natural life of the excited state or $\tau=0.25\times 10^8$. The constant k is rather uncertain as it really is the diffusion constant for excited Mg atoms in a foreign gas atmosphere. We may assume, however, that k is $\lambda c/3$ and for argon under standard conditions this has the value 0.112. When c, the mean molecular velocity, and λ, the mean free path, are corrected for the temperature of 500°C used in the experiment, λ and hence the pressure p may be determined for any of the values of α^2 listed above. When the values of N are plotted against log p, we obtain the broken curve shown in Fig. 2. The scale chosen for N is quite abitrary, but it will be noticed that the curve as drawn is in general agreement with the experimental curves. While the slope of the curve at 1 mm pressure is more nearly like that of neon, than argon, its saturation value is reached around 50 mm which is in fair agreement with the experimental curve for argon. The argon used in this experiment was not very pure and this may account in part for the discrepancy between experimental and theoretical curves. There is also considerable error in experimental values of the intensities. The remarkably close agreement, however, indicates that the life of the Mg 2^3P_1 state must be very nearly 4×10^{-8} sec. If the value were reduced to 2×10^{-8}, the saturation value would occur about 25 mm which would agree very well with experimental data.

This remarkably close fit of the theoretical and experimental curves undoubtedly proves that the general conditions proposed to explain the curves of Fig. 2 are correct. *It proves that collisions of excited metastable atoms with the walls are collisions of the second kind*, and furthermore, proves without any doubt that the *action of a noble gas* particularly argon or neon, *in enhancing lines from metastable states, is one of reducing diffusion to the walls.* Finally, the life of the Mg 2^3P_1 state is proved to be approximately 4×10^{-3} sec.

Discussion of Results on 2852.

It has already been pointed out that the intensity of the 2852 line diminishes with pressure of the foreign gas. Neon and He show the least diminution over the pressure range. Argon and N_2 have a very pronounced effect while H_2 appears to cause the greatest diminution. The same conditions that reduce 2852 also diminish the singlet lines terminating on the 3^1P state. Referred to the triplet line 3838, the 2852 line is diminished to the same extent as the singlet lines. H_2, however, is an exception. Here, the 2852 line shows a diminution of one-thirtieth in the pressure range that reduces the singlets only one fifth. This quenching of the 2852 line must be similar to the quenching of Hg resonance radiation found by Wood,[9] Cario[10] and Stuart. The quenching action of H_2 is attributed to the action of the excited Hg atom in dissociating the H_2 molecule. Since the Mg 3^1P state has an energy of 4.4 equivalent volts, an atom in that state can readily dissociate the H_2 molecule. Mg atoms would then return to the normal state without radiation. This process should in no way involve the intensity of the 4571 line.

In the case of gases other than H_2, the diminution of the singlet lines and the 2852 line cannot be explained as any result of collisions of the second kind. The life of the 3^1P state is one millionth that of the 3^3P_1 state and collisions of the second kind should be far more effective for the state with the longer life. We have already seen, in the case of the noble gases, that collisions of the second kind are ineffective with the 3^3P_1 state, and, accordingly, we can hardly expect them to account for the decrease observed in the intensity of the singlet members. Since the intensities of these singlets are measured with reference to a triplet, it would seem that the higher pressures favor the triplet series rather than the singlets. Similar effects were found by Frayne and Montgomery[7] in Hg vapor in which increased vapor pressure reduced all the singlets relative to the triplets. Professor Ornstein[11] has recently offered an explanation of this differentiation between singlet and triplet lines at high pressures. It appears that higher pressure of the emitting vapor or a foreign gas give similar results.

In conclusion the author desires to thank Professor I. S. Bowen for his many suggestions and advice in interpreting the experimental results. He also wishes to thank Dr. W. V. Houston for assistance in the mathematical work and Dr. M. Muscat for assistance in the experimental work.

[9] R. W. Wood, Phys. Zeits. **13,** 353 (1912) and numerous later papers.
[10] G. Cario, Zeits. f. Physik **10,** 185 (1922).
[11] L. S. Ornstein. Zeits. f. Physik **51,** 34(1928).

NEW TERMS IN THE SPECTRA OF Al I, Ga I, AND In I

By William D. Lansing
University of Illinois

(Received June 15, 1929)

Abstract

The spectra of Al, Ga, and In were investigated in a tungsten vacuum furnace. Lines arising from the term $sp^2\ ^2D$ were discovered in Al I. $A\ ^2P-{}^4P$ combination was found in In I from previous data.

FURNACE spectra offer a very useful means of classifying spectra due to neutral atoms. Temperature excitation is perhaps preferable to electron bombardment because of the large amount of energy involved, requiring only short exposures. The excitation may be varied by changing the temperature, and in addition absorption lines aid in the identification of low terms.

The spectrum of aluminum in the furnace has been investigated by Frayne and Smith[1] and by Sur and Majumdar.[2] Since they list only absorption lines and do not agree even on that, it was thought desirable to repeat the work.

The furnace was a tungsten strip furnace described by Paton and Rassweiler.[3] The under-water spark of copper was used as the continuous source. At a temperature of 1400°C the first two members of the sharp and diffuse series were absorbed. Higher members of these series were out of the range studied. At 1500°C the first members of the sharp series (3961 and 3944A), which are the resonance lines, were emitted. At 1800°C the sharp and diffuse series were emitted, and in addition two lines at 3057.16 and 3050.08A. At about 2200°C the following unclassified lines were emitted.

Table I. *Unclassified lines of Al. Tungsten strip furnace at 2200°C.*

Int.	λI.A.	ν (vac.)	Int.	λI.A.	ν (vac.)
6	3066.16	32604.6	10	3057.16	32700.6
4	3064.31	32624.1	3	3054.69	32727.1
0−	3060.56	32664.3	8	3050.08	32776.5
2	3060.00	32670.3			

These lines are all due to Al I. At 1800°C no known lines of Al II were radiated, and at 2200°C only those lines of Al II belonging to transitions between low terms were observed, and these were weak.

The furnace spectra of gallium and indium were also tried. Absorption of the first few members of the sharp and diffuse series of Ga were observed. No emission of Ga and only very faint emission of the resonance lines of

[1] Frayne and Smith, Phys. Rev. **27**, 23 (1926).
[2] Sur and Majumdar, Phil. Mag. **1**, 451 (1926).
[3] Paton and Rassweiler, Phys. Rev. **33**, 16 (1929).

In was observed. This was probably due to the rapid escape of the heated vapor from the furnace.

Frayne and Jarvis[4] have observed five unclassified lines excited in indium vapor by 6.9v electrons. These lines are obviously low-excitation lines, since they come out with the lines due to low terms.

These lines in Al and In are undoubtedly due to transitions between low terms in the atom. The only low terms having sufficient energy and not already discovered are the b^4P, b^2D, b^2S, and b^2P terms arising from the sp^2 configuration. In Al I the bP terms are known,[5] and the irregular doublet law predicts that the lines $aP-bS$ should lie about 1950A.[6] The separations of the lines are not right for the a^2P-b^4P combination. Three of the lines seem to form a diffuse doublet, and the irregular doublet law confirms the classification which is given below.

TABLE II. *Classification of three Al I lines.*

Int.	λI.A.	ν (vac.)	Δν	Classification
0	3060.56	32664.3		$a^2P_2-b^2D_2$
			36.3	
10	3057.16	32700.6		$a^2P_2-b^2D_3$
			112.2	
8	3050.08	32776.5		$a^2P_1-b^2D_2$

The five indium lines come from the b^4P terms, as shown in the table below. The wave-lengths and intensities are taken from Exner and Haschek and corrected to I. A.

TABLE III. *Classification of five In lines.*

	b^4P_1		b^4P_2		b^4P_3
a^2P_1	2858.19 (1)		2775.36 (1)		—
	34976.9	1043.8	36020.7		
	2212.2		2212.7		
a^2P_2	3051.19 (1)		2957.02 (2*R*)		2836.90 (3*R*)
	32764.7	1043.3	33808.0	1431.4	35239.4

A strong unclassified line due to In I at 2306.07A probably belongs to one of the other terms coming from the configuration sp^2. No such terms of Ga I have yet been observed An unclassified line at 3020A given by Exner and Haschek may come from one of these terms. It is expected that the work on Ga and In will be continued using a tube furnace to prevent escape of the metallic vapor.

The author wishes to take this opportunity to express his acknowledgement to Professor A. P. Carman for the facilities placed at his disposal, and to Professor R. F. Paton for the help and encouragement given during the course of this investigation.

[4] Frayne and Jarvis, Phys. Rev. **29**, 673 (1927).

[5] Bowen and Millikan, Phys. Rev. **26**, 150 (1925).

[6] Selwyn (Phys. Soc. London **41**, 402 (1929)) has discovered a pair of lines in the arc between Al electrodes in nitrogen with wave-lengths 1936.45 and 1932.25. This pair has the separation 112 of Al I exactly, and he rightly attributes it to the $aP-bS$ combination.

THE INFRA-RED ABSORPTION SPECTRA OF ORGANIC NITRATES

By E. K. Plyler and P. J. Steele
University of North Carolina

(Received June 24, 1929)

Abstract

The infra-red absorption of four organic nitrates has been studied in the region from 1.0 to 7.5μ. The liquids used are methyl nitrate, ethyl nitrate, propyl nitrate and butyl nitrate. Two absorption bands at 1.40μ and 2.96μ are attributed either to an OH linkage or water. All other bands are attributed to the carbon-hydrogen linkage and as an additional CH_2 group is introduced, two characteristics appear, namely, the intensity of all bands decreases and a shift of from 0.01 to 0.06μ to longer wavelength occurs. No characteristic absorption spectra of the NO_3 group have been found to exist in the organic nitrates. Previous workers have found that the carbon-hydrogen linkage gives regions of intense absorption at about 3.43, 6.86, 8 to 10 and 12 to 18μ. In the present work an intense band was observed at 6.7μ but the observations were not carried past 7.5μ and the other two fundamental frequencies were not observed. However, from observed bands there has been calculated four regions of intense absorption, which are assumed to be the fundamental frequencies and all other bands observed are attributed to a combination or overtones of these fundamentals.

ORGANIC liquids which contain carbon and hydrogen have been found to have many similarities in their infra-red absorption bands and some success has been had in identifying the bands as due to certain groups of atoms within the molecule. A good idea of the energy changes which give rise to the absorption spectra has been obtained in methane from the experimental work of Cooley[1] and the theoretical work of Dennison.[2] Easley, Fenner and Spence[3] have studied the halogen derivatives of methane and have found the effects produced by the substitution of the halogens for hydrogen. The present investigation was undertaken to see what modifications are produced in the infra-red absorption bands of the methyl, ethyl, propyl and butyl groups by having a nitrate ion used instead of a single atom. Also, it is of interest to note the absorption spectrum of the nitrate ion in organic compounds so that it may be compared with the absorption spectrum of the nitrate ion in inorganic compounds.

Experimental Procedure

A Hilger infra-red spectrometer with a quartz prism was used from 1 to 2.6μ, the slit including about 0.02μ. The readings were taken at intervals of 0.02μ but the individual points are not shown on the curve to avoid crowding. The absorption cell was made by separating two pieces of glass with lead or

[1] Cooley, Astrophys. J. **62**, 73 (1925).
[2] Dennison, Astrophys. J. **62**, 84 (1925).
[3] Easley, Fenner and Spence, Astrophys. J. **67**, 185 (1928).

lead foil. In this way cells of the necessary thickness could be obtained. From 2.6μ to 7.5μ a rock-salt prism was used, the effective slit width being about 0.07μ at 6.5μ. Microscope cover glasses were used for the windows of the cells from 2.6 to 4.5μ and then rock salt, cut and polished, was used

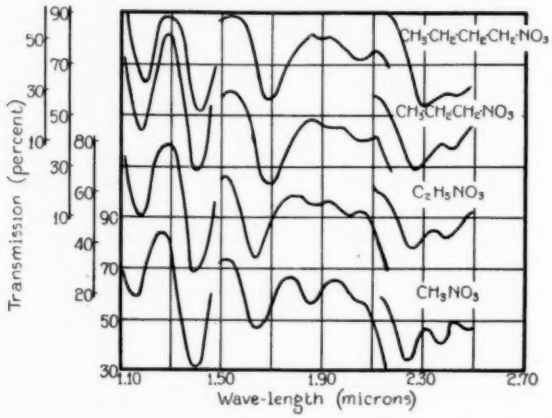

Fig. 1. The infra-red absorption spectra of methyl, ethyl, propyl and butyl nitrates from 1.1 to 2.5μ. The thickness of cells used: 15 mm from 1 to 1.5μ; 0.5 mm from 1.5 to 2.2μ; 0.3 mm from 2.2 to 2.5μ.

from 4.5 to 7.5μ. No correction was made for the loss of intensity at the windows; this usually amounted to about 10 or 15 percent. In some cases it was found necessary to seal the windows on to the lead or foil and Le Page's glue was used for this purpose. Some cells were made with the glue and

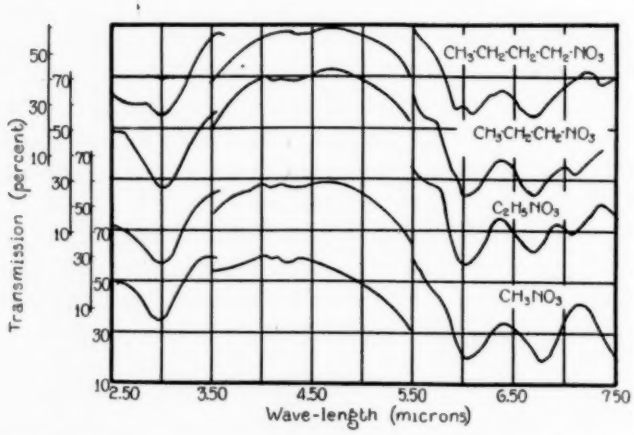

Fig. 2. The infra-red absorption spectra of methyl, ethyl, propyl and butyl nitrates from 2.5 to 7.5μ. The thickness of cells used: 0.12 mm from 2.5 to 5.5μ; 0.03 mm from 5.5 to 7.5μ.

some without it, but no difference greater than would be expected due to observational errors was found between the two types of cells.

The organic liquids for this work were prepared by standard methods in the chemical laboratory of the University of North Carolina. The liquids

were dried over an excess of calcium nitrate until the vapor pressure of the liquid became equal to the vapor pressure of the drying agent. This was done to render the liquids water free. The liquids prepared for this study are methyl nitrate, ethyl nitrate, propyl nitrate and butyl nitrate.

Results and Discussion

A complete curve for each liquid is given in Fig. 1 and in Fig. 2. Since the bands cannot be located from these curves with accuracy on account of the small scale used, a list of all bands observed is given in Table I.

Table I. *List of all observed absorption bands between 1 and 7.5μ.*

Methyl Nitrate	Ethyl Nitrate	Propyl Nitrate	Butyl Nitrate
1.16μ	1.18μ	1.18μ	1.20μ
1.40	1.40	1.40	1.42
1.64	1.64	1.68	1.70
1.86	1.86	2.06	2.06
2.02	2.02	2.28	2.30
2.24	2.26	2.40	2.44
2.36	2.38	2.58	2.58
2.48	2.54	3.02	3.02
2.96	3.02	4.30	4.28
4.12	4.34	6.04	5.92
4.30	6.04	6.70	6.10
6.02	6.70	7.06	6.70
6.74	7.06		6.88
			7.12

By comparing the curves certain characteristics are seen. The intensity of the bands decrease as the CH_2 group is introduced between the CH_3 and NO_3 groups. The first band, which occurs at 1.16, 1.18 and 1.20μ in the methyl, ethyl, propyl and butyl nitrates, respectively, has a percent transmission of 60 in the methyl, 50 in the ethyl, 45 in the propyl, and 35 in the butyl. The other intense bands, except those at 1.40μ and 2.96μ, decrease similarly in percent transmission as the complexity of the molecule is increased, although there is no uniformity in the amount of decrease. There is a very noticeable tendency of the bands to shift to longer wave-lengths as a CH_2 group is introduced. The first band observed in this work at 1.16μ in methyl nitrate shifts to 1.18μ in the ethyl and propyl nitrates and to 1.20μ in the butyl nitrate. This shift to longer wave-lengths occurs in the bands at 1.16, 1.64, 2.24, 2.36, 2.48 and 4.30μ in the methyl nitrate and corresponding bands in the other liquids.

The bands at 1.42μ and 2.96μ show very little change in intensity or in position for the different nitrates. This probably shows that these bands are produced in a different way from the characteristic bands of the CH linkage[4] which have just been noted. At first it was thought that these bands were produced by the nitrate ion. By the work of Schaefer and Schubert[5] the

[4] In accordance with the custom of other observers some bands are attributed to energy changes of certain groups of atoms in the molecules (such as CH linkage). However, it is more accurate to consider each band as produced by an energy change of the molecule as a whole rather than by certain groups of atoms within the molecule.

[5] Schaefer and Schubert, Ann. d. Physik 577 (1918).

fundamentals of the bands of nitrate ion are about 7.3μ, 13.74μ and 15.58μ. We would expect to find overtones and combination bands in the near infra-red region. Since no bands of much intensity were observed between 3.5μ and 5.5μ, it must be concluded that the bands at 1.42μ and 2.96μ are not higher overtones or combination bands including overtones which may be attributed to the nitrate ion.

These bands may be attributed to a rearrangement within the molecule so that a hydrogen atom becomes associated with one of the oxygen atoms of the nitrate ion. This change within the molecule does take place in the NO_2 group and if present in nitrate ion would probably cause all the nitrate bands to be modified. If this re- arrangement takes place, there would be characteristic OH bands as found in alcohol. These bands occur for the alcohols at about 1.57 and 3.06μ.

The bands at 1.42μ and 2.96μ may also be due to a small amount of water left in the liquid when it was made or taken up by it from the air. From the work of Collins[6] the water bands in this region occur at 1.44μ, 1.95μ and 3.00μ for room temperature and Coblentz[7] has measured the water bands in the longer wave-length region to be at 4.75 and 6.00μ. In all the liquids an intense band was found at 6.00μ. There is considerable doubt as to what causes these bands may be attributed, but from their position in the spectrum and intensity t does not seem probable that they are produced by the CH linkage or the nitrate group.

It is remarkable that no bands which are very intense may be attributed to the nitrate ion. Only in the region from 7μ to 7.5μ are found bands which correspond to the inorganic nitrates. The intensity of these bands are much sma ler than for the inorganic nitrates and it may be that these bands are not due to the nitrate ion but to the CH linkage. A 20 percent solution in water of potassium, calcium, lead and lithium nitrates in each case showed very intense bands with maxima of absorption occurring between 7.15 to 7.4μ for the different solutions. Pringsheim[8] has been able to get strong Raman lines which indicate a band at about 7.2μ for the nitrates in a solution of water.

It is evident that the nitrate ion in organic compounds does not produce bands at all similar to the nitrate ion in inorganic compounds. This difference in the two types of compounds is probably due to the influence of the CH group on the nitrate ion in the organic compounds.

An attempt has been made to classify the bands which may be attributed to the CH linkage. E lis[9] made a study of a number of compounds and found that all the near infra-red bands of CH compounds could be attributed to overtones of the fundamental at 6.44μ. Barnes and Fulwei'er,[10] and later

[6] Collins, Phys. Rev. **26**, 771 (1925).
[7] Coblentz, Investigations of Infra-Red Spectra, Part 3, Page 17.
[8] Pringsheim, Zeits. f. Physik **50**, 741 (1928).
[9] Ellis, Phys. Rev. **27**, 298 (1926).
[10] Barnes and Fulweiler, Jour. Am. Chem. Soc. **49**, 2034 (1927).

Ellis,[11] showed that the band at 3.28μ must be an overtone. Easley, Fenner and Spence[3] found that it was necessary to assume four fundamental frequencies in order to account for the bands observed by them in the halogen derivatives of methane. One of the writers has shown that all organic liquids,

TABLE II. *Combinations of the intense observed bands.*

Methyl	Ethyl	Propyl	Butyl Nitrate	Combinations
obs.	obs.	obs.	obs.	
1.16μ	1.18μ	1.18μ	1.20μ	$3\nu_1$
1.64	1.64	1.68	1.70	$2\nu_1$
1.86	1.86			$\nu_1+\nu_2+\nu_3$
2.06	2.02	2.06	2.06	$\nu_1+\nu_3+\nu_4$
2.24	2.26	2.28	2.30	$\nu_1+\nu_2$
2.36	2.38	2.40	2.44	$\nu_1+\nu_3$
2.48	2.54	2.58	2.58	$\nu_1+\nu_4$
6.74	6.70	6.70	6.70	ν_2

containing carbon and hydrogen, which have been measured thus far have a system of bands in near infra-red with many similar characteristics. It was shown that if four fundamentals are assumed for the carbon-hydrogen compounds, all the more intense bands in the near infra-red can be arranged in a similar series by attributing the bands to the overtones and combinations of the fundamentals. In addition to this series there occurs in some compounds another series of bands which may be attributed to other groups within the molecule, such as an OH group. In Table II the close similarity between the different nitrates studied is readily seen. Due to the great intensity of the band at 3.00μ, the fundamental at about 3.35μ, ν_1, scarcely appears.

The fundamental at 6.70μ, ν_2, has been observed in the four compounds and the position is almost the same for each one, but the complexity of this band increases as each CH_2 group is added.

Three intense bands have been observed at 2.24, 2.36 and 2.48μ in methyl nitrate and corresponding bands in the other nitrates. By comparison with the absorption bands of benzene and other organic liquids containing only carbon and hydrogen, these bands are attributed to the combinations $\nu_1+\nu_2$, $\nu_1+\nu_3$, and $\nu_1+\nu_4$, where ν_3 denotes the fundamental which has a wave-length from 8 to 12μ, and ν_4 the fundamental from 12 to 18μ.

The wave-length of ν_1 may be calculated from the two overtones observed at 1.16μ and 1.64μ for methyl nitrate and at corresponding positions for the other nitrates. Since only one of the fundamental bands has been observed in the experimental work, it was found that most of the observed bands must be considered also as calculated values in order to find the wave-length of the fundamentals. For this reason only the observed bands are given in Table II and the combination is assigned by analogy to the absorption spectra of other organic compounds. These combinations will be discussed more fully in a future paper which will treat of various types of absorption bands found in organic liquids.

[11] Ellis, Phys. Rev. **31**, 310 (1928).

THE INFRA-RED ABSORPTION SPECTRUM OF HYDROGEN SULPHIDE

By A. H. Rollefson
University of Wisconsin

(Received June 27, 1929)

Abstract

The infra-red absorption bands of hydrogen sulphide in the regions of 4.2, 5.6, and 8.0μ were investigated by means of a prism-grating spectrometer. A narrow, intense absorption band was observed at 4.2μ, but could not be resolved. The 5.6μ band observed by Coblentz was not found. Evidence is presented to show that the band observed by Coblentz might have been due to an impurity. Thirty-four lines of the band in the region of 8.0μ were observed.

THE analysis of the fine structure of the infra-red absorption bands of gases in connection with its bearing on molecular structure has been very satisfactory in the case of the diatomic gases. For triatomic molecules, however, the spectra observed have usually been too complex to permit analysis of the fine structure. Water vapor has been extensively studied but without yielding very satisfactory results. With the resolving power of the present instruments, good resolution can be obtained only for those molecules which have small moments of inertia, i.e., those molecules which contain only one atom heavier than hydrogen.

The purpose of the present investigation was to study the fine structure of the infra-red spectrum of hydrogen sulphide in the hope that it might yield a fine structure more readily analyzed than that of water vapor or, in any case, that it would furnish additional data for the study of triatomic molecules.

Coblentz,[1] using a low dispersion prism spectrometer, found weak absorption bands for hydrogen sulphide at 4.24, 5.60, 7.12, 7.78, 8.46, 9.65, 10.08, 10.7, and 11.0 microns. The author has investigated a considerable portion of this region with a high dispersion grating spectrometer. No fine structure was obtained in the case of the 4.2 micron band, but 34 lines were observed in the region of 8 microns.

Apparatus

The apparatus was an auto-collimating, prism-grating spectrometer very similar in design to that used by Sleator and others at the University of Michigan.[2] Radiation from the source was focused on the slit of the double spectrometer by a mirror of 20 cm focal length. The absorption cell was placed immediately ahead of this slit. The prism spectrometer produced a spectrum which was brought to a focus on the slit of the grating spectrometer.

[1] Coblentz, "Infra-Red Spectra." (Washington, 1905).
[2] Sleator, Astrophys. J. **48**, 125 (1918).

After dispersion by the grating, the radiation was focused on an adjustable slit behind which was placed the receiving thermopile. The focal length of the mirrors of the spectrometer was 40 cm.

The double spectrometer was inclosed in a wood case which was sealed to the table top with paraffin. The top portion of the case could be swung out of the way when adjustments were being made. The edges of the top and base which came in contact were lined with felt weather-strips to make a fairly tight joint. The source S was mounted in a separate case together with the first mirror and the absorption cell. The joints of this case were also sealed with paraffin and the case was sealed directly to the spectrometer case, the only opening between the two being the first slit. The top was removable.

The apparatus was thus protected from air currents and rapid fluctuations of temperature. The air in the case was partially dried by means of calcium chloride and sulphuric acid to protect the rock-salt prism and the rock-salt windows of the absorption cell. A quantity of potassium hydroxide was placed in the case to absorb any hydrogen sulphide which might escape from the absorption cell.

The source of radiation was a d.c. Nernst glower. The glowers used were rated at 0.8 and 1.2 amperes but were operated on a considerably lower current as it was found that this increased the life of the glower without materially decreasing the energy available in the regions under investigation. The glower was surrounded by a water jacket which absorbed most of the heat liberated by the glower.

The prism was a thirty degree rock-salt prism mounted on a table especially constructed for this purpose in these laboratories. A plane mirror was mounted directly behind the prism so as to reflect the light back through the prism at an angle not far from minimum deviation.[2]

The gratings. The gratings were ruled at the University of Michigan by Dr. Barker and were made available through the kindness of Professor H. M. Randall. They were of the echelette type ruled with 2880 lines to the inch. Two gratings were used, one of which concentrated energy in the region from 3.5 to 6.0 microns; the other from 5.0 to 9.0. These are later referred to as gratings $A10$ and $A6$ respectively.

The gratings were mounted on a spectrometer table the scale of which could be read to one minute intervals by means of a vernier. A slow motion screw on the grating circle was calibrated so that settings could be made by measuring the angle through which the screw had been turned, the circle being used only for reference. This method gave consistent results and permitted setting at smaller intervals. The circle was read by means of a telescope mounted outside the case.

The thermopile and galvanometer. The thermopile was a Coblentz 14-junction, Bi-Ag linear thermopile, of 9.6 ohms resistance, mounted directly behind an adjustable slit which was calibrated so that the slit width could be read from a micrometer screw. The surface of the receivers was 13 mm by 1 mm which was sufficient to collect all the energy falling on the slit for a slit

width of 0.5 mm or less but did not utilize the full amount of energy for a 1 mm slit. The thermopile was enclosed in a brass case with limiting diaphragms in front and mounted on a heavy tripod. The case was surrounded by a wood box filled with cotton for better thermal insulation.

The current from the thermopile was measured by means of an iron-clad, astatic galvanometer with a resistance of 4.5 ohms. While the galvanometer usually had to be adjusted at the beginning of each run, no difficulty was found in securing a sensitivity of 1×10^{-10} amperes per millimeter deflection with a lamp and scale at a distance of two meters. Occasional difficulty was experienced with a pronounced shift of the zero position of the galvanometer upon closing the circuit through the thermopile. As this shift varied considerably in magnitude, it was attributed to a thermal e.m.f. some place in the circuit. This e.m.f. was compensated for by impressing an opposing e.m.f. on the circuit so as to bring the galvanometer back approximately to its position on open circuit.

The absorption cells. Two absorption cells were used, one with mica windows and the other with rock-salt windows. The mica cell was a brass tube 5″ by 2.5″ with the ends cut at an angle of sixty degrees with the axis of the tube to eliminate interference effects due to the thin mica windows.[3] The mica windows were mounted with a wax made of beeswax and resin and the inside of the cell was coated with paraffin to prevent the action of the hydrogen sulphide on the brass walls. The cell was provided with a side tube at either end for introducing the gas to be investigated. Compensating windows of mica were mounted on a support attached to the cell and the cell was mounted so that either the cell or the compensating windows could be swung into the path of the light. Each window and its corresponding compensating window were cut from the same piece of mica which had been tested between crossed nicols to insure uniformity of thickness.[3]

The rock-salt cell was constructed in a similar manner except that the ends were normal to the axis of the cell. This cell was 6″ long and 2″ in diameter. The rock-salt windows were plates about 3/16″ thick split from a crystal of rock salt, ground flat on sandpaper and emery cloth, and polished with rouge and water on a block of pitch made of turpentine and resin.

The hydrogen sulphide was generated in a Kipp generator using calcium sulphide and dilute hydrochloric acid. The gas was washed by bubbling it through water and dried by passing it over calcium chloride and phosphorus pentoxide. The cell was filled by flushing it for a short time with the gas, the effluent being absorbed by a solution of sodium hydroxide.

Adjustments and Method of Taking Data

All adjustments were made by means of visible light. The zero position of the grating was determined by taking an energy curve with the grating turning through the zero position and finding the position of maximum energy. Grating *A*10 was calibrated by measuring five absorption lines of

[3]Meyer and Bronk, Astrophys. J. **59**, 252 (1924).

HCl and using the wave-lengths given by Colby and Meyer.[4] A check was made by taking an energy curve to show the absorption of the atmospheric CO_2 in the path of the light and comparing the results with those obtained by Barker.[5] Grating *A*6 was calibrated by measuring the absorption of atmospheric CO_2 and comparing the curve with that obtained with grating *A*10. The grating constant was found to be the same for both gratings, $K=17.612$ microns.

The wave-length of the radiation falling on the thermopile is given by[6]

$$\lambda = K \sin\theta \tag{1}$$

where θ is the angle through which the grating has been turned from its zero position, and K is the grating constant. We may calculate the range of wave-lengths included in the slit by means of the formulae:[7]

$$d\lambda = K\cos\theta d\theta, \quad d\theta = d/2f \tag{2}$$

where θ is the grating angle as above, $d\theta$ is the change in the grating angle to move the center of the image of the slit across the thermopile slit, f is the focal length of the mirror, d is the slit width, and K is the spectrometer constant.

Observations were taken by setting the prism and grating at known positions and observing the deflections of the galvanometer with the absorption cell alternately in and out. Several readings were taken at each point. The absorption was taken as the ratio of the difference between the readings of the galvanometer with the cell in and the cell out to the deflection with the cell out. In measuring the absorption in a particular region, the grating was set at a definite angle which was read on the grating circle by means of the short focus telescope mounted outside the case. The grating angle was then changed by means of the micrometer screw previously mentioned.

The correction for slit width is small and does not need to be considered in this type of work. The readings were reduced to the same temperature, 20°C. No correction was made for the difference in absorption between the cell windows and the compensating windows because this difference was small and would not affect the frequencies of the absorp-

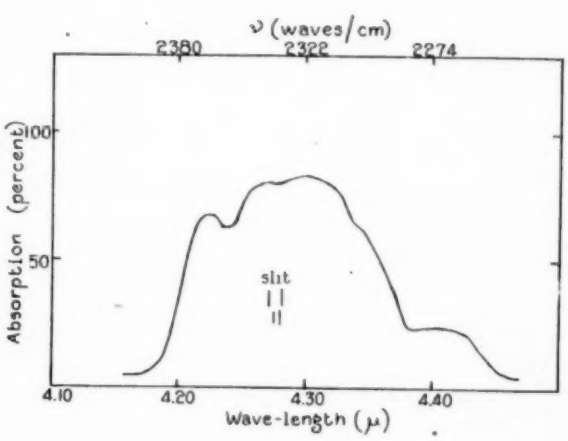

Fig. 1. 4.2μ band.

[4] Colby and Meyer, Astrophys. J. **53**, 302 (1921).
[5] Barker, Astrophys. J. **55**, 391 (1922).
[6] Sleator, Astrophys. J. **48**, 125 (1918).
[7] Imes, Astrophys. J. **50**, 251 (1919).

tion lines. We are interested in the frequencies rather than in the absolute absorption.

Results

4.2 micron band. The absorption in this region is shown in Fig. 1. The entire curve was gone over at least twice with $\frac{1}{2}$ mm slits. Portions of the curve were investigated with $\frac{1}{4}$ mm slits but no indication of fine structure was obtained. For this region, the mica cell was used. A few check points were taken later with the rock-salt cell and were found to agree very well.

5.6 micron region. The region from 4.83 to 6.48 microns was investigated for absorption with 0.5 mm slits but no indication of absorption was found.

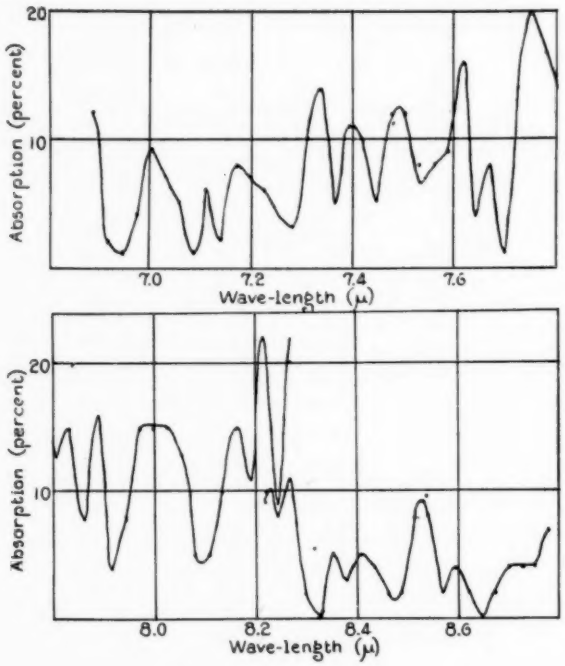

Fig. 2. Preliminary run.

In order to facilitate rapid exploration, observations were taken by watching the galvanometer reading as the cell was moved alternately in and out. If no change was observed, this was taken as an indication that there was no absorption. At the end of one of the runs, the absorption in the 4.2 micron region was checked in the same manner and a maximum absorption of about 90 percent was found, indicating that the cell was well filled with hydrogen sulphide.

Coblentz[1] gives an absorption band at 5.6 microns with a maximum absorption of 17 percent as compared with 21 percent in the case of the 4.2 micron band. With our narrower slit, we should have expected to find a region of very strong absorption, at least 50 percent, if this band is a real hydrogen sulphide band. Coblentz shows an absorption band for SO_2 in this

region which is almost identical with that which he gives for H_2S,—and it is the only band which shows any similarity. In the case of SO_2, he gives two curves, one for ordinary SO_2 and the other for the same gas when purified by fractional liquefaction and distillation. The two curves practically coincide except for a marked change in the intensity of the 5.6 micron band. It is quite possible, therefore, that the 5.6 micron band which he observed may have been due to an impurity which was present in both cases.

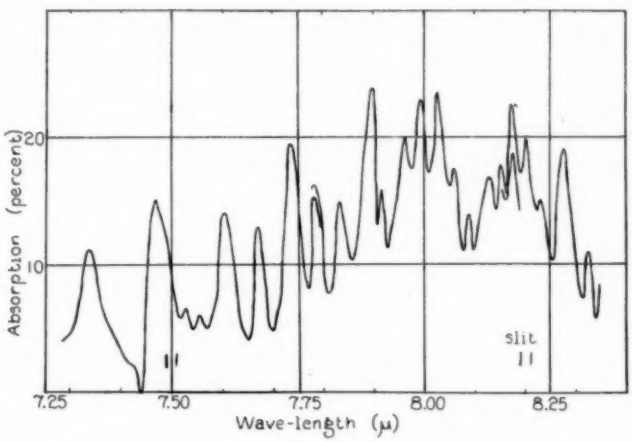

Fig. 3. Final run.

8.0 micron region. The results for this region are shown in Fig. 2, Fig. 3 and Table I. The entire region from 6.89 to 8.78 microns was covered in a preliminary survey taking readings at intervals of 0.027 microns. The portion from 7.3 to 8.35 microns was covered by a more careful survey with readings taken at intervals of 0.009 microns, a small portion (from 8.35 to 8.15 microns) being taken at intervals of 0.0045 microns.

TABLE I. *Observed lines. 8.0 micron region.*

Line No.	L (μ)	Wave-No. (waves/cm)	Line No.	L(μ)	Wave-No. (waves/cm)
1	6.885	1453.4	15	7.994	1250.9
2a	7.000	1428.6	16	8.026	1245.9
2b	7.040	1420.5	16b	8.058	1241.0
3	7.115	1405.5	17	8.088	1236.4
4a	7.180	1392.8	18	8.126	1230.6
4b	7.235	1382.2	19	8.150	1227.0
5	7.335	1363.3	20	8.175	1223.2
6	7.402	1351.0	21	8.208	1218.3
7	7.480	1336.9	21b	8.232	1214.7
8	7.607	1314.6	22	8.276	1208.3
9	7.671	1303.6	23	8.325	1201.2
10	7.739	1292.2	24a	8.360	1196.2
11	7.785	1284.5	24b	8.410	1189.1
12	7.835	1276.3	25	8.527	1172.7
13	7.893	1266.9	26	8.594	1163.6
13b	7.916	1263.3	27a	8.71	1148.1
14	7.963	1255.8	27b	8.78	1139.0

As the available energy in this region was small, it was necessary to work with 1 mm slits, but in spite of this handicap a considerable amount of fine structure was obtained. Unfavorable weather conditions combined with lack of time prevented the duplication of the entire curve. It was possible, however, to duplicate portions of the curve and the results were of such a nature that the author feels confident that the remainder of the curve cannot be in error to any great extent. The energy available on the long wave-length side of the curve was small and this difficulty, combined with those mentioned above, precluded the extension of the curve to longer wave-lengths. On the short wave-length side, the absorption of the water vapor in the air became troublesome and it was not considered feasible to carry the observations further into this region under existing conditions.

The wave-lengths and wave-numbers of 34 lines observed in this region are given in Table I. Good agreement is found between the preliminary and final curves in every case except for the two lines designated as 6 and 18 respectively. It is hoped that these data may aid in the development of the theoretical interpretation of the band structure for triatomic molecules.

In conclusion, the author wishes to express his appreciation to Dr. C. E. Mendenhall for his advice and encouragement throughout the investigation and to Dr. L. R. Ingersoll for his assistance in the last part of the experimental work.

THE CATHODE DROP IN AN ELECTRIC ARC

By S. S. Mackeown
California Institute of Technology, Pasadena, California

(Received March 14, 1929)

Abstract

By making the assumption that the total cathode drop occurs in a distance less than one mean free path from the cathode, Poisson's equation can be solved. If the experimental values of 4000 amperes per square centimeter, and 10 volts are used for the current density at the cathode, and the cathode drop in a mercury arc, values for the electric field existing at the surface of the cathode can be determined for varying percentages of the current carried by positive ions. If 5% of the current at the cathode is carried by positive ions, the field existing at the surface of the cathode exceeds 5×10^5 volts per cm. This is probably sufficient to furnish the necessary electron current by "field" currents produced by this high field. The whole cathode drop occurs within a distance of approximately 2×10^{-5} centimeters, so that the original assumption is justified.

AN ARC is differentiated from a glow discharge primarily by the current density at the cathode and the magnitude of the cathode drop. In a glow discharge the current density at the cathode is normally a small fraction of an ampere per square centimeter, and the cathode drop is usually greater than 100 volts. In an arc, on the other hand, the current density at that portion of the cathode which is carrying current, is of the order of hundreds or thousands of amperes per square centimeter and the cathode drop is of the order of 10 volts. From these facts it can readily be concluded that in the case of a glow discharge most of the current at the cathode is carried by positive ions and only a small percentage by free electrons leaving the cathode. On the other hand in the arc the current is carried primarily by free electrons leaving the cathode and a smaller amount by the positive ions striking the cathode.

In the case of an arc, in which the cathode is not a heated filament, the free electrons have generally been thought of as thermions emitted by the cathode "hot spot."[1] Recently, however, Langmuir[2] has suggested that the positive space charge, causing the cathode drop, may exert a strong enough electric field at the surface of the cathode to cause a large "field" current from the cathode, even though the latter may be too cool to emit thermions. Compton[3] has developed this idea further and from energy considerations believes that in the mercury arc the electrons emanating from the cathode are due primarily to a high electric field and not to thermal emission. The purpose of the present analyses is to show that such a theory is consistent with such data as are available.

[1] Compton, Phys. Rev. **32,** 492 (1928).
[2] Langmuir, G. E. Rev. **26,** 735 (1923); Science **58,** 290 (1923).
[3] K. T. Compton, Jour. A. I. E. E. **46,** 1192 (1927).

The electric field existing at the surface of the cathode, for any given current density of electrons and positive ions, and for a given cathode drop can be determined by using Poisson's equation. If distance and potential difference are measured from the boundary of the cathode drop farthest from the cathode, then Poisson's equation gives

$$\frac{d^2V}{dx^2}=-4\pi\rho=-4\pi\left(\frac{j}{v}-\frac{i}{u}\right) \tag{1}$$

where j and i are the current density carried by the positive ions and electrons respectively, and v and u are the velocities of the positive ions and electrons. We will assume now that the whole cathode drop occurs within one mean free path. This assumption will be found to be consistent with the results obtained from the solution of this equation. Then both j and i are constant and independent of x. Moreover the velocities v, and u, are given within the cathode drop by the following equations:

$$\tfrac{1}{2}Mv^2=Ve \qquad\qquad \tfrac{1}{2}mu^2=(V_c-V)e \tag{2), (3}$$

where M is the mass of the positive ion, m, the mass of the electron and V_c is the potential of the cathode. Substituting in Eq. (1) the values of v, and u from equations (2) and (3) we obtain

$$\frac{d^2V}{dx^2}=-4\pi\left[j\left(\frac{M}{2Ve}\right)^{1/2}-i\left(\frac{m}{2(V_c-V)e}\right)^{1/2}\right] \tag{4}$$

This can readily be integrated once and gives

$$E^2=\left(\frac{dV}{dx}\right)^2=16\pi\left\{j\left(\frac{MV}{2e}\right)^{1/2}+i\left(\frac{m(V_c-V)}{2e}\right)^{1/2}-i\left(\frac{mV_c}{2e}\right)^{1/2}\right\} \tag{5}$$

when the boundary condition, that $\partial V/\partial x=E=0$ when $x=0$, is assumed. This expression does not integrate into a simple function and it is simpler and better to proceed with a graphical integration. Equation (5) can be rewritten as

$$E^2=7.57\times10^5\left\{j(1845WV)^{1/2}-i\left[(V_c)^{1/2}-(V_c-V)^{1/2}\right]\right\} \tag{6}$$

where E is measured in volts per cm, j and i in amperes per cm^2, V and V_c in volts, and W is the ordinary atomic weight of the positive ion.

The value of the electric field at the cathode is given by

$$E_c^2=7.57\times10^5(V_c)^{1/2}\left\{j(1845W)^{1/2}-i\right\}. \tag{7}$$

This equation will serve to determine the field existing at the cathode provided the values of the cathode drop (V_c), the density of the positive ion current reaching the cathode (j) and the density of the electron current from the cathode (i), are known.

For the case of the mercury arc no reliable data are available to determine the values of j and i, accurately. The cathode drop V_c, lies close to 10 volts.[4]

[4] Killian, Phys. Rev. 31, 1122 (1928).

The current density at the cathode $(i+j)$ is given as 4000 amperes per square centimeter.[5] Using these values we can calculate E_c for varying ratios of j to i. This has been done and the results plotted in Fig. 1. This curve shows that for values of $j=0.05i$ the field at the cathode exceeds 5×10^5 volts per centimeter and for $j=0.30i$ this field exceeds 1.3×10^6 volts per centimeter. There are no data available for the electric field necessary to produce an electron current of 4000 amperes per square centimeter from a mercury surface. In this laboratory it has been found that the field at which current begins to appear from a tungsten wire in a vacuum is variable, being very much lower for the case of a surface contaminated by impurities than for a clean surface that has been "conditioned." Moreover the current increases extremely rapidly as the field is increased beyond that necessary to produce the first perceptible current. Since mercury has a lower work function than tungsten, it is probable that an electron current could be produced by a lower field in the case of mercury than in the case of tungsten. Since the surface of

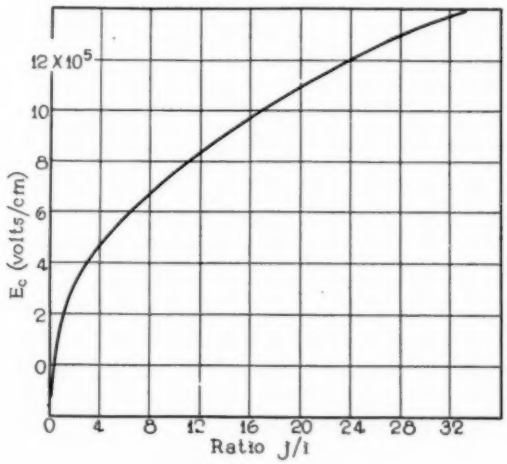

FIG. 1

the mercury is covered with impurities it is reasonable to suppose that a field of the order of 5×10^5 volts per centimeter is sufficient to produce an electron current of 4000 amperes per centimeter square. It is probable that the ratio of j to i does not stay constant at the cathode but may vary, increasing as the surface of the cathode becomes "conditioned," and thus producing a larger field. The fact that the cathode spot moves so rapidly about the surface of the mercury may be explained by the fact that the surface acting as cathode is quickly conditioned by the discharge and that the spot moves to a neighboring position where the mercury surface is contaminated by impurities, and where electrons can be extracted more readily by the electric field. Not only does the cathode spot move rapidly over the surface of the mercury but the mercury surface is depressed. Very probably the electrons come from the irregular edge of this crater which then is immediately depressed, due to the vapor pressure of the mercury which is heated by the bombardment of positive ions at the cathode spot. This would

[5] Güntherschulze, Zeits. f. Physik **11**, 74 (1922).

also account for the rapid movement of the cathode spot, since the electrons always come from the edge of the crater, which is then depressed by the increased vapor pressure at that point.

Equation (5) has been solved graphically on the assumption that $j=0.05i$. This graphical solution gives both the potential V and the electric field E as a function of the distance from the cathode. In Fig. 2 both the electric field and the potential, measured now from the surface of the cathode have been plotted against the distance from the surface of the cathode. It is seen that practically the whole cathode drop occurs within less than 3×10^{-5} centimeters from the surface of the cathode. As this distance is less than the mean free path of a mercury molecule at the temperature generally existing in the mercury arc, the original assumption is justified.

If it is assumed that a field as great as 1.3×10^{6} volts per centimeter is necessary to produce an electron "field" current of 4000 amperes per square centimeter, then $j=0.30i$ and the cathode drop will occur within a distance of 10^{-5} centimeters from the surface of the cathode.

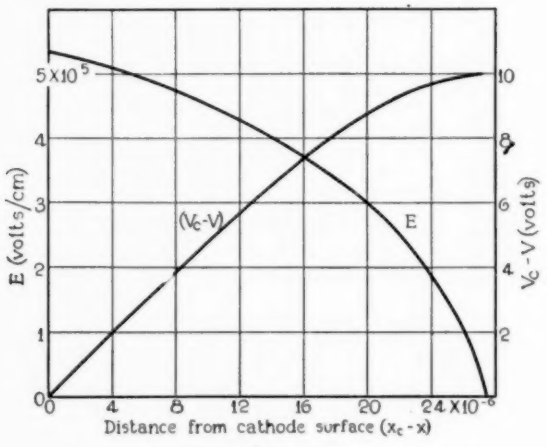

FIG. 2

It should be noted that the assumption has been made that the density of electricity ρ is continuous. This is not true when we consider distances as small as 10^{-5} centimeters. Poisson's equation however may be used if ρ is considered as a time average of the density of electricity. Actually the field existing at the surface of the cathode will be greater than that calculated due to the fact that ρ is not continuous.

Probably in most electric arcs, even in air, electrons are pulled from the surface of the cathode by the high electric field existing there. In certain cases, as for instance in the carbon or tungsten arc, the temperature of the cathode spot is high enough so that probably thermions contributed also to the "field" currents produced by the high electric field existing at the cathode.

In conclusion it may be stated that if five percent of the current reaching the cathode of a mercury arc, is carried by positive ions, there must exist at the surface of the cathode an electric field of approximately 5×10^{5} volts per centimeter. It is believed that this field is adequate to produce the electron current necessary for the maintenance of the arc.

THE DIELECTRIC CONSTANTS OF ARGON AND NEON

By A. B. Bryan
Department of Physics, Rice Institute

(Received July 3, 1929)

Abstract

The heterodyne beat method has been used to measure at room temperatures the dielectric constants of argon and neon relative to air. The value for air is assumed to be 1.000589 and the values found for argon and neon are 1.000574 and 1.000148 respectively, for normal temperature and pressure. Simultaneous refractive index measurements agree with previous determinations and indicate that the gases contain no appreciable impurities. An oscillator employing a shield grid tube is described for which the frequency is very little affected by changes in the various battery voltages.

Apparatus

THE heterodyne beat method has been used to measure the dielectric constants of argon and neon. The apparatus is a modification of that used in a previous work.[1] Two radio frequency oscillators are used, a 1651 kc crystal controlled oscillator of an ordinary type and the special shield grid oscillator shown in Fig. 1. The frequency of the beat note between these two oscillators is compared with that of an electrically driven tuning fork as in the previous work. Capacity changes caused by changing the gas pressure in the test condenser C are compensated by changing the capacity of condenser Cc, thus maintaining a constant frequency as indicated by a constant beat note. The condensers C and Cc and the arrangement for varying

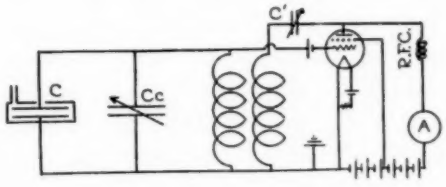

Fig. 1. Shield grid oscillator.

the gas pressure are the same as previously used. However, the test condenser has been dismantled and reassembled and its capacity is apparently now larger than before. A Jamin refractometer has been attached to the apparatus to permit refractive index measurements which are useful as an indication of the purity of the gases.

The oscillator shown in Fig. 1 has proven satisfactory in that its frequency is quite constant and very little influenced by changes in the various battery voltages. A type SP122 tube is used with voltages 3.3, −1.5, 45 and 135

[1] A. B. Bryan and I. C. Sanders, Phys. Rev. **32**, 302 (1928).

volts on the filament, control grid, shield grid and plate respectively. The grid circuit coil has 11 turns of No. 14 bare copper wound on 4 inch paper tubing and spaced about 0.75 cm. It is made in two sections the distance between which may be varied for rough adjustment of the frequency. The plate circuit coil has 19 turns of the same wire spaced 0.3 cm and is 5.5 inches in diameter. It is supported outside of and coaxially with the grid circuit coil. The feed back condenser C' is a small variable air condenser having seven semicircular plates 3 cm in diameter, spaced about 0.17 cm. No shielding is used, the adjustments of Cc being made from a distance by suitable means.

The following results show the effect of various factors on the oscillator frequency. Increasing the filament voltage by 10 percent produces a frequency decrease of about 0.5 cycle per second. Decreasing it by the same amount causes a frequency increase of 1.1 cycles per second. Increasing or decreasing the shield grid voltage by 10 percent increases or decreases the frequency by 26 cycles per second. Increasing or decreasing the plate voltage by 10 percent increases or decreases the frequency by 2.8 cycles per second. Increasing the setting of C' from one third to one half maximum decreases the frequency by 1200 cycles per second and incidentally raises the d.c. plate current from 1.37 to 1.68 milliamperes.

The frequency normally decreases steadily at the rate of about 1.3 cycles per second in one minute and Cc must be decreased by 0.005 divisions per minute to hold it constant. This drift is probably caused principally by the slow rise in room temperature which always occurs while measurements are being made.

Results

The experimental results are shown in Table I. As in the previous work the readings have been taken in a way which eliminates the slow steady frequency drift and have been made on various parts of the scale of Cc. The second column shows the absolute temperature, the third the change in pressure of the gas in the test condenser and the fourth the resulting capacity change in divisions on Cc. The last column gives the capacity change for a pressure change of one atmosphere and a tempreature of 0°C, obtained from δC_1 on the assumption that the effect is directly proportional to the pressure change and inversely to the absolute temperature. The measurements on air are made to calibrate the apparatus, the previously found value $K = 1.000589$ for air being used. Since $K-1$ is proportional to δC we have for argon $K-1 = 0.000589\ (1.949/2.001) = 0.000574$ and for neon $K-1 = 0.000589\ (0.5026/2.001) = 0.000148$.

Dry carbon dioxide free air was used. The argon and neon were purchased in liter flasks and were supposed to be specially purified. No additional purification was attempted except drying over P_2O_5. Refractive index measurements made after the gas was in the apparatus give 0.000292, 0.000282 and 0.0000663 as the values of $n-1$ for air, argon and neon, respectively, sodium light being used. The first two are in good agreement with previous deter-

minations.[2] The value for neon seems to be about one percent low and may indicate a slight helium impurity but the difference is probably within the range of experimental error.

The only previous dielectric constant measurement on either argon or neon seems to be that of Braunmühl[3] on argon. He also uses the heterodyne beat method and his value 1.000571 is in as good agreement with the above as

TABLE I. *Change in capacity of test condenser as pressure of gas is changed.*

Gas	T	δP	δC_1	δC
Air	297.1	53.32	1.293	2.006
"	297.3	53.38	1.288	1.997
Argon	296.8	53.25	1.265	1.963
"	297.1	43.47	1.027	1.954
"	297.3	43.48	1.025	1.951
"	297.5	52.85	1.235	1.935
"	296.4	52.32	1.235	1.948
"	297.0	44.06	1.035	1.942
				mean 1.949
Neon	299.1	51.59	0.315	0.5084
"	299.4	51.63	0.310	0.5006
"	299.9	52.75	0.317	0.5017
"	300.0	52.77	0.315	0.4986
"	299.1	53.76	0.323	0.5003
"	299.1	53.86	0.325	0.5025
"	299.4	53.91	0.322	0.4978
"	299.6	48.56	0.293	0.5033
"	299.8	48.58	0.297	0.5103
				mean 0.5026
Air	299.2	53.60	1.287	2.000
"	299.4	53.61	1.287	2.001
"	299.7	51.07	1.225	2.001
"	299.9	51.11	1.225	2.001
				mean 2.001

could be expected, especially since it is based on the somewhat uncertain value 1.000547 for oxygen. The gases were purchased from Air Reduction Sales Company, 342 Madison Avenue, New York, who state that the argon was as pure as is commercially practicable but probably contained a very small fraction of one percent of nitrogen, the actual quantity being too small to be determined by analysis. They also state that the neon contained less than one percent of helium and that no other impurities were present in either of the gases.

[2] Landolt-Börnstein Tabellen.
[3] H. J. v. Braunmühl, Phys. Zeits. **28**, 141 (1927).

THE RECOMBINATION OF IONS AND OF IONS AND ELECTRONS IN GASES

By Lauriston C. Marshall
Physical Laboratory, University of California, Berkeley

(Received May 16, 1929)

Abstract

Coefficient of recombination of ions, produced by x-rays, as function of x-ray exposure time, initial ion concentration and time of recombination.—The present work constitutes a study of the recombination of ions and of ions and electrons in gases, by means of a new direct method, using constant radiation from a Coolidge x-ray tube as the ionizing agent, together with a rotating commutator shutter. This method permits wide limits of independent variation of: (1) x-ray exposure (t'); (2) initial ion concentration (n_0); (3) time of recombination (t). Results in air show that α, previously assumed constant and equal to 1.6×10^{-6} actually varies as a function of t' and of t. It is high, 4×10^{-6} or more, for small values of the above quantities and drops rapidly to nearly a constant value. α is also found to be a function of n_0. These facts can only be explained on the assumption that the ions are not initially uniformly distributed, but are in pairs along the paths of the x-rays. This leads to fictitiously high calculated values of α corresponding to low apparent values of n_0 and n, erroneously computed on the assumption of random distribution. As t', and with it n_0 and also t, increase, α approaches a constant value between 0.8 and 0.9×10^{-6}, which is probably nearly the true value. This result lends strong support to the theory of Thomson that the process of diffusion plays the major role in the initial stages of the mechanism of recombination; i.e. in bringing ions together.

Coefficient of recombination in argon: mechanism of recombination, formation of negative ions by electron attachment to impurities.—In argon, where electrons remain free for appreciable intervals, α is nearly constant. For the same time intervals it has only about half the value found in argon-oxygen mixtures, where the electrons attach rapidly, or the value found in dry air. On the basis of the kinetic theory α would be expected to be the same in argon as in air. The constancy of α with t and t' is due to the rapid achievement of random distribution when free electrons are present. The value of α indicates that the coefficient of recombination for electrons and positive ions is less than for positive and negative ions. This conclusion is in agreement with the results of Kenty on recombination between electrons and positive ions in argon. Consequently α, as observed in pure argon, is not a true measure of the recombination of positive and negative ions, but serves as an indication of the rate of negative ion formation through the attachment of electrons to impurities present.

Introduction

ATTEMPTS at formulating an adequate theory of recombination of positive and negative ions, in gases near atmospheric pressure, and of ions and free electrons in these gases under similar conditions, have in recent years met with considerable difficulty owing to inadequate information on the following points:

1. Whether the fundamental mechanism of ion recombination may be ascribed: (a) to the attractive forces between the ions according to the

treatment of Langevin;[1] or (b) to the random heat motions as provided in the more recently published theory of J. J. Thomson.[2]

2. Whether one may state with assurance that the coefficient of recombination, designated henceforth as α, is constant with time as *assumed* in previous investigations, or if it does vary, why it does so.

3. The unknown role of free electrons in recombination; for electrons have, in the last ten years, been shown to remain free for appreciable periods of time in many gases, even at high pressure.

It seemed essential, therefore, to undertake measurements which might help to clarify these questions especially in relation to the third point, evience for which had been claimed by Rümelin as a result of a study of the recombination of ions within short time intervals after ionization. A direct method of study of recombination, following ionization by x-rays, was suggested to the writer by Professor L. B. Loeb. This seemed capable of greater flexibility and control than the previous methods used, due to the development of modern x-ray technique. After two years' time the elaborate equipment required to carry on measurements under satisfactory conditions was assembled and the results obtained this year appear to have entirely fulfilled the expectations. It is the purpose of this paper to describe the method and the preliminary results obtained.

Method of Measurement

Reference to the accompanying diagram (Fig. 1) will make the following description more clear. The development of the Coolidge x-ray tube, supplied with a constant high-potential direct current, has made the production of constant x-radiation possible for long intervals of time. The intensity may be determined, over a wide range, by the variation of either current through the tube or applied voltage, or both. Provision is made to vary the duration of the ionizing flash of x-rays, in a chamber, by means of a sector, variable from 0° to 90°, cut out of a solid brass disk, rotating at any desired speed. The same shaft carries a commutating mechanism, which may be adjusted relative to the sector. Thus the ions may be swept from the ionized volume at any time after the x-ray flash has ceased. The x-rays are limited by means of a series of square slits of large aperture, and directed in a nearly parallel beam into the ionization chamber, through a thin aluminum window. Here a volume of gas is ionized, between two parallel horizontal plates, and the beam is allowed to pass out through another window in the rear of the chamber. The plates are so placed, with relation to the path of the x-rays, that no appreciable diffusion of the ions, to them, may take place in the range of time intervals over which measurements are made. Also care is taken, in the design and placing of the slits, that practically no scattered radiation shall be incident upon the plates. The lower plate is connected alternately, by the commutating mechanism, to the high voltage for sweeping out the ions,

[1] P. Langevin, Ann. de Chimie et Physique **28**, 403 (1903).
[2] J. J. Thomson. Phil. Mag. **47**, 337 (1924).

and to ground through a high resistance. Thus the plate is at zero potential during the x-ray exposure and the period of recombination. A relay grounds the electrode permanently when the final measurement of charge is made. The upper collecting electrode is surrounded by a grounded guard ring and connected to the quadrant electrometer. Thus the ions are swept from a sharply defined volume of ionization of about 63 cm³. The process is cyclic, the exposure to x-rays, the lapse of time for recombination after cutting off of the x-rays, and the sweeping out of the ions being repeated in succession during each complete rotation of the commutating shaft. The control of each of these functions is completely independent of the others over a wide

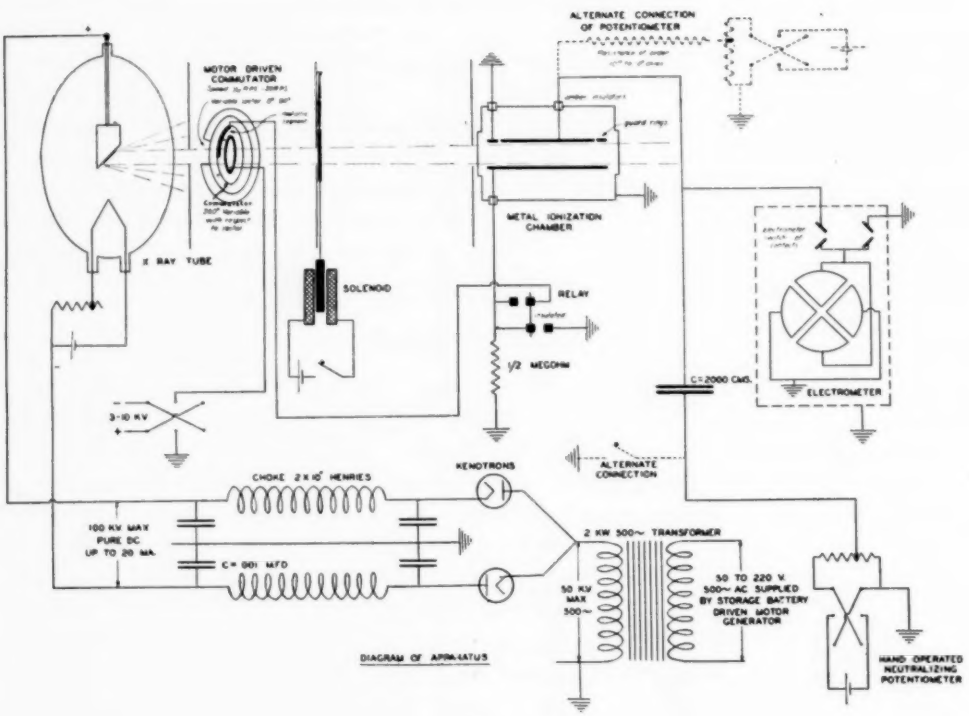

Fig. 1.

range, determined by the relative settings of the variable sector and commutating mechanism, and the speed of rotation. The chamber and electrometer are shunted by a large capacity and a single measurement is allowed to extend over sufficient time (30 seconds to 4 minutes) to build up a conveniently measureable charge on this system. This charge is neutralized, as it grows, by a hand-operated potentiometer, with one of the two methods indicated in the diagram. Thus the effective potential, on the upper plate, is kept very near to zero at all times. The ions are formed and permitted to recombine free from the influence of stray fields.

The method of neutralization indicated by the solid lines in the diagram is the least accurate. This was the first developed and used in the measure-

ments on air, which are described later. The upper plate may be kept as close to zero potential as the amount of charge collected in a single cycle. Due to sluggishness of the electrometer, however, the variance may be much greater. Moreover, it becomes necessary to time the period over which the reading is taken by means of the sliding shutter. This method is, therefore, not practical for measurement in gases in which free electrons are present, because of their high velocities, even in very small fields. For measurements in air and in mixtures where electrons are not free for appreciable intervals, it suffices. α may then be calculated from the relation

$$\alpha=\frac{300eVNT}{C\epsilon R}\cdot\frac{1}{t}\left(\frac{1}{r}-\frac{1}{r_0}\right)$$

where e is the electronic charge, V the volume ionized, N the speed of commutator in r.p.s., T the time of observation, C the capacity of the electrometer system, ϵ the voltage of the potentiometer battery. R is a multiplying factor, entering because the capacity, to the lower plate of which the potentiometer is connected, does not comprise the total capacity of the system. The time t is the recombination time as determined by setting of the commutator. r_0 is the potentiometer reading corresponding to $t=0$, and r the potentiometer reading corresponding to $t=t$.

With the second method, indicated by the broken lines in the diagram, the variation of the collecting electrode from ground may never exceed the potential built up in a single revolution of the commutator. Naturally this may be made very small by properly increasing the shunt capacity in the electrometer system. If, moreover, the proper value of high resistance is chosen, the variation may be made well within the limit set above. As before, the values of r_0 and r are read directly from the potentiometer, in volts, when equilibrium is reached. α is now given by the relation

$$\alpha=\frac{1.59\times10^{-19}RNV}{\epsilon}\cdot\frac{1}{t}\left(\frac{1}{r}-\frac{1}{r_0}\right)$$

where R is the value of the high resistance in ohms, N the speed of the commutator in r.p.s., V the volume ionized, ϵ the voltage of the potentiometer battery, t the recombination time, r_0 the potentiometer reading corresponding to $t=0$, r the potentiometer reading corresponding to $t=t$.

In both systems a series of measurements was made with the same exposure to x-rays, t', and the same commutator speed. Different relative settings of commutator with respect to sector are used to determine first r_0 and then corresponding values of r for different values of t. Such a series of observations is designated as a run. In all cases, readings for both positive and negative charge are taken.

The voltage induced on the electrometer by the high field used for sweeping out ions is very small. This is because the inter-electrode capacity of the plates in the ionization chamber is very small compared to the total capacity of the electrometer system, and the two capacities are in series

with each other and the high potential during the application of the field. In taking readings with the first method, the field is first applied. The electrometer deflects slightly to a new position which is taken as the zero during the measurement. The shutter is then opened and the measurement proceeds. Actually the system is at true ground potential except when the field is applied. The constant deflection here is then due to the sluggishness of the electrometer. When sufficient charge has been collected the shutter is closed and the lower plate of the chamber is permanently grounded by means of of the relay. Final neutralization with the potentiometer is made by adjusting to the original zero point. With the second method of measurement, the presence of the shunting leak resistance together with the high total capacity of the system and the sluggishness of the electrometer, renders the inductive effect of the field so small that it cannot be observed.

Gases were purified[3] with procedure along the lines of standard technique. Air was filtered and dried thoroughly. The argon was obtained from the General Electric lamp works. Its purification was not carried beyond the removal of all substances having high electron affinity, and drying. Consequently a small amount of nitrogen was present in the samples of argon on which measurement was made.

Results

1. *Air.* All measurements in air were taken with the first method described. A sequence of runs was made, starting with short x-ray exposures t', small values of recombination time, t, and extending to longer intervals. The variation of these two quantities was systematic, the value of t' and the range of variation of t being doubled in each successive run. This was accomplished merely by halving the commutator speed in each case. The x-ray intensity was held constant with respect to current and voltage on the tube for a complete series of runs. In this manner, results were obtained for values of t' beginning with 0.0156 seconds and ending with 0.5 seconds. This range made possible the production of ions of various ages over a wide range of concentrations. At the longer intervals of 0.25 and 0.5 seconds, equilibrium between the rate of formation and of recombination during the flash was reached. The equality of total numbers of ions produced in the two cases stood as proof. The above procedure provided a series of overlapping ranges of t between the limits 0.0015 sec. and 1.2 sec., the range covered in each run being 24 fold. Variation of t within a run was also systematic, each successive value being made double the preceding one. The values of α and n_0 were calculated from the readings thus obtained, in the manner previously described. These results were also pictured graphically by plotting α as a $f(t)$ for each run. The initial concentration, n_0 was also plottd on the same diagram as a $f(t')$. The result is shown in Figures 2 and 3. Figure 3 is a magnification of Fig. 2 shown in order to facilitate comparison of the results for short time intervals. For this reason, only the first two points on curve V and the first one on curve VI appear on Fig.3. The points on the

[3] L. B. Loeb, Phys. Rev. **19**, 24 (1922); Phil. Mag. **43**, 230 (1922).

curve labeled n_0, give a picture of the range of variation of n_0 and t' and the shape of the curve clearly illustrates the approach to equilibrium. A glance at the curves showing α as $f(t)$ brings out some very interesting features, as follows:

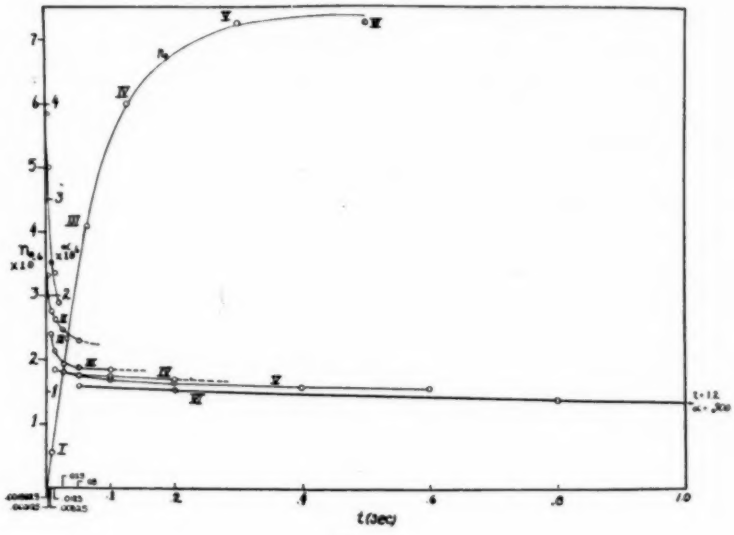

Fig. 2.

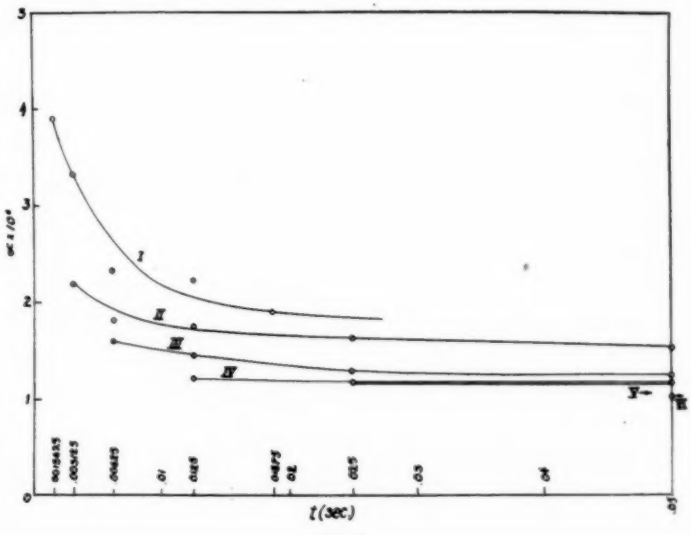

Fig. 3.

1. *α is by no means a constant with time* as apparently observed previously by the majority of experimenters. On the contrary α starts at a high value, about 4×10^{-6}, for $t'=0.0156$ and $t=0.00156$, and drops off very rapidly during the run.

2. As t' and t are increased the drop becomes less sharp and at the longer time intervals the curves become nearly straight, showing only a gradual, but nevertheless definite, falling off in the value of α.

3. If the calculations for these longer time intervals are carried out as indicated previously, the dropping off of α is more rapid than that shown by the curves given. This was found to be due to the effects of diffusion. Since the edges of the beam are far from the plates, diffusion to the latter will not occur. The process of diffusion, as time goes on, will, however, increase the volume, V, in which the ions are contained. This quantity falls in the numerator of the expression used in calculation. If, therefore, we use the original uncorrected volume in determining α, an apparent value is obtained, for longer intervals, t, which is too low, and the variation due to this cause must be corrected for.

Since $dn/dt = -\alpha n^2$ and $n = N/V$, where N is the total number of ions in the volume V, $dn = dN/V - NdV/V^2$. The last term is very small, compared to the first, and may be neglected so that $dn = dN/V$. Now $V = lx^2$, where l is the length of the ionized volume and x its width. Because of diffusion, x varies with time. The quantity l remains practically constant; for it is to be remembered that this dimension is determined by the guard ring and that the gas in either direction along the length of the ionized region is also uniformly ionized. Therefore the chance of ions diffusing in or out of the volume from either end is equal. Thus we need only concern ourselves with the change in V due to increase in x. If we let x_0 be the original width of the ionized volume, then $x = x_0 + \overline{2\Delta x}$. Now $\overline{\Delta x} = [(2/\pi)\overline{\Delta x^2}]^{1/2}$ and $\overline{\Delta x^2} = 2Dt$, so $\overline{\Delta x} = (4Dt/\pi)^{1/2}$. In this we are only considering diffusion along the x direction. The general three dimensional case gives $\overline{\Delta S^2} = 6Dt$. Now D, the coefficient of diffusion of the gas, is given by $D = 0.0236K$, where K is the ionic mobility in centimeters per second per volt per centimeter. Then, if we let V_0 be the originally ionized volume, and remember that $V_0 = lx_0^2$, we find that $V = V_0 + bt^{1/2}$. b is a constant involving the coefficient of diffusion and the dimensions of the ionized volume, i.e. $b = 4.512\ x_0 D = 4.512 V_0 D/x_0$. The differential equation then reads

$$\frac{dN}{N^2} = \frac{-\alpha\, dt}{V_0 + bt^{\frac{1}{2}}}$$

which on integration yields

$$\alpha = -\frac{10.18lD}{4.512(Dt)^{1/2}/x_0 - \log\cdot(1+4.512(Dt)^{1/2}/x_0}\left(\frac{1}{N} - \frac{1}{N_0}\right)$$

or, in terms of potentiometer readings, by the first method of neutralization

$$\alpha = -\frac{300eNT}{C\epsilon R}\cdot\frac{10.18lD}{4.512(Dt)^{1/2}/x_0 - \log\cdot(1+4.512(Dt)^{1/2})/x_0}\left(\frac{1}{r} - \frac{1}{r_0}\right).$$

In the runs for which t' was large, an initial correction was also made in x_0, for the diffusion which took place during the exposure. The equation

above affects the value of α very little for small values of t, but renders the falling off more gradual for the longer times. The curves, as shown, in Figs. 2 and 3 are corrected in this way.

In as much as some photo and longer range recoil electrons are lost from the volume, during the process of ionization, before they could attach to form ions, the positive and negative readings differed at the start, i.e. $r_{0-} \neq r_{0+}$. Moreover the rate of decrease was not quite the same. This latter effect was attributed to the fact that the positive and negative ions present have different rates of diffusion, due to the different mobilities, the positive rate being less than the negative. The accuracy of these first measurements did not warrant very great refinement in calculation. Therefore, a coefficient of diffusion was used determined from the average value of the two mobilities. This is $D=0.0236\times 2=0.047$, which is as close as D is really known.

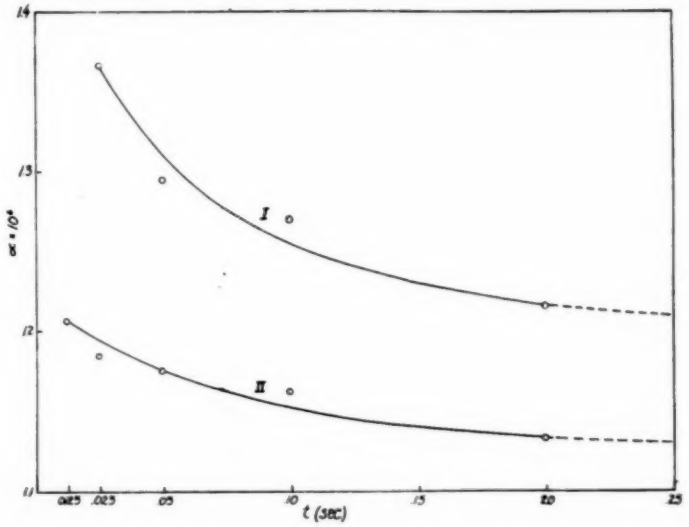

Fig. 4.

α, as determined from the positive and from the negative readings, is not quite the same. Owing to the use of a common value for D, the average value of α was used in plotting and may be safely assumed to represent the true condition of affairs within the limits of error.

The systematic variation of t', carried out at constant x-ray intensity, produces not only an ageing effect in the ions from run to run, but also a marked change in the number produced. Some measurements were therefore made, using the same values of t' and t, but with different x-ray intensities The intensity was varied by means of the electron current through the tube keeping the applied voltage constant. Thus the ions in each case might be said to have been formed in the same manner, since the x-rays are of equal hardness. The only difference, then, in the conduct of two runs with corresponding intervals, t' and t, lay in the number of ions formed initially. A comparison of two such runs is shown in Figure 4. These curves correspond

to curve IV in Figure 3, and are seen to be of the same general type. *α is however consistently much smaller here on curve II than on curve I. Also the lower curve does not show such a sharp rise in α for smaller values of t.* It is important to state that the values of this curve were taken with a higher initial density of ions than was the case on curve I.

The same effect was noted in measurements, taken in argon to which 1 centimeter partial pressure of oxygen in the form of air had been added. The result is shown by the curves, in Fig. 5, which correspond to curve III in Fig. 3. The runs were taken for $t' = 0.0139$ sec and t from 0.00625 sec to 0.15 sec. A ratio of initial ion densities of about 3:1 was obtained. The drop in α, with increase in density, is seen here to be much more pronounced than in the previously discussed case. As before, the lower curve, (curve II), corresponding to higher concentration, does not rise as sharply for small

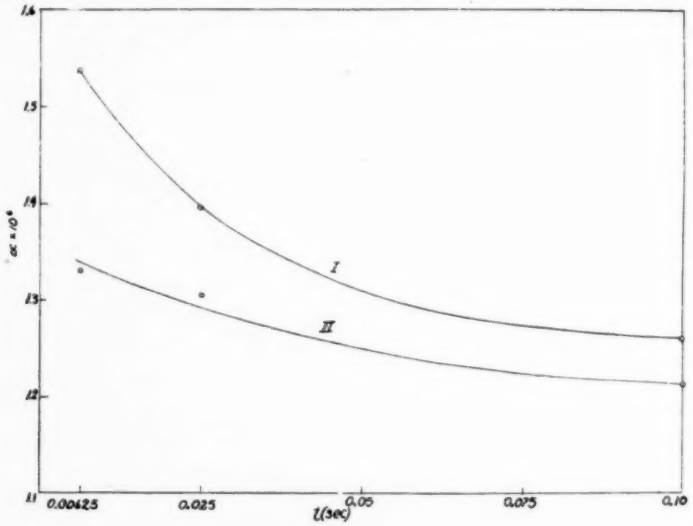

Fig. 5.

values of t. The significance of these results in relation to others obtained, will be discussed later.

Although the accuracy of the readings obtained by this method is well within $\pm$ 2 percent, the accuracy of determination of α cannot be so great. In the first place, the value of α depends on the difference, $(1/r) - (1/r_0)$, and a variation of $\pm$ 2 percent, in r or r_0, introduces a variation in α which may be much greater and depends on the relative values of r and r_0. In addition, as pointed out, the value of D is not known with certainty, and this introduces an unknown error in this correction. Finally the present measurements were undertaken only as a preliminary survey of the field, with the new method, for the purpose of determining the real conditions existing. Although the method is absolute, no attempt was made to secure high accuracy in this regard, because of lack of time after significant results were obtained. More accurate results can be obtained when certain portions of the equipment are

changed to meet the unforeseen difficulties encountered in these measurements. Work is at present under way with a view to extending the field. So far as the relative values of α are concerned the accuracy may be claimed to be fairly high. The absolute values may be said with confidence to hold within a range of ± 10 percent.

2. *Argon.* Thus far the results obtained have apparently had very little bearing on the originally stated goal of this experiment, i.e. the determination of the role of the free electron in recombination. Results obtained by Loeb,[4] on attachment of electrons to molecules, make it possible to estimate that in air any free electrons present will attach to molecules, chiefly of oxygen within 10^{-5} sec after separation from the parent molecule. Consequently it is safe to state that in the measurements thus far described we have been concerned only with recombinations between positive and negative ions. It seemed highly desirable to obtain a series of observations in a gas in which electrons do remain free for an appreciable time. Such gases are hydrogen, nitrogen and argon. Argon was chosen because of the extremely high degree of ionization obtainable with moderate x-ray intensities. A series of runs was made, as before, over ranges of t' from 0.0139 sec to 0.0556 sec, and t, between the limits 0.00625 sec and 0.15 sec. Since the velocity of electrons in a unit field is of the order 10^3 times that for ions, the rate of diffusion must be high. Therefore the first method of measurement described proved impractical. The second method was consequently resorted to and gave satisfactory preliminary results. The negative as well as the positive readings were carefully taken. Free electrons were present in profusion, as evidenced by the behavior of the negative readings as compared with the positive. Even during the short exposure time of 0.0139 sec, enough electrons diffused from the volume to make the intital negative readings far smaller than the positive. As t increased, the rate of decrease of the negative charge was much greater than that of the positive. In the time intervals used, the positive charges could diffuse only a very short distance so that their rate of disappearance was taken to indicate the trend of recombination. The original differential equation, $dn/dt = -\alpha n^2$, assumes equal numbers of positive and negative ions present during the process, and therefore cannot apply here. Consequently the method of calculation of α must also be changed. The modification is as follows:

Let n_+ be the number of positive ions per cc, n_- the number of electrons per cc, α the coefficient of recombination, t the time of recombination, n_0 the number of negative charges initially present (at $t=0$), n' the number of positive ions initially present and n the number of positive ions present after a time t.

Then we write

$$dn/dt = -\alpha\, n_+\, n_-.$$

The disappearance of the negative charges may be ascribed to two causes, namely: recombination and diffusion from the region between the plates.

[4] L. B. Loeb, Proc. Nat. Acad. Sci. **7**, 5 (1921); Phys. Rev. **17**, 89 (1921); J. Franklin Inst. **197**, 45 (1924); Phil. Mag. **46**, 1088 (1923).

This change is shown, as a function of t, in the negative readings. It was assumed that n_- might be expressed as a function of t as follows:

$$n_- = a/(1+bt).$$

Then at $t=0$, $a=n_0$, and we may write

$$n_- = n_0/(1+bt).$$

When this expression is substituted for n_- in the above equation, integration yields the following expression for α

$$\alpha = \frac{b}{n_0}\,\frac{\log n'/n}{\log (1+bt)} = \frac{b}{n_0}\,\frac{\log r'/r}{\log (1+bt)}.$$

Values of n_0, r' and r were measured and calculated as described in the second method. It remained to determine the proper value of b. The values of n_- were plotted as a function of t, yielding curve I in Fig. 6. Then, using n_0 and another point on the curve, b was computed from the relation $b=(n_0-n_-)/n_-t$. Proper choice of b gave a calculated series of values represented by the curve II in Fig. 6. This fit was considered to be sufficiently close to give values of α well within the limits of error.

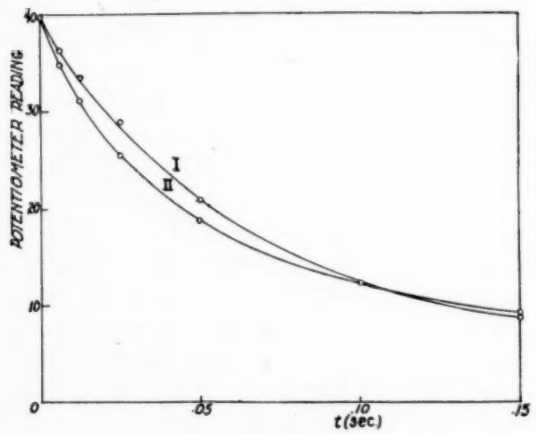

Fig. 6.

The results obtained are shown by the curves in Fig. 7. Curve I corresponds to curve III in Fig. 3. Curve III in Fig. 7 represents a run taken with a longer interval t' and corresponds to curve V in Fig. 3. The curves marked n' and n_0 show the change in these quantities with t'. All these curves are plotted in the same manner as in Fig. 3. The difference in the rate of increase of n' and n_0 is most striking. During the exposure times used, n' does not even approach equilibrium, while n_0 very quickly reaches a maximum. The latter effect may be ascribed to the rapid diffusion of the electrons so that the rate of loss very soon approaches the rate of generation. Most striking, however, is the shape of the curves showing α as a $f(t)$ and the *low values of* α

obtained. These are, in general, about half the corresponding values in air. On the basis of the kinetic theory, α, for argon, would be expected to be about equal to α for air. The sharp drop in the value of the coefficient, which was observed in air for these conditions, is here absent. The significance of these facts will be discussed later.

Two errors enter the above determinations which make the value of α uncertain. The first is introduced by the loss of electrons from the volume ionized. The plates in the chamber were circular, and not designed for this type of measurement, so that electrons may travel several centimeters to the side before passing from the region between the plates. It is therefore possible for the electrons to leave the volume of ionization, and in which the positive ions stay, and still be collected when the charge is swept to the upper plate. This will lead to the measurement of a spuriously high value of n_0 or

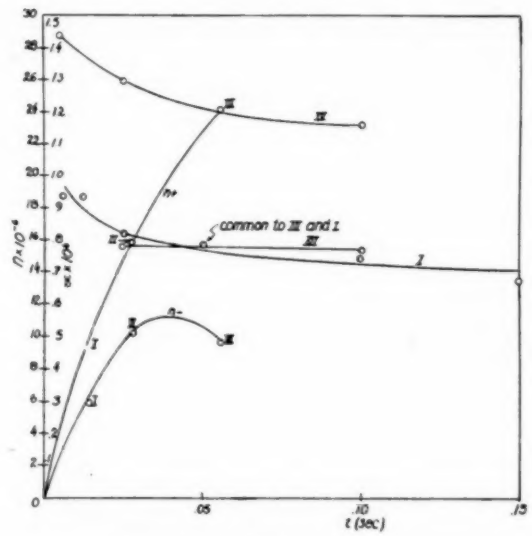

Fig. 7.

n_-, corresponding to given values of n' or n. Such an effect would tend to produce a calculated value of α lower than the actual one. On the other hand, electrons diffusing upwards to the collecting plate will tend to increase the measured values of n_0 and n_- and decrease those of n' and n. This is an effect in the opposite direction. Obviously diffusion in and out of the ends will be equal. Electrons lost to the lower plate will not affect the reading, inasmuch as this electrode is grounded except when the ions are being swept out. It is estimated that the two effects will about compensate each other and that the value of α obtained is true within the limits $\pm$ 10 percent. Naturally a series of experiments with a chamber designed to eliminate these effects would be most desirable. Such measurements are now being undertaken in this laboratory.

3. *Argon mixed with air.* The measurements in argon, to which 1 cm partial pressure of O_2 in the form of air was added, afford interest when compared

with these just described. Curve IV in Fig. 7 corresponds to curve I and is identical with curve I in Fig. 5 and represents the value of α in the mixture. The runs are identical, with the exception of a slight difference in the x-ray intensities used. *The values of α are seen to have risen to the corresponding ones for air.* (curve III, Fig. 3). There was no sign of the presence of free electrons and the positive and negative readings were nearly equal. In calculating and plotting α the same system of averaging was employed as described in the work with air.

Previous Investigations

The earliest direct[5] measurements were made by Townsend[6] Rutherford,[7] and McClung, [8] who used either air-blast methods or methods in which a gas was ionized by a flash of x-rays and the number of ions remaining after a time t was measured relative to the initial ions present. The coefficient of recombination α is then calculated from the solution of the well-known differential equation

$$dn = -\alpha n^2 dt,$$

which reads

$$\alpha = \frac{1}{t}\left(\frac{1}{n_t} - \frac{1}{n_0}\right)$$

where n_t and n_0 are the number of ions per cm^3 after a time t, and the initial number at $t=0$ respectively. The values of n_t and n_0 are computed from the numbers of ions observed, divided by the volume ionized. These earlier observers found that the value of α so observed was constant and equal to about 1.6×10^{-6} for air. Inasmuch as these results were obtained at a time when the control of experimental conditions was much inferior to that possible later and did not eliminate the effects of diffusion, the conclusions drawn from them, which have been only too generally accepted, must be regarded with caution. More recently Rümelin[9] and Plimpton[10] have carried the measurements further. The work of both these men was excellent, but the conditions under which they worked did not allow of the independent control of the variables, ionization flash period, t', recombination time, t, and ion concentration, n_0, now possible. Both these observers found that, for very short

[5] Other measurements have been made by many workers including Langevin (reference 1); Bragg and Kleeman, Phil. Mag. **11,** 466 (1906); Kleeman, Phil. Mag. **12,** 273 (1906); Hendren, Phys. Rev. **21,** 314 (1905); Erikson, Phil. Mag. **18,** 328 (1909); Thirkill, Proc. Roy. Soc. **A88,** 488 (1913); Phillips, Proc. Roy. Soc. **A83,** 246 (1909); and Retchinsky, Ann. d. Physik **17,** 518 (1905). The methods employed by these workers were more or less "indirect" so that they did not permit independent control of the important variables t', t and n_0 and thus the effects which are here under discussion were masked.

[6] J. S. Townsend, Phil. Trans. Roy. Soc. **193,** 157 (1900).

[7] E. Rutherford, Phil. Mag. **44,** 422 (1897).

[8] A. McClung, Phil. Mag. **3,** 283 (1902).

[9] Rümelin, Ann. d. Physik **43,** 821 (1914).

[10] S. J. Plimpton, Phil. Mag. **25,** 65 (1913).

time intervals, t' and t, α was high and not constant, dropping rapidly to lower values as the time intervals t' and t increased. Rümelin interpreted his high values as being due to an initial rapid recombination of free electrons and positive ions, an erroneous interpretation as the present results show. Plimpton correctly ascribed his results to an initial non-random distribution of ions due to the mechanism of ionization, a distribution which became more nearly random through diffusion of the ions as time progressed This interpretation, it will be seen, is in good accord with the results herein described. The non-random nature of the initial ionization in the meantime had been discussed theoretically by Jaffe,[11] particularly for the case of α-particle ionization where the columnar effects are much more pronounced than for ionization by x-rays. Finally while the present work was in progress Schemel[12] carried out measurements on α-ray ionization by a direct method of measurement. His results are excellent and are made the basis for discussion in a theoretical paper by Jaffe.[13] While they deal with a more troublesome mode of ionization the conclusions are in good accord with the conclusions of Plimpton and those independently arrived at from the present work before the paper of Schemel's came into the writer's hands. The complications due to α-particle ionization, however, have made the absolute evaluation of α in the work difficult, as pointed out by Jaffe, so that the results of the present investigation may serve to throw some light on this subject.

Discussion of Results

The first feature to excite interest is the unusual variation of the coefficient of recombination as evidenced by the results obtained in air. Except in the measurements of Rümelin and Plimpton and very recently Schemel the sharp increase of α, for short time intervals, t, has not been observed before. Recent investigations have led to a rather clear picture of the mechanism of x-ray ionization.[14] It is now fairly certain that the ions are formed, initially, in pairs. In most of these the ions are separated by relatively small distances. Especially is this true in gases and mixtures such as air, where the electrons attach quite rapidly to form negative ions. It is fairly safe to assume that in air the average initial distance between the ions in a pair is of the order 10^{-3} cm or less. This would correspond to a concentration of 10^{9} ions/cc, with uniform distribution throughout the volume and only 10^{-3} cm between any two ions of a pair. Now an initial concentration of the order 10^{6} ions/cc, such as calculated for small values of t from the observed readings and assumed volume, corresponds to a distance between ions of 10^{-2} cm at uniform distribution. These facts lead to a clear picture of the conditions existing as the x-rays are cut off following a *short* exposure. The ions must be scattered in pairs rather irregularly throughout the volume,

[11] G. Jaffé, Ann. d. Physik **43,** 249 (1914); **75,** 391 (1924).
[12] J. Schemel, Ann. d. Physik **85,** 137 (1928).
[13] G. Jaffé, Ann. d. Physik **1,** 977 (1929).
[14] A. H. Compton, X-Rays and Electrons, pp. 227–314.

along the paths of the x-rays and photo and recoil electrons. Due to the fact that some diffusion has taken place between ions formed at the beginning of the x-ray flash, we shall have distances within pairs ranging from less than 10^{-3} cm to somewhat over this amount. Consequently, though there be but 10^6 ions in each cm^3 of gas, the effective concentration may amount to 10^7/cm^3 or more. In order to see the effect of such a condition on the results, it is well to consider the simple expression for α.

$$\alpha=\frac{1}{t}\left(\frac{1}{n}-\frac{1}{n_0}\right)=\frac{1}{nt}\left(\frac{n_0-n}{n_0}\right)=\frac{1}{nt}\left(1-\frac{n}{n_0}\right).$$

Now calculation gives $n=N/V$ and $n_0=N_0/V_0$ where N and N_0 represent the total measured numbers of ions in volumes V and V_0 respectively. Then we may write

$$\alpha=\frac{1}{Nt/V}\left(1-\frac{NV_0}{N_0V}\right)$$

The value of α depends on the quantities n_0 and n, which are computed from the ratios N_0/V_0 and N/V. N_0 and N are found by measurement. The values of V and V_0 used are the *total volumes over which the ionization is distributed*. These are consequently much higher, for small values of t' and t, than the effective volumes, which are determined by the distribution in pairs just described. That is to say n, as we determine it is much smaller than the effective n which is influencing recombination, and which, for a given measured N, corresponds to a much smaller effective value of V. Consequently, for a given calculaton, since our evaluation of n and n_0 is much too small, the apparent value of α will be correspondingly high. For a given run, i.e. a given exposure time, t', the error in n_0 will be constant. However, as t increases the ions begin to diffuse apart. The effective value of V is closer to the assumed one and the determination of n is less in error. Consequently the apparent value of α, though still high, will drop off, the drop becoming more gradual as t increases. In other words, we have measured the total number of ions present as a function of t and from this have computed erroneous values of n_0, and of n as a function of t, obtaining a value of α which varies as shown in the curves. The effective value of n_0 and the actual variation of the effective values of n with t, is determined by the initial distribution and the processes of diffusion which ensue. This time varitaion may or may not be such as to make the true value of α constant.

As we increase t' from run to run two things occur. First, the ions are older, when measurement is started, and consequently have had more time to diffuse apart. Second, the total concentration is greater due to the increased exposure to x-rays. Therefore the effective and computed values of n_0 become more nearly the same, and the ions need not diffuse so far before the effective and apparent values of n become equal. The value of α, thus calculated, is lower and drops less sharply with t. Finally at the longer values of t', distribution is nearly uniform before observation of recombination is

begun. The apparent and true values of α coincide and are very nearly constant at least for the longer intervals t. As mentioned before, lack of quantitative knowledge concerning the initial conditions of distribution prevents our determining definitely whether the true value of α is constant for the smaller values of t. The experimental evidence however, indicates quite strongly that it is,and that the predominating effect,causing the observed falling off of α, is that described above. The strongest proof of this conclusion lies in the drop observed in the values of α for identical runs, when only the concentrations were increased. This is also in accord with the observed drop, at the beginning of successive runs, for the same values of t. A comparison of the curves, in Fig. 3, with each other, and with the corresponding ones in Figs. 4 and 5 will make the matter strikingly clear.

It is to be noted that the final value of 0.8 to 0.9×10^{-6} toward which α tends in these experiments, is only about half the previously accepted one. It is believed that the value here given is more nearly correct in view of the fact that this result was obtained by a *direct* method, in which the sources of error could be foreseen and avoided, and which made use of the high degree of development of modern experimental technique.

These results also distinguish definitely between the two opposing viewpoints, i.e. of Langevin and J. J. Thomson, mentioned in the introduction, concerning the fundamental process of recombination. If, as assumed by Langevin, the bringing of the ions together be due to the mutual effect of their electric fields, we should expect a very high and practically constant value of α. This would be especially so, inasmuch as the ions are known to be formed so close together initially. The field, if the dominating factor, would also prevent diffusion apart and there should be no marked apparent decrease of the coefficient with time. The contrary is seen to be true. Hence the results obtained seem to be thoroughly in accord with the fundamental assumption of Thomson, i.e. that the ions are brought into the immediate neighborhood of each other by their heat motions and the role of the electrical forces is secondary.

The next feature which claims the attention is the behavior of the coefficient in argon. As stated, we now know that electrons do not attach to atoms of argon to form negative ions. The results set forth here would then indicate that the rate of recombination of electrons with positive ions in argon is very slow compared to the recombination in argon contaminated with oxygen, where electrons are no longer free. This conclusion is borne out by the recent results of Kenty,[15] concerning the recombination of positive ions with electrons following electrical discharges in very pure argon. It is found that the apparent coefficient of recombination between electrons and positive ions in argon is of the order 10^{-10}.

The observed recombination in pure argon must then take place between positive ions and negative carriers of a nature other than electronic. Undoubtedly the electrons must attach to molecules of impurity present in the

[15] C. Kenty, Phys. Rev. **32**, 624 (1928).

sample of gas used, thus forming negative ions. That sufficient impurity was present to permit such a process to take place is very likely to be the case inasmuch as a metal ionization chamber was used. In such chambers spectroscopically pure gas can still contain impurity enough to cause fairly rapid attachment. The gas was, however, sufficiently pure to make the rate of attachment relatively slow, as shown by the numbers of free electrons observed. The measurements obtained, therefore, are not to be regarded as a true indication of the rate of recombination between electrons and positive ions, but rather as the rate of attachment of electrons to molecules of impurity. This view is nicely substantiated by the effect of adding small quantities of O_2. The percentage of impurity was then sufficiently great to allow rapid attachment, probably within 10^{-3} to 10^{-4} seconds. All evidence of free electrons disappeared, and the recombination rose to the same rapid rate as previously observed in air.

It was also pointed out that the sharp drop in α at short time intervals was absent in pure argon, as evidenced by the flatness of the curves in Fig. 7. The rate of electron diffusion is so rapid in argon that even at the short times involved the distribution of charge was probably completely uniform.

The experiments are now being continued by Mr. Overton Luhr, to whom the writer wishes to extend sincere thanks for his assistance and suggestions in the carrying out of the work in the last stages of this complicated method. Most of all it is desired to thank Professor Loeb, at whose behest the problem was undertaken, for his unfailing interest and kind assistance, rendered both by advice and suggestion, throughout the course of the experiments.

FACTORS AFFECTING THE NATURE OF IONS IN AIR.

By Henry A. Erikson
Physics Laboratory, University of Minnesota

(Received June 10, 1929)

Abstract

This paper embodies the results of an attempt to determine some of the conditions which affect the nature of ions in air. It is shown that drying agents like $CaCl_2$ and P_2O_5 are not sufficient for drying purposes and that cooling by means of liquid air is essential for the more complete results. In air dried in this manner the initial positive ion transforms into the final ion very slowly, if at all. Results are also given confirming Tyndall, Grindley and Sheppard, that the ionizing process itself gives rise to impurities affecting the ions. It is shown that the effect of water is modified by the presence of the impurities due to ionization. The requirements essential in any method for the study of ions are given at the close of the paper.

IN GATHERING evidence as to the nature of gaseous ions, it is very necessary to keep in mind the purity of the medium involved. Each ion experiences 10^{10} collisions per second. As an ion can attach itself to a neutral body and in certain cases can transfer its charge to other neutral bodies forming an ion often of different mobility, it is clear that impurities may lead to results which are quite misleading. The object of this paper is to publish some results which throw additional light on this situation. It is necessary that the various effects along this line be clarified before we can hope for success in formulating a theory.

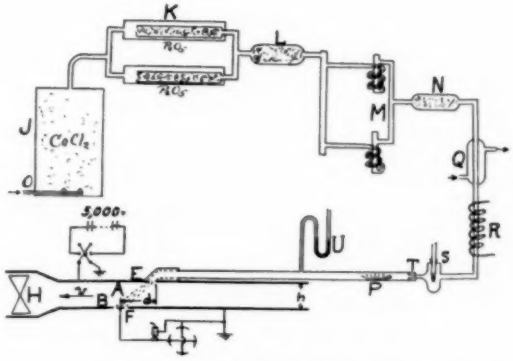

Fig. 1. Diagram of apparatus.

The Effect of Drying the Air

The apparatus used was essentially the same as described in an earlier paper.[1] The arrangement of driers was as shown in Fig. 1.

Air from the compressed air system in the building was passed into the tank J at O. The steel tank J was 40 cm in diameter and 92 cm high and

[1] Erikson, Phys. Rev. **33**, p. 403 (1929).

was nearly filled with granules of $CaCl_2$. The air then passed through two iron tubes K in parallel. In each of these was contained a glass tube 5 cm in diameter and 110 cm long. These glass tubes contained glass-wool and P_2O_5. The air then passed through a glass-wool strainer L, then through two copper coils M in parallel. The copper tubing of each of the coils was 0.6 cm in side diameter and 375 cm long wound in 25 turns. These coils could be immersed in liquid air. The air then passed through glass tubing to the glass-wool strainer N. The strainer N quickly became covered with frost so that the air was strained while cold. The air then passed through a glass Liebig condenser Q, than through a glass tube R wound with a nicrome heating ribbon. The current in the heater R was regulated so that the thermometer S registered room temperature. The air dried in this manner then passed into the auxiliary tube TE. The flow of air was regulated so that the pressure of the air in TE was the same as the room pressure as registered by the gauge U containing sulphuric acid. The tube TE was of brass and was 2 cm in diameter and 100 cm long.

A polonium plate was placed at P in the auxiliary tube TE. The polonium P could be placed at different distances from E, where the ions entered the main stream of room air passing through the apparatus due to the fan H. The age of the ions could then be altered by altering the position of P. The speed of the air in the auxiliary tube TE was 160 cm/sec. The speed of the main air stream in the tube ABH was 3300 cm/sec. The difference of potential between the plates AB was of the order of 5000 volts. The time, therefore, required for the ions to pass from E to F was of the order of 0.0003 sec. This short time required for the ionic measurement is very essential on account of the rapid transformation which the ions often undergo. In many cases the above time is amply short, in other cases it is evidently too long. This is true when a small percent of acetylene is present or for example, when the positive ion formed in the impurity due to ionization comes into the presence of water vapor.

Effects Due to Drying the Air

In Fig. 2 are given results showing the effect of the different driers. The polonium was 18 cm back from E and therefore corresponds to an ion-age of about 0.11 sec.

Curve A was obtained when air passed through the auxiliary tube TE directly from the room. The maximum n is due to the initial ions and represents a mobility of 1.87 cm/sec per volt/cm. The maximum m is for the final ion and represents a mobility of 1.36 cm/sec per volt/cm. The relative proportion of these two ions depends upon the age. With the polonium at E, only the initial ion n is obtained, but with the polonium at T, only the final ion m is obtained.

Curve B, Fig. 2, was obtained when the air passing through the auxiliary tube TE had passed through the $CaCl_2$ tank J, only, and then through the coils M without having the coils immersed in liquid air. The other conditions were the same as for A. It is here seen that the initial ions have disappeared, thus giving only the final 1.36 ion m.

Curve *C*, was for the same conditions as for *B* but with the P_2O_5 driers *K* added. It is here seen that there has been no appreciable change from *B*. A similar test with the P_2O_5 driers alone showed no change from *B*. Comparing curves *B* and *C* with curve *A*, shows that something favorable to the formation of the final ion had been added. On account of the long closed system this effect can not safely be attributed entirely to the P_2O_5 and $CaCl_2$.

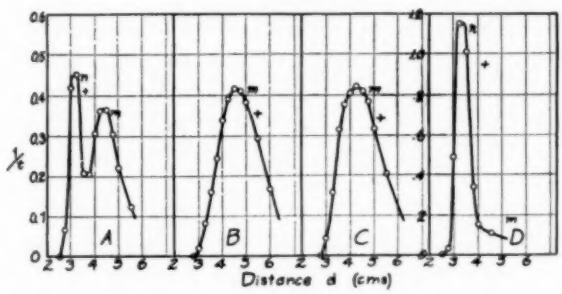

Fig. 2. Showing effect of drying agents.

Curve *D*, Fig. 2, was obtained when the air passed through the $CaCl_2$ tank *J* only and then through the coils *M* immersed in liquid air, the polonium being at 18 cm from *E* as before. It is here seen that initial ions *n*, are present and that there is only a trace of the final ions *m*. A condition now prevails which makes it difficult for the final ions *m* to form. We are no doubt here dealing with the real initial air ion. The negative ion during the above procedure remained unchanged. Its maximum agrees with that of the initial ion *n*.

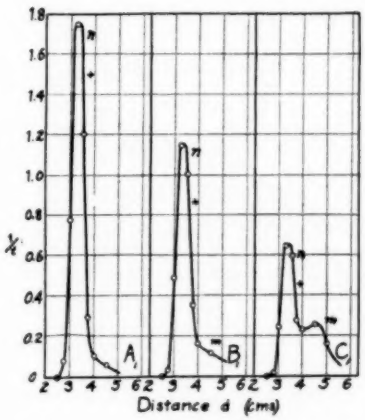

Fig. 3. Showing ageing of initial ion in dry air.

In Fig. 3 are shown results obtained when the air passing through the auxiliary tube *TE* was dried by passing through the $CaCl_2$ tank *J* and through the coils *M* immersed in liquid air. Curve A_1 was obtained when the polonium was at *E*, giving an ion-age of about 0.02 sec. It is seen that only the initial ion *n* is present.

Curve B_1 was obtained with the polonium 18 cm from E, giving an ion-age of 0.1 sec. Only a trace of the final ion m is here present.

Curve C_1 was obtained with the polonium 80 cm from E. This corresponds to an ion age of about 0.5 sec. It is here seen that there are less of the ions n and that final ions m have formed. The negative ion during the above remained unchanged. This indicates that in air dried in this manner the positive ion changes into the final ion with age. The transition is, however, much slower than in the case of room air, or in the presence of the impurities added by the $CaCl_2$ or P_2O_5 drying chambers. There is a question if the small change observed is due to a small amount of impurity still remaining in the air, as for example, the impurities due to the ionization.

Effects Due to Drying Nitrogen

A commercial cylinder containing nitrogen of 99 percent purity was connected through a reducing valve to the system immediately before the glass-wool strainer L, Fig. 1. The driers J and K were disconnected. The nitrogen thus passed successively through M, N, Q, R, and S into the auxiliary tube at T.

The results are shown in Fig. 4. Curves A_2 and B_2 are for the negative and positive ions when the polonium was 70 cm from E thus giving ions about 0.4 sec. old. The nitrogen passed through the coils M without liquid-air

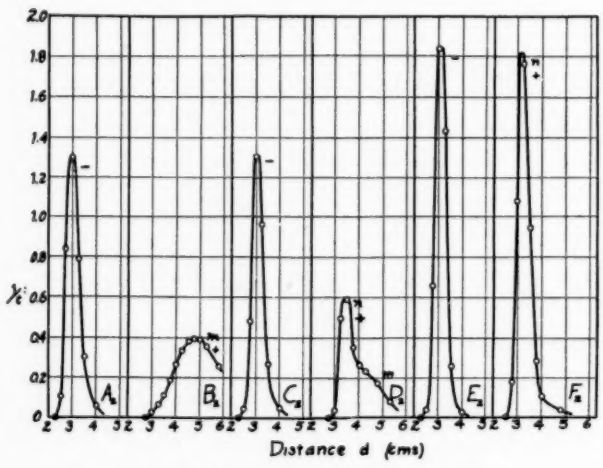

Fig. 4. Showing effect of drying nitrogen.

cooling. It is seen that the normal negative ion, mobility 1.87, is present and that only the final 1.36 positive ion m is present.

Curves C_2 and D_2 are for the negative and positive ions when the nitrogen passed through the coils immersed in liquid air, the polonium being 70 cm from E as before. It is here seen that the negative is unchanged. The positive, however, has changed and now consists primarily of initial 1.87 ions n. There are, however, also a few final 1.36 ions m, comparable to Curve C_1, Fig. 3, which was for the polonium at 80 cm.

Curves E_2 and F_2 were obtained with the polonium close up to E thus giving ions about 0.02 sec. in age. The coils were immersed in liquid air. Here there is present only the normal negative ion and the initial positive ion n, both having the same mobility. The fact that the negative ion is normal in nitrogen at this short age must mean that the free electrons known to exist in nitrogen become attached when entering the main room-air stream at E.

It is thus seen that the results with nitrogen are smilar to the results for air, and that the final ion forms more quickly in nitrogen taken directly from the cylinder without liquid-air drying. With the liquid-air drying, however, it is seen that the initial ion attaches itself with difficulty.

Impurities due to Ionization

Tyndall, Grindley and Sheppard[2] suggested that impurities may be formed which are due to the ionizing action of the rays and obtained results indicating this. In order to test this point, a rectangular brass chamber 7.4 cm square and 23 long was inserted between S and T, Fig. 1. No special care was taken to clean the surfaces of the chamber. A metal rod connected to earth extended through this chamber and into the tube TE. This gave a potential

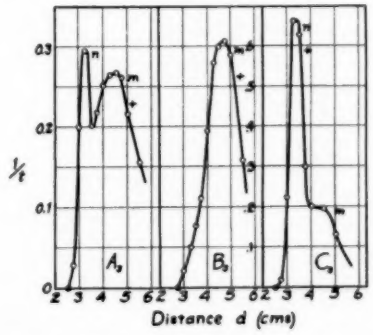

Fig. 5. Showing effect of ionizing air in a metal chamber.

of 5000 volts between the rod and the chamber and tube. A powerful source of beta-rays was introduced into the chamber. The air in the chamber was thus ionized very heavily but the ions were removed by the time the air passed the downstream end of the rod. The polonium was placed a short distance downstream from the end of the rod thus reionizing the air, and giving ions of an age of about 0.3 sec. The air was dried by passing through the $CaCl_2$ tank J and the coils M immersed in liquid air.

The results are shown in Fig. 5. Curves A_3 and B_3 were obtained simultaneously, that is, after a reading for A_3 without the beta-rays had been obtained, the rays were introduced into the chamber and a reading for curve B_3 obtained. This procedure more fully insures identical conditions. It is thus seen that curve A_3, which is for air which had not been ionized, shows the presence of initial ions n, whereas curve B_3, which is for air which

[2] Tyndall, Grindley and Sheppard, Proc. Roy. Soc., **A121**, 185 (1928).

had been ionized, shows that the initial ions have been transformed. It is thus clear that the ionizing process gives rise to something which greatly enhances the transition into the final ion. Presumably this is due to the formation of oxides of nitrogen and ozone.

Direct Effect of the Chamber

In Fig. 5, Curve C_3 was obtained under conditions similar to those for curve A_3, but without the chamber. It is here seen that without the chamber, mostly initial positive ions are obtained whereas with the chamber the final ions predominate as shown by curve A_3. The chamber itself had a contaminating effect.

In order to test further the effect of ionization, a glass bulb W, 12 cm in diameter was inserted between S and T, Fig. 1. The upper side had been caved in so as to form a recepticle into which the decayed emanation tubes giving beta-rays could be placed. A rod X connected to earth passed centrally in the auxiliary tube ET, as shown in Fig. 6. The auxiliary tube was at 5000 volts, thus giving a field which removed the ions due to the beta-rays in W from the air before it reached the polonium P, where it was reionized.

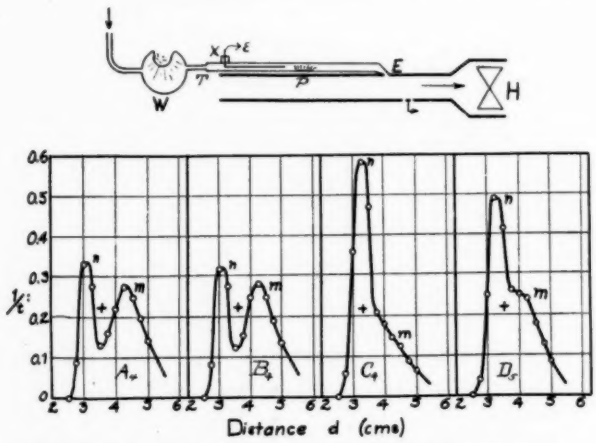

Fig. 6. Showing effect of impurities due to ionization.

The results are shown in Fig. 6. Curve A_4 was obtained when room air entered directly into the vessel W. This shows the presence of initial ions n and final ions m. Curve B_4 was obtained when the room air entering W was heavily ionized by the beta-rays. No appreciable change from A_4 was obtained. n had been slightly lowered and m slightly raised. This unchanged result is apparently due to the water present in the room air which, as will be seen later, has an opposite effect to that of the impurity due to ionization in dry air.

Curve C_4 Fig. 6, was obtained with no rays in W and the air dried by passing through tank J and the coils M immersed in liquid air. It is seen as before that practically all the ions are initial ions n. Curve D_4 was obtained under identical conditions as for C_4 but with the beta-ray tubes in the re-

cepticle in *W*. It is seen that final ions *m* have been formed. The day was cold and dry so that the room air passing through the main tube *AB*, Fig. 1, had a low humidity.

The curves in Fig. 7 were obtained when a glass bulb *W*, 12 cm in diameter was inserted between *S* and *T*, Fig. 1. Through an opening at the top a thin aluminum capsule 2.6 cm in diameter and 5 cm long was inserted. This capsule could be filled with the beta-ray tubes thus ionizing the air in *W* more heavily than in the case of Fig. 6.

Curves A_5 and B_5 are for room air without beta-rays and with beta-rays in the aluminum capsule. As in A_4 and B_4 in Fig. 6, no appreciable differ-

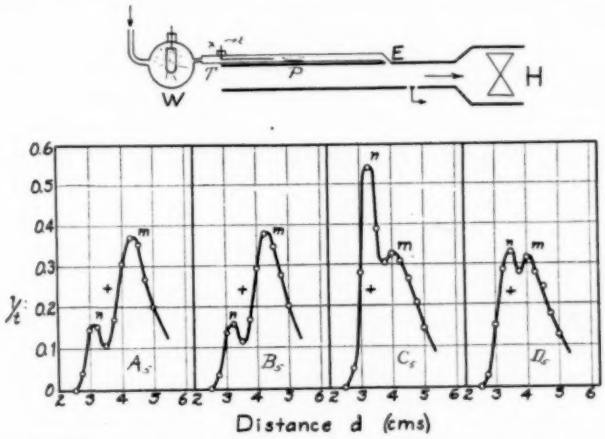

Fig. 7. Showing effect of impurities due to ionization

ence was obtained. Only a slight lowering of *n* and raising of *m* was obtained. Curve C_5 was obtained when the air entering *W* passed through the tank *J* and the coils *M* immersed in liquid air. No rays were present in the aluminum capsule in *W*. It is seen that more final ions *m* were present there than in the case of C_4, Fig. 6, presumably due to greater contamination by the vessel *W*. Curve D_5 was obtained with the rays in *W*, conditions otherwise being the same. It is seen that there is a marked diminution in the number of initital ions similar to D_5 Fig. 6.

It is therefore apparent that impurities are formed in the ionization process which increases the rate of transition of the initial into the final ion.

The Effect of Water

In order to test the effect of humidity, distilled water was added to bulb *W*. The air passing over this evaporated the water.

The results are shown in Fig. 8. Curve A_6 was obtained when the bulb *W* was dry and the entering air had passed through the tank *J* and coils *M* immersed in liquid air. No rays were present in *W*. Practically only initial ions *n* are present. Curve B_6 was obtained when distilled water was placed in the bulb *W*; no rays were present in *W*. It is seen that final ions *m* have formed. These are due to the ageing of the initial water ions as was shown in an earlier paper.

Curve C_6 was obtained with the conditions the same as for B_6 except that that the beta-ray bulbs were placed in the receptacle in W. It is seen that fewer final ions m and more of the initial ions n were present than in the case of air containing moisture alone. The final ion m in B_6 is, on the writer's view, a two-molecule water ion. This ion apparently is simplified back to a

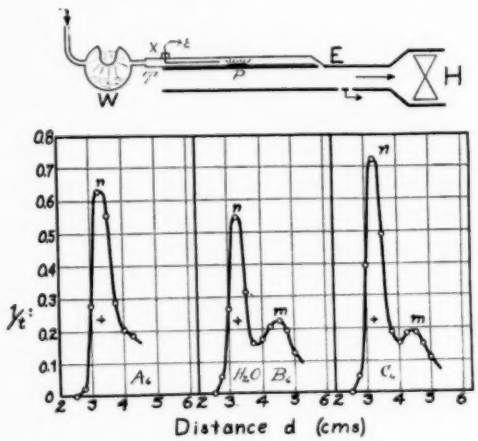

Fig. 8. Showing effect of water and the ionization impurity.

one molecule ion n. The behavior is as if the impurity due to ionization deprives the ion m of a water molecule or that the impurity is molecular and gives up an electron to the ion m and itself becoming a one molecule positive ion n. By means of a modified method it will be possible to clarify this point.

Discussion of Results

From the above it is apparent that in a study of the air ions it is necessary to work under very definite conditions. In the first place the air must be thoroughly dried. Drying by passing through concentrated H_2SO_4 adds an impurity which alters the ions. From the above, drying agents like $CaCl_2$ and P_2O_5 apparently do the same. Even a closed vessel, especially if of metal, alters the ions. Any drying process must include cooling by means of liquid air and careful straining while the air is cold to remove water dust, etc. When the air has been thoroughly dried, the transition of the initial positive ion into the final positive ion is very slow, being of the order of one second for half-value. This transition even, may be due to traces of impurity still remaining. On the writer's view the initial positive ion is one molecule large. It has the same mobility, namely of the order of 1.87 cm/sec per volt/cm, as the negative air ion which is also one molecule large. The negative ion does not change with time. The initial positive ion, however, does change with time into a definite ion of a lower mobility, of the order of 1.36 cm/sec per volt/cm. This ion is, on the writer's view two molecules large. The rate of transition into the slower ion depends upon the character of the impurity present. If water is added to the dry air the initial air

ion becomes a one molecule water ion (H_2O^+). This is undoubtedly due to the fact that the ionizing potential of H_2O is of the order of 13, where as that of N_2 or O_2 is of the order of 16. This permits an electron to pass from H_2O to N_2^+ or O_2^+. The H_2O^+ ion thus formed and being one molecule large has the same mobility as the N_2^+ or O_2^+ ions and also the same as the N_2^- or O_2^- ions.

The H_2O^+ ion, it was found in an earlier investigation, unites with another molecule forming the slower 1.36 ion. This transition is quite rapid having a half-value period of the order of one-tenth second.

It is apparent from the work of Tyndall, Grindley and Sheppard and from the above results that in air the ionizing process itself gives rise to molecules which will alter the ions. This impurity, which presumably is an oxide of nitrogen, is very rapid in its attack on the initial one-molecule positive air ion, resulting in a positive two-molecule ion of mobility 1.36. This transition is so rapid that even to minimize it introduces a serious experimental difficulty. In fact, it practically bars the use of a closed vessel method. The ions will have to be drawn out of the ionized region in a time which is shorter than the time necessary for the impurity to act. Care will then also have to be exercised that the air which was ionized does not itself enter the measuring vessel.

As seen above if water is also present the situation is further complicated. The ionizing impurity and the water both attack the initial air ion and the ions so formed, have themselves an interaction.

It thus seems that any method in order to give clarifying results must accomplish the following: 1. It must remove the ions from the ionized regions in an interval not to exceed 0.001 sec after formation; 2. It must not admit any of the air from the ionized region into the measuring part; 3. It must have a region through which the ions pass and to which definite impurities may be added for varying intervals of time; 4. It must permit the ions to be removed from this region into a region of definite character such as pure dry air; 5. It must permit the measurement to be made in a definite interval preferably not in excess of 0.001 sec. The writer has begun the use of a method embodying these features.

The author wishes to thank the Exceutive Committee of the Graduate School of the University of Minnesota for its financial aid in this research.

ADSORPTION OF AIR AND WATER VAPOR ON ROCK-SALT SURFACES

By J. H. Frazer*
Department of Physics, University of California

(Received May 27, 1929)

Abstract

With a method previously described the adsorption of air on rock-salt surfaces is measured as a function of temperature, and the temperature at which complete outgassing occurs is determined. An estimate of the thickness of the film is given, and also the approximate speed at which it forms. The effect of water vapor on the surface is observed, and it is shown that exposure to water vapor has no permanent effect on the surface as long as the partial pressure of the water vapor is kept below that of a saturated sodium chloride solution at the same temperature. This, however, is true only of cleavage surfaces; polished surfaces are less stable against the action of water vapor.

WHEN light, plane polarized at 45° to the plane of incidence, is reflected at a certain definite angle from the sharp boundary between two isotropic dielectric media, the reflected light should be plane polarized. Experimentally this is not quite so; the light is almost always more or less elliptically polarized. This elliptical polarization is explained by saying that the boundary between the two media is not a mathematical plane, but that there is a gradual transition from the properties of the first to those of the second medium. The mathematical expression for this elliptical polarization,[1] to the first order in $1/\lambda$ is:

$$\rho=\frac{\pi}{\lambda}\,\frac{(\epsilon_1+\epsilon_2)^{1/2}}{\epsilon_1-\epsilon_2}\int_{Z_2}^{Z_1}\frac{(\epsilon-\epsilon_1)(\epsilon-\epsilon_2)}{\epsilon}dZ.$$

Where ρ is the "coefficient of ellipticity," i.e., the ratio of the minor to the major axis of vibration of the reflected elliptically polarized light: ϵ_1 is the dielectric constant in the 1st medium; ϵ_2 is the dielectric constant in the 2nd medium; ϵ is the dielectric constant in the transition layer; and λ is the wave-length of the light used, and the integral extends over the region of variable ϵ.

This surface or transition layer, the region within which the optical properties are different from those of either medium, might originate in one or more of the following ways:

(1) The interface might have irregularities small in comparison with the wave-length of light. This would not produce scattering, but two planes drawn tangent to the tops and bottoms of these irregularities would then enclose a region in which there would obtain a dielectric constant to the first approximation the mean of those of the two media.

* National Research Fellow.

[1] Drude, Lehrbuch der Optik, p. 272.

(2) There might be material adsorbed at the interface, which would then constitute a transition layer.

(3) The temperature agitation of the surface would result in a roughening of the surface which would be in addition to (1) above.

(4) Even in the case of the reflection of light from a "molecularly plane" surface at the absolute zero of temperature there would still be an effective transition layer because the surface ions or molecules are in a different condition from those in the interior.

It will be noted that the expression for the ellipticity involves, besides the thickness, also the dielectric constant. This means that in order to evaluate the thickness we must know the dielectric constant, not only its average value, but its value as a function of position as we proceed from medium (1) to medium (2). However, the error made by assuming the dielectric constant to be constant within the layer is small. Neglecting this it is frequently possible, by assigning reasonable values to the dielectric constant, to get a fair approximation to the thickness, and it is always possible to set a minimum thickness, namely,

$$l=\frac{\rho\lambda}{\pi(1+n^2)^{1/2}}\,\frac{n+1}{n-1}.$$

The ellipticities were experimentally determined by reflecting light from the surface under investigation at the polarizing angle, and measuring photometrically the ratio of the amplitudes of the two beams transmitted by the

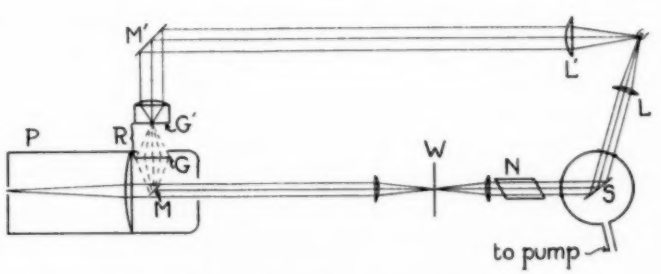

Fig. 1. Diagram of apparatus

nicol analysing prism (a) when set to transmit light vibrating perpendicular to the plane of incidence, and (b), when set to transmit light vibrating parallel to the plane of incidence.

The apparatus used, a diagram of which is given below, is practically that employed in a previous investigation,[2] the principal change being that light from the same source is used both for reflection from the surface under investigation and for illuminating the photometer. This made the readings independent of any fluctuations in intensity of the light source, and correspondingly increased the reliability of the readings.

[2] J. H. Frazer, Phys. Rev. **33**, 97 (1929).

Experimental

A piece of rock salt, as free as possible from striations, cloudiness, etc., was ground and polished to a small angle (5–10 degrees) to the cleavage plane. The crystal was then cleaved along the cleavage plane nearest parallel to the polished surface, so that a narrow angle prism resulted, and reflection from the cleavage plane could be gotten without an interfering reflection from the back surface. This crystal was then put, as quickly as possible, into the apparatus, and the apparatus evacuated. The ellipticity was read. The temperature of the apparatus was then raised, and readings taken until they reached a constant value. Then a second higher temperature was established, and readings again taken until they became constant, and so on. The curve given below is the temperature plotted against the equilibrium values of the ellipticity, which is roughly proportional to the thickness of the adsorbed layer. It will be observed that the curve reaches a minimum at about 330° and again starts to rise very slightly; but this last rise is within the limit of experimental error. At temperatures above 400° the readings became very unreliable, going up and down again with no apparent regularity while the temperature was kept constant.

These fluctuations were interpreted to mean evaporation and recondensation of the NaCl, since it was found that cooling a part of the container by a blast of cold air while it was at this temperature would stabilize the readings. The air blast would be expected to prevent recondensation, and so maintain a steady surface condition of continuous evaporation.

I then tried exposing the crystal to the action of water vapor. A new, freshly cleaved crystal was put in the apparatus, and the apparatus evacuated and sealed off from the pump. Then a liquid air bottle was removed from around a side tube containing a saturated solution of sodium chloride; this warmed up to room temperature, establishing in the apparatus the vapor pressure of a saturated sodium chloride solution. This was necessary to prevent condensation of water on, and solution of, the crystal surface. After standing for several hours, the readings showed no change, indicating that the amount of water vapor adsorbed was smaller than could be detected experimentally. The water vapor was then frozen out with liquid air, and the apparatus heated to 350°. On cooling to 30° and establishing a pressure of 5 mm water vapor pressure, the ellipticity increased from 0.00887 to 0.00108, coming back to its original value 0.00887 on being reheated and re-evacuated.

Interpretation

Obviously, neither the "intrinsic surface effect" ((4) at beginning of paper) nor the degree of polish is a function of temperature. Therefore, this effect must be ascribed to adsorbed material, and to the temperature vibrations of the surface. The amount of adsorbed material, and its contribution to the ellipticity, would decrease with increasing temperature; on the other hand, the temperature vibration of the surface, and its contribution to the ellipticity, would increase with increasing temperature. Applying this to the above, we see that the thickness of the layer decreases up to 330° and from

there on remains constant to within the limits of experimental error. This means that on increasing the temperature, the decrease in ellipticity due to the progressive outgassing of the surface overshadows the increase in ellipticity due to increased thermal agitation of the surface up to temperatures of 330°. From there on the algebraic sum of the two effects is zero, as far as can be told experimentally.

We can get a maximum value, and an order of magnitude for this temperature roughening of the surface in the following way. We take into account the surface ions only, and consider them as an aggregate of uncoupled linear harmonic oscillators, and evaluate the root mean square position. Multiplying this by two will give us the layer thickness. We get the same result for the linear oscillator classically and quantum-mechanically, namely

$$(\overline{x^2})^{1/2} = \left(\frac{KT}{8\pi^2 m\nu^2}\right)^{1/2}, \quad \text{or} \quad \Delta Z = \left(\frac{KT}{2\pi^2 m\nu^2}\right)^{1/2}$$

Even if this layer has its maximum effect on the ellipticity, this effect would be experimentally undetectable; so we are justified in ascribing this effect to adsorbed layers alone.

Below is given the curve representing a plot of ellipticity against temperature.

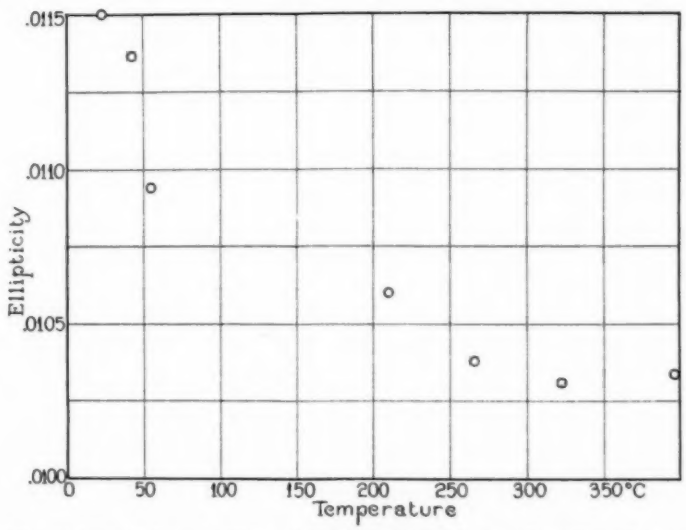

Fig. 2. Adsorption of air on sodium chloride. Ellipticity as function of temperature.

Above the temperatures indicated in the diagram, there was evidence of evaporation, and we felt safe in assuming that the minimum of this curve represented a condition of no adsorption. If this is so, then the total thickness of adsorbed layer adsorbed at room temperatures can be assigned a limit, namely 6×10^{-8} cm.

Attention must be called to the fact that these figures represent equilibrium values at the indicated temperature and degree of evacuation used

(10^{-5} on a McLeod gauge, with liquid air trap). If the crystal be outgassed at a temperature above 330° and the temperature lowered, it requires only about 30 min. for the equilibrium thickness of layer corresponding to the lower temperature to be established, and this thickness, within the experimental error, is independent of the pressure within the limits of 760 and 10^{-5} mm.

Since the dielectric constants of water and air are not known for such thin layers, we can only assign a lower limit to the thickness of the layer, and if we wish, make what seems a reasonable assumption about the dielectric constant, and then make our calculations. In the case of water vapor and air, we might take the dielectric constant of liquid water, and calculate that of air from the dielectric constant of atmospheric air and the known density of liquid air by Lorentz's[3] formula. Doing this, we find that the values we so get are not very far from being those calculated as a minimum, and so they seem reasonable values. This would mean that in the above curve we would interpret the maximum ordinate as corresponding to a layer thickness of 6×10^{-8} cm and the minimum ordinate as a zero layer thickness. This is probably right to within the experimental error.

Further, the experiments were quite conclusive in that exposure to a vapor pressure of water less than that of a saturated solution of sodium chloride produces no permanent change in the surface. (This was *not* so in the case of a polished surface; these deteriorated at a much lower pressure, although the limit was not found.)

[3] Lorentz, Theory of Electrons, p. 144.

THE COMPRESSIBILITIES AND THERMAL PRESSURE COEFFICIENTS OF CERTAIN LIQUIDS

By Joel H. Hildebrand
Chemical Laboratory, University of California

(Received June 10, 1929)

Abstract

Values for the compressibilities of heptane, acetone, carbon tetrachloride, benzene, carbon disulfide, ethylene chloride, ethylene bromide and bromoform, obtained by Westwater, Frantz and Hildebrand from their direct measurements of the thermal pressure coefficient, $(\partial p/\partial T)_v$, were subject to a small error which is here corrected. The corrected values are compared with some recalculated from the adiabatic compressibilities directly measured in 1913 by Tyrer, and obtained recently by Freyer, Hubbard and Andrews by the aid of a sonic interferometer. The data from the three sources and methods show excellent agreement. Values are given for the constant $v^2T(\partial p/\partial T)_v$, from which can be calculated the coefficients of thermal pressure or of compressibility at various temperatures by the aid of existing data for the densities and coefficients of expansion. In the following list the first number for each substance represents the coefficient of thermal pressure at 20°, the second the compressibility at $20° \times 10^7$ and the third the value of the above mentioned constant: Heptane, 8.66, 1430, 5420; acetone, 11.32, 1260, 5305; carbon tetrachloride 11.47, 1060, 1325; benzene, 12.58, 966, 4800; carbon disulfide, 12.67, 938, 2340; ethylene bromide, 15.20, 633, 936; ethylene chloride, 14.17, 818, 2640; bromoform, 15.32, 594, 537. The unit of pressure is the atmosphere, v is the specific volume.

NOT long ago, the writer, with the collaboration of W. Westwater and H. W. Frantz[1] published values for $(\partial p/\partial T)_v$ (which we will call the thermal pressure coefficient, $T(\partial p/\partial T)_v$ being the thermal pressure), for eight liquids and a number of their mixtures. These values were directly determined by making use of what was in principle a constant volume thermometer. From them the authors calculated the corresponding compressibilities by the aid of the cofficients of expansion. The compressibilities so obtained were somewhat higher than many of those recorded by other observers. Part of the disagreement is due to an error in our calculation. We used the equation $(\partial p/\partial T)_v = \alpha/\beta$, where α and β are, respectively, the cofficients of expansion and compressibility. This is true at 0°C, but since the coefficient of expansion is ordinarily defined as $\alpha = (1/v_0)\,(\partial v/\partial T)_p$, and the coefficient of compressibility as $\beta = (-1/v)\,(\partial v/\partial p)$, where v is the specific volume at 1 atmosphere and t°C, v_0 the same at 0°C, our values for β should be multiplied by v_0/v. In giving corrected values, we have availed ourselves of the data given in the International Critical Tables, except that the coefficient of expansion and density of bromoform are from the recent measurement in this laboratory.[2] The resulting values are still larger than most of those found in the literature,

[1] Westwater, Frantz and Hildebrand, Phys. Rev. **31**, 135 (1928).
[2] A. Sherman and J. Sherman, J. Am. Chem. Soc. **50**, 1119 (1928).

but are strikingly comfirmed by two sets of values, one by Tyrer[3] calculated from the observed adiabatic compressibility, and another recently published by Freyer, Hubbard and Andrews,[4] who determined the velocity of sound by a sonic interferometer, which gives the adiabatic compressibility from which, in turn, the isothermal compressibility was calculated. This calculation requires data for the density, the thermal expansion and the specific heat. The last named experimenters used the same data for these quantities as were used by Tyrer, but since newer data are available, we have recalculated their results for the liquids we measured by the aid of data taken from the International Critical Tables.

Table I gives in columns 2 and 3 the adiabatic coefficients of compressibility at 20°C, obtained for these liquids by Tyrer and by Freyer, Hubbard

TABLE I.* *Thermal pressure coefficients and compressibilities at 20°C. The unit of pressure is the atmosphere.*

Liquid	Adiabatic compressibility Tyrer	F., H. & A.	Specific heat	Density, ρ	$\partial v/\partial T$ $\times 10^3$	Thermal pressure coef. $\partial p/\partial T$ Tyrer, F., H. & A.	W., F. & H.		Isothermal compressibility, β, $\times 10^5$ Tyrer, F., H. & A.	W., F. & H.		$v^2 T \partial p/\partial T$
Heptane		111.4		0.6836	1813		8.61	8.66		143.9	143.0	5420
Acetone		90.6	2.182	0.7901	1805		11.35	11.32		125.6	126.0	5305
Carbon tetrachloride	72.45	72.8	0.836	1.5941	763	11.54	11.49	11.47	105.3	105.8	106.0	1325
Benzene	66.25	65.8	1.69	0.8787	1382	12.68	12.73	12.58	95.8	95.4	96.6	4800
Carbon disulfide	59.95	59.8	1.005	1.2624	942	12.78	12.82	12.67	93.0	92.7	93.8	2340
Ethylene bromide				2.1805	441			15.20			63.3	936
Ethylene chloride				1.2537	926			14.17			81.8	2640
Bromoform		41.2		2.8912	315			15.32			59.4	537

* The author is indebted to Mr. A. Wachter for help in the calculations.

and Andrews, respectively. The original observations extend through a range of 50 to 80 degrees but we reproduce here only the values for 20°, since the variation with temperature is adequately taken care of by a relation given below. The specific heats, in column 4, are probably subject to greater error than any of the other factors involved, but fortunately the formula whereby the isothermal compressibilities are calculated reduces the error to about one-third. In the sixth column we give $(\partial v/\partial T)_p$ instead of the ordinary coefficient of expansion, to avoid the confusion mentioned in the opening paragraph. In the seventh and eighth columns are given the values of $(\partial p/\partial T)_v$, a very important thermodynamic quantity, calculated from the adiabatic compressibilities, β_H, from the two sources, by aid of the formula

$$\left(\frac{\partial p}{\partial T}\right)_v = \left(\frac{\beta_H}{\rho \partial v/\partial T} + \frac{0.1013T}{C_p} \cdot \frac{\partial v}{\partial T}\right)^{-1}.$$

In the ninth column are the values of the same coefficient directly determined by the author and his collaborators.

The next three columns give values of the isothermal compressibility,

$$\frac{1}{v}\left(\frac{\partial v}{\partial p}\right)_T \text{ or } \rho\left(\frac{\partial v}{\partial p}\right)_T,$$

[3] Tyrer, J. Am. Soc. **103**, 1675 (1913).
[4] Freyer, Hubbard and Andrews, J. Am. Chem. Soc. **51**, 759 (1929).

where ρ is the density corresponding to each value of the coefficient of thermal pressure, calculated from the latter by the aid of the density and expansion coefficient, by the aid of the relation

$$\left(\frac{\partial p}{\partial T}\right)_v \left(\frac{\partial v}{\partial p}\right)_T = -\left(\frac{\partial v}{\partial T}\right)_p.$$

The agreement between the values of the coefficients of thermal pressure and of compressibility from the three sources is very striking, especially when it is remembered that they are derived from as many independent methods, and it goes far towards establishing the fact that the lower values for the compressibility obtained for these substances by many other investigators are of inferior accuracy.

The variation of β with temperature can be calculated with considerable accuracy by the relation used by Westwater, Frantz and Hildebrand, i.e. that $v^2T(\partial p/\partial T)_v$ is constant. Evidence for this was given in their paper and it is further comfirmed by the data of the other workers cited in this paper. We will give here only the values of the constant for benzene.

Temperature:	10	20	30	40	50	60	70
Tyrer:	4800	4815	4830	4830	4810	4820	4810
F., H. and A.:	4813	4820	4815	4820	4805		

We therefore give in the last column of Table I, values of this constant, representing weighted means, from which, by the aid of values of the density and of $(\partial v/\partial T)_p$, readily obtainable from the International Critical Tables, one may readily calculate either coefficient, that of thermal pressure or of compressibility at 1 atmosphere and any ordinary temperature.

NOTE ON THE THEORY OF ACOUSTIC WAVE FILTERS

By R. B. Lindsay
Sloane Physics Laboratory, Yale University

(Received July 5, 1929)

Abstract

Comparison is made of the lumped impedance theory of Stewart and the more recent transmission theory of Mason. It is found that for the low frequency pass and single band types the former theory gives to a very close approximation the same frequency limits for the transmission region as the latter. The weak point of the former is the high frequency pass type, where Stewart's formulae are semi-empirical. The connection between these and the corresponding formulae of Mason is investigated.

THE development of the acoustic wave filter has been due mainly to G. W. Stewart[1], who first presented the theory and constructed actual filters. His theory given in the first of the papers noted below (hereafter referred to as *loc. cit.*) assumes lumped acoustic impedances in the main line and branch lines postulating that the air in each section of the filter moves as a whole and that the length of each is short compared with one wavelength of the sound. More recently Mason[2] has worked out a more general theory of the acoustic filter and has applied it to several special cases. It does not appear, however, that anyone has clearly pointed out the relation between the two theories to account in particular for the generally excellent agreement with the experimental data of Stewart's admittedly approximate theory. It is the aim of the present article to make this clear.

Considering the accompanying schematic diagram (Fig. 1) of an infinite filter in which the branches (represented here for simplicity as simple ori-

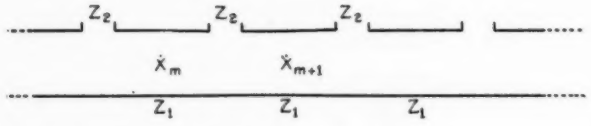

Fig. 1. Diagram of acoustic filter.

fices) are assumed arbitrary in nature, the lumped impedance theory, neglecting viscosity damping, (loc. cit. p. 531) deduces the relation

$$\dot{X}_{m+1}/\dot{X}_m = e^{Y} \tag{1}$$

where

$$\cosh Y = 1+\tfrac{1}{2}Z_1/Z_2. \tag{2}$$

[1] G. W. Stewart, Phys. Rev. **20**, 528 (1922); **23**, 520 (1924); **25**, 90 (1925).
[2] W. P. Mason, Bell System Technical Journal **6**, 258 (1927).

In these equations $\dot{X}_m$ denotes the volume current at the beginning of the m^{th} section, while Z_1 is the acoustic impedance of one section of the main conduit and Z_2 that of one of the recurrent branches. Both Z_1 and Z_2 are here supposed to be pure reactances, so that their ratio is real. Transmission without attenuation occurs only when Y is a pure imaginary, i.e. $-1 < \cosh Y < +1$. Hence the limits of the transmission region will be given by the equations

$$Z_1/Z_2 = 0, \; Z_1/Z_2 = -4. \tag{3}$$

In the theory of Mason, which may perhaps be called the branch transmission theory since it is most simply developed by considering transmission through a conduit with a side branch[3] it is found that the relation corresponding to equation (1) above is

$$\dot{X}_{m+1}/\dot{X}_m = e^{-iW} \tag{4}$$

where

$$\cos W = \cos 2kl + (iZ/2Z_2) \sin 2kl. \tag{5}$$

There is a similar relation for the pressures[4]. In the Eq. (5) $2l$ = length of one section i.e. the distance between successive branches, Z_2 is the branch impedance as before, but Z is *not* the same as Z_1. Rather we have $Z = \rho_0 c/S$, where ρ_0 is the equilibrium density of the air, c the velocity of sound and S is the area of cross section of the main conduit. It is seen that Z is the acoustic resistance of the plane wave in the conduit. As usual, $k = \omega/c = 2\pi\nu/c$, where ν is the frequency. Transmission without attenuation occurs only when W is real, i.e. for $1 > \cos W > -1$. Hence on this theory the limits of the transmission region are given by the transcendental equations (Mason, reference 2, p. 267)

$$(iZ/2Z_2) = -\cot kl, \quad (iZ/2Z_2) = \tan kl. \tag{6}$$

We have now to investigate the relation between Eqs. (3) and (6). Suppose first that kl is very small, corresponding to short sections and low frequencies. Neglecting higher powers of kl than the first, Eqs. (6) become

$$2ikl\,Z/Z_2 = -4, \quad 2ikl\,Z/Z_2 = 0 \tag{7}$$

From the value of Z, it is seen that these take the form of Eqs. (3) provided we set $Z_1 = 2ikl\rho_0 c/S$. But this is precisely $i\omega M_1$ where M_1 = (mass of air per section)$/S^2$ is the inertance of one section of the conduit. Now for the low frequency pass and the single band type filters Stewart (loc. cit. p. 541 ff) assumes Z_1 to be just of this form, and hence to the above mentioned approximation the two theories give identical results.

The situation is different if l is no longer small and if high frequencies are considered, as is the case with the high pass filter, the simplest type of which is a tube with simple orifices as branches. Here since $Z_2 = i\omega M_2$

[3] G. W. Stewart, Phys. Rev. **26**, 688 (1925).

[4] See the above noted article of Mason, p. 266, and allow for change in notation.

(inertance only in the orifice) the lumped impedance theory can not define Z_1 as above. In this case Stewart (loc. cit. p. 538) assumes that Z_1 is due to a combination of inertance M_1 and capacitance C_1 in parallel, that is

$$Z_1 = i\omega M_1/(1 - M_1 C_1 \omega^2) \tag{8}$$

where M_1 is as given above and $C_1 = V/\rho_0 c^2 = 2lS/\rho_0 c^2$. As an alternative choice, he also tried

$$Z_1 = -i/C_1\omega \tag{9}$$

corresponding to $M_1 = \infty$ in (8). There is little justification for either of these, except on empirical grounds, as was pointed out by Stewart. There is, indeed, some argument in favor of attributing capacitance to the conduit in this case, but no one knows *a priori* how much. However, the choice (8) led to rather good agreement with experiment, and we wish to see why. Substitution and reduction of (8) yield

$$Z_1 = i\rho_0 c/S \cdot 2kl/(1 - 4k^2l^2)$$

and if $Z_2 = i\omega M_2 = i\omega\rho_0/c_0$, where c_0 is the acoustic conductivity of the orifice, the low frequency limit is given by

$$c_0/2kS = -(1 - 4k^2l^2)/kl. \tag{10}$$

For the same limit the second of Eqs. (6) gives

$$c_0/2kS = \tan kl \tag{11}$$

whence there is agreement between the two theories for this case only if

$$\tan kl = -(1 - 4k^2l^2)/kl$$

which is not an identity but is approximately satisfied for kl in the immediate neighborhood of $(1/3)^{1/2}$. As a matter of fact this condition is met approximately in most of Stewart's data on the high pass filter (loc. cit. p. 548). Recalculation, using the limit given by Eq. (11) gives somewhat better agreement with the experimental results, which are, of course, themselves not too precise.

It is perhaps worthy of comment that the assumption which attributes capacitance only to the conduit (see Eq. (9)) gives low frequency limits about *half* as large as the experimental values. Thus if we assume[5] $Z_1 = -4i/C_1\omega$, the second of Eqs. (3) gives for the low limit

$$c_0/2kS = kl \tag{12}$$

instead of (11). If $kl < 0.6$, the difference between kl and $\tan kl$ is less than 13 percent and the calculated frequencies differ in percentage by roughly half this. This explains why Stewart's F' values (loc. cit. p. 547 and Table III p. 548) are about half the right order of magnitude.

[5] This fact has been called to my attention by Professor Stewart.

The conclusion we reach then is that as far as the low pass and single band type filters are concerned the lumped impedance theory is as good in practice as Mason's branch transmission theory.[6] The weak point of the former lies in the high pass case, but the above discussion shows that even here it is possible to give it a reasonably satisfactory interpretation. Its greater simplicity will undoubtedly continue to render it preferable to the branch transmission theory in the practical construction of filters. Reference may here be made to a forthcoming article by G. W. Stewart and C. W. Sharp[7] in which further comparison between the two points of view is made on the basis of more recent experimental data. The measurements here referred to are of the so called *characteristic* or *mid-series* impedance, i.e. the impedance with which it is necessary to match a *finite* filter terminated half way between two successive branches in order that it may act as an *infinite* filter. On the lumped impedance theory this is $(Z_1Z_2+Z_1^2/4)^{1/2}$, while the branch transmission theory (Mason, loc. cit. p. 265) yields for the same quantity

$$p_m/\dot{X}_m=Z_0=Z\left(\frac{1+iZ/2Z_2\cdot\tan kl}{1-iZ/2Z_2\cdot\cot kl}\right)^{1/2}. \tag{13}$$

For kl small, substitution and reduction show that to the approximation already employed in establishing Eqs. (7) these two impedances are identical.

I am indebted to Professor Stewart for discussion of the material in this article.

[6] This statement neglects the presence of the additional bands found in these types of filter, which are perhaps more easily interpreted on Mason's theory. But see Phys. Rev. **25**, 90, (1925) for Stewart's interpretation.

[7] Stewart and Sharp, Journal of the Opt. Soc. Amer. **19**, 17 (1929).

EXTENSION AND PERIOD OF A CONICALLY WOUND SPRING

By O. B. Ader*
Department of Physics, Duke University

(Received May 31, 1929)

Abstract

By imposing certain restrictions on the shape of a conically wound spring, it is valid to assume that the extension under a load is due entirely to torsion. It is found that the extension is then given to an approximation by the expression:

$$Z=\frac{2MgR^3L}{3\pi nr_1^4}$$

Mg is the load, R is the radius of the end coil, L and r_1 are respectively the length and radius of the wire of which the spring is made, and n is its rigidity modulus. For a truncated conically wound spring, this expression becomes:

$$Z=\frac{2MgN(R+r)(R^2+Rr+r^2)}{3nr_1^4}$$

N is the number of coils of the spring, and r is the radius of the small end coil. By making certain assumptions the period is shown to be:

$$T=2\pi\left(\left(1+\frac{xm}{M}\right)\frac{z}{g}\right)^{1/2}$$

m is the mass of the spring, and X is a function of the ratio of the radii of the two end coils.

Introduction

THE conically wound spring is in quite general use, but it does not lend itself so readily to theoretical treatment as does the helical. Consequently, while the theory of the helical spring is well developed,[1] the conically wound spring presents a field for investigation which is practically untouched. If this type of spring is defined as a uniform wire wound in such a way that the elastic central-line lies upon a right cone and cuts all the generators under the same angle, the equations

$$X=ce^{au}\cos u \qquad Y=ce^{au}\sin u$$
$$Z=be^{au}$$

where a, b, and c, are constants, and u is the general parameter, may be taken to represent the elastic central-line. These equations offer one method

* A paper presented to the American Physical Society April, 1928. The writer wishes to express his thanks to Professor G. D. Collins who suggested this problem and whose constant interest has been a strong incentive to persist. He is indebted to Professor W. W. Elliott for a helpful suggestion which lead to a solution.

[1] Kelvin and Tait. "Treatise on Natural Philosophy," part II, pp. 139–144.

of solution to the problem of the conically wound spring, but a less tedious method will be presented here.

Extension of a Conical Spring

The quantity of stored energy in a twisted straight rod is given by the expression:

$$Q=\tfrac{1}{4}\pi n r_1^4(d\theta/ds)^2 l$$

l is the length of the rod, $d\theta/ds$ is the rate of twist, r_1 is the radius of the rod, and n is its rigidity modulus. Consider a small element ds of a conical spring, i.e. a conically wound spring which terminates at the apex of the cone. It is evident that since the twisting torque is a variable, the rate of twist will be a variable. Hence the stored energy of this particular element is:

$$dQ=\tfrac{1}{4}\pi n r_1^4(d\theta/ds)^2 ds$$

provided the element ds is normal at all times to the plane of the line of action of the force due to the load and the radius of the coil. In the development of the equations of the elastic central-line, this restriction may be shown to lead to the result that

$$a=R/L \tag{1}$$

R is the radius of the end coil, and L is the length of the spring measured along the wire. The expression for the torsional couple on a rod or wire of circular cross section is:

$$Mga_1=\tfrac{1}{2}\pi n r_1^4 d\theta/ds$$

a_1 is the arm of the couple, r_1 is the radius of the rod, n is its rigidity modulus, and $d\theta/ds$ is, as above, the rate of twist. Utilizing the last three equations, and integrating between the limits L and O, there results:

$$Q=\frac{(Mg)^2R^2L}{3\pi n r_1^4}.$$

If Z is the extension the spring undergoes, it follows from Hook's law that $Q=\frac{1}{2}MgZ$, and hence

$$Z=\frac{2MgR^2L}{3\pi n r_1^4}. \tag{2}$$

The corresponding expression for the helical spring is:

$$Z=\frac{2MgR^2L}{\pi n r_1^4}.$$

Comparing these two equations, the following relationship between the helical and conical spring may be noted: When a given weight is applied, the extension of a conical spring is equal to one-third the extension of a helical spring made of wire of the same dimensions and the same modulus of rigidity,

the helical spring having a radius equal to the radius of the end coil of the conical spring.

Modification for Truncated Conically Wound Spring

It is now comparatively easy to modify the above result to fit the case of a truncated conically wound spring which has a coil of radius r at the upper end and a radius R at the lower end. Imagine the wire of a truncated conically wound spring to be extended upward to the apex of the cone so that it becomes a spring whose extension is given by Eq. (2). Now by using the relationship (1), and by a simple composition of known extensions given by Eq. (2), the result for the truncated conically wound spring is found to be:

$$Z=\frac{2MgL(R^2+Rr+r^2)}{3\pi nr_1^4}.$$

Or, since L is in general difficult of measurement, we may approximate it and write[2]

$$Z=\frac{2MgN(R+r)(R^2+Rr+r^2)}{3nr_1^4} \tag{3}$$

N is the number of turns of wire in the coil.

Period of Conically Wound Spring

From Eqs. (1) and (2), it is evident that the velocity of any element along the wire of a conical spring may be expressed as $2Mga^2S^3/3\pi nr_1^4$, where S is the distance of the element measured along the wire. The fact that the velocity of the element of a conical spring varies in this way with the cube of the distance along the wire, can be used to determine the expression for the kinetic energy of the truncated spring when vibrating with a load. However, in order to apply this principle to the truncated spring, it is necessary as in the calculation of the extension to imagine the truncated spring as an integral part of a larger conical spring. Then by a simple composition of extensions, and by a determination of the dimensions of the hypothetical part of the conical spring in terms of the known dimensions of the truncated spring, it is possible to work back to the real case. This method gives for the kinetic energy of the truncated conically wound spring:

$$E=\frac{1}{2}m\dot{Z}^2\left[\frac{2+6K+12K^2+13K^3+9K^4}{14(1+K+K^2)^2}\right]$$

$\dot{Z}$ is the instantaneous velocity of the vibrating load, m is the mass of the spring, and K is the ratio, r/R. Assuming that the system is conservative, the expression for the period is found to be:

[2] In the October, 1928, issue of the J.O.S.A. & R.S.I., R. B. Abbott developes by another method a different expression, namely $Z=MgN(R+r)(R^2+r^2)/nr_1^4$. This expression does not agree so well with experimental data now available as does the one developed in this paper.

$$T=2\pi\left(\left(1+\frac{xm}{M}\right)\frac{z}{g}\right)^{1/2}$$

where X is the value of the fraction of mass of the spring which enters into the expression for its kinetic energy. The calculated values which this fraction assumes for various values of K are given below.

TABLE I.

K	Fraction	K	Fraction	K	Fraction	K	Fraction
0	0.1429	0.25	0.1861	0.55	0.2480	0.80	0.2978
0.05	.1503	.30	.1961	.60	.2583	.85	.3071
.10	.1585	.35	.2063	.65	.2685	.90	.3161
.15	.1673	.40	.2167	.70	.2785	.95	.3249
.20	.1764	.45	.2271	.75	.2883	1.00	.3333
		.50	.2376				

Equation (3) has been checked experimentally with good agreement. Using a small phosphor-bronze spring, the values found were:

$$Mg=980\times 2.392 \text{ dynes}$$
$$N=112.5 \text{ turns}$$
$$R=0.9115 \text{ cm}$$
$$r=0.4115 \text{ cm}$$
$$r_1=0.026 \text{ cm}$$
$$n=4.36\times 10^{11} \text{ dynes/cm}^2$$

From direct measurement, the extension was found to be 1.60 cm. The value calculated by the above data gives 1.605 cm, an error of 0.3 percent, which is within the limits of experimental error. Using the same spring with a load of 9.955 grams, an experimental value of 6.70 cm was found for the extension, as compared with 6.682 cm by formula, an error of less than 0.3 percent.

BOOK REVIEWS

English and Science. PHILIP B. MCDONALD. Pp. viii+192. D. van Nostrand Company, New York, 1929. Price $2.00.

This book is planned primarily for engineering students and aims to interest them in the proper use of English in their technical work, particularly with letters and reports, the preparation of which forms so large a part of their later professional activity. Besides this, the book is extremely stimulating and interesting to research workers who have to prepare technical papers. The senior associate editor of the Physical Review strongly recommends that authors of papers to be presented for publication herein follow its recommendations regarding conciseness and choice of words. In the concluding chapters the author suggests how an engineer or other technical expert whose general cultural background is deficient may begin to remedy his deficiency by reading in the history and biography of his specialty.

A study of the monograph shows that Mr. McDonald has some deep-seated prejudices against lawyers and women, but aside from these biases the selection of examples and the comments thereon are extremely happy.

L. W. MCKEEHAN

Gmelin's Handbuch der Anorganischen Chemie. Eighth edition edited by R. J. MEYER. **System-Nummer 21: Natrium,** pp. 992+xviii+xxxiii, 75 figs., price RM 150. **System-Nummer 31: Radium und Isotope,** pp. xvii+iv+80, 4 figs., price RM 15. **System-Nummer 59: Eisen,** Teil A—Liefering 1 pp. 224, price RM 33. Verlag Chemie, Corneliusstrasse 3, Berlin W 10 Germany, 1929.

Thus far there have appeared twelve volumes of this completely rewritten eighth edition of Gmelin's classic which when complete will comprise more than seventy volumes of information about all the known elements. Although written primarily for chemists the information given includes, with very complete bibliography, almost all that is known of the physical properties of the elements and their compounds.

The work is extremely valuable to the physicist. It provides for him a means of ready access to the literature of almost any subject provided he can remember, as is usually the case, what elements have been studied in that connection. The treatment given each subject is not very critical. A sentence or two summarizes the work of each author in the field but as a bibliography of source material it is invaluable. The volumes are well indexed and analytically arranged for convenient reference.

JOHN T. TATE